LIST OF TABLES

LIST OF FIGURES

CONTENTS

ACKNOWLEDGEMENTS

I would like to thank my supervisor, Professor H. Scholz who has guided and helped me through the time I have spent on this dissertation. I am also most grateful to him for organising funding through the Portland Cement Institute and the Foundation for Research and Development. Funding from the University is also deeply appreciated.

Mr. John Dyer provided invaluable assistance in helping me to set up the test equipment and placing the beams in the rig for which I am indebted.

Thanks also to Mike de Vitto of Concor Technicrete, who helped me in the supervision of the casting of the beams and Colin Keel of Haggie Rand, who donated the first lot of prestressing wire.

Thanks to my mother, June Eagleson and to Michele Edens, who haven't failed to provide me with anything but encouragement, especially through heavy times of work.

ABSTRACT

This dissertation deals with cracking of partially prestressed concrete members. Four series of beams with different types and combinations of prestressed and unprestressed steel were cast, ranging from reinforced concrete through partially prestressed concrete to fully prestressed concrete. The beams were subjected to bending by two point loads in order that a pure moment region could be set up and all crack width measurements were made here. Crack measurements have been analyzed with the objective of formulating improved crack width predictions.

As a result of this study, the equation from ACI 318-83[18] and CAN3-A23.3-M84[19] and the equation by Suri and Dilger[20] were improved upon, by the inclusion of variable cracking factors which take account of the type of prestressed steel and method of prestress used, and the amount of prestress present.

The applicability of the proposed method for prediction of crack width is shown by comparing predicted crack widths to measured crack widths from previous research. By comparison the predicted crack widths, using the cracking factors obtained from the test beams, were similar to those using the factors suggested by Scholz[14], but were an improvement over those when using the factors suggested by Suri and Dilger[20].

DECLARATION

I declare that this dissertation is my own unaided work. It is being submitted for the degree of Master of Science in Engineering in the University of the Witwatersrand, Johannesburg. It has not been submitted before for any other degree or examination in any other University.

F. Eagle

28th day of FEBRUARY 1994

CRACK WIDTH OF PARTIALLY PRESTRESSED CONCRETE FLEXURAL MEMBERS WITH DIFFERENT METHODS OF PRESTRESS

Victor Fraser Ross Eagleson

A dissertation submitted to the Faculty of Engineering, University of the Witwatersrand, in fulfilment of the requirements for the degree of Master of Science in Engineering

Johannesburg, 1994

It should be noted that Hognestad[9] made various incorrect assumptions:

- a uniform tensile stress is assumed across the section, while in fact Park and Paulay[6] have shown that the distribution is variable.

- crack width is assumed to be constant throughout the section.

2.2.2 No slip theory

Base et al[12] assumed that no slip occurs between the steel and concrete. They proposed that crack width was at a maximum at the tensile face, decreasing to zero at the reinforcing bar implying that the crack width is dependent on the deformations of the concrete surrounding the bar. Wedge shaped cracks would result from such cracking. Their suggested equation was:

$$W = 3,3c\,\frac{f_s h_2}{E_s h_1} \qquad [2.2]$$

Beeby[16] modified no-slip theory to develop his equations for prediction of crack width in reinforced concrete, as described in section 2.2.4.

2.2.3 The statistical approach by Gergely and Lutz

Gergely and Lutz[13] examined existing equations of the time that calculated crack width in reinforced concrete members. They found that values predicted by these equations varied considerably and suggested their own equation based on a statistical analysis. Park and turn determine the crack spacing. The concrete tensile stress would thus increase to a maximum halfway between two cracks, while the steel stress was a minimum here. New cracks would then form between initial cracks until a stabilized crack spacing had been reached.

The equation by Hognestad[9]

$$a_{min} = \frac{A_e f_t}{u \Sigma O} \qquad [2.1]$$

predicted that a new crack would form only when the spacing between two already existing adjacent cracks was greater than twice the minimum crack spacing, a_{min} for that particular member (as shown in Figure 2.1), assuming that the tensile strength of the concrete had been exceeded in that portion of the member. However, he found through experiments that the average crack spacing was one and a half times his suggested minimum spacing, ie. $1{,}5a_{min}$. On this basis, Hognestad[9] suggested an equation for maximum crack width, other improved equations were derived by CEB[10] and Kaar and Hognestad[11].

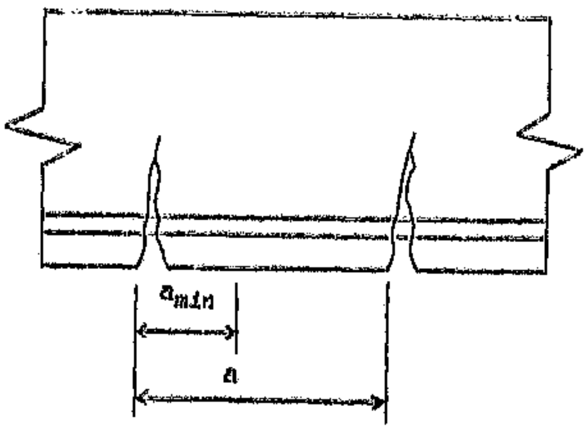

Figure 2.1 Crack spacing due to classical theory

width that is acceptable to the general public is dependent on personal opinion. This is reflected in the different recommendations of Park & Paulay[6] and Park & Gamble[7] who suggest 0,25 mm to 0,38 mm, and Leonhardt[8] who suggests 0,20 mm as the visually acceptable limits.

2.2 The Mechanism of Cracking in Prestressed and Reinforced Concrete

Three types of cracking can occur in concrete structures:

- due to flexural stresses
- due to plastic settlement of the concrete
- due to volumetric changes, generally caused by shrinkage

Much of the existing theory on cracking of partially prestressed concrete members is adapted from research performed on reinforced concrete and hence it is pertinent at this point to examine the mechanism of flexural cracking in reinforced concrete. Cracking due to plastic settlement and cracking due to volumetric changes have been omitted since they are outside the scope of this research. Several theories have been advanced, but Park and Paulay[6] have identified the most relevant ones which will be briefly summarised below.

2.2.1 Classical theory

It was believed that initially cracks formed randomly wherever the tensile strength of the concrete had been exceeded. At a crack, it was assumed that only the steel carried the tensile stress, which implied that slip between the steel and the surrounding concrete occurred. However, it is the bond that enables the generation of tensile stress in the steel. The allowable bond stress in since it is of high strength and hence even a small percentage of its cross sectional area lost due to corrosion can cause a considerable reduction in strength. Protection of the prestressed steel can be one of three types:

(1) In pretensioned members, the prestressed steel comes into contact with the concrete which forms a passivating layer, in the same manner as described above.

(2) In post tensioned bonded members, once the stressing of the steel is complete, grout is injected into the ducts. This grout forms the protective layer on the steel.

(3) In post tensioned unbonded members, the prestressed steel comes into contact neither with concrete nor grout. Therefore grease is injected into the ducts after stressing, or in some cases, the prestressed steel is supplied in ducts that have already been greased.

Both the permeability and the cover are the main factors influencing corrosion of the steel, while research on the correlation between the crack width and corrosion is inconclusive. At present, it is thought that the passivating layer on the steel remains unchanged for crack widths up to 0,4 mm[5].

2.1.2 Aesthetic considerations

According to reference 5, cracks are visually unacceptable to the public since they can cause alarm with regard to the safety of the structure. The reference also states that a definite limit on the maximum crack

2 DETAILED FORMULATION OF THE PROBLEM

2.1 Introduction

Engineers are often more concerned with the performance of an element at the ultimate limit state than with the behaviour at the at the serviceability limit state. However, when dealing with concrete structures excessive cracking and deflection can have far reaching effects. The prosecuted examination focuses on the cracking behaviour of partially prestressed members. An improved calculation method for the crack width prediction of such members is sought. Two reasons for crack control are apparent:

- protection of the prestressed and unprestressed steel against corrosion.

- aesthetic considerations.

2.1.1 Protection of the prestressed and non prestressed steel against corrosion[4]

Hydration of concrete produces a number of alkaline by-products, the main one being calcium hydroxide having a pH of 13. When these compounds come into contact with bonded steel, a passivating protective layer of ferric oxide is formed. This passivating layer may be broken down mainly by carbon dioxide, which reacts with the calcium hydroxide to form calcium carbonate which has a pH of only 8. This is detrimental to the protection of the steel since the lower the pH of the passivating layer, the less effective it is against stopping corrosion.

It is especially important to protect prestressed steel

(3) With lower values of prestress, the compressive strength of the concrete at transfer need not be as high as for a fully prestressed member, leading to cheaper concrete, if transfer stresses are governing. The problem of cracking due to bursting in the end zones is also diminished.

(4) Low prestress produces relatively small elastic shortening and creep shortening, hence reducing the loss of prestress. Also as a result of the lower prestress, volumetric changes in the concrete will be less, therefore reducing the possibility of cracking at fixed member connections.

(5) Tadros[3] observed that a partially prestressed member is capable of carrying the same load as a fully prestressed member significantly earlier for the same concrete strength because of the reduced stresses at transfer. Hence the shuttering may be stripped much earlier and therefore used more economically.

(6) Most importantly, fully prestressed sections can result in brittle solutions. The predominant requirement of service, in particular cracking, can produce overprestressed sections in terms of the ultimate limit state, resulting in a low ductility capacity of the member. Such members are not suitable for moment redistribution or plastic analysis and design.

steel.

1.2 Reasons for using partially prestressed concrete

Traditionally, prestressed concrete flexural members were designed for no cracking under full service load. However, it was then realised that fully prestressed members did not always offer optimum structural performance and were not necessarily the most economic. Hence partially prestressed concrete was recognised as being a viable alternative to both reinforced and fully prestressed concrete. With this recognition, reinforced and prestressed concrete are not seen as two completely separate entities, but as boundaries of a spectrum, of which partially prestressing is a transitional stage. The reasons for using partially prestressed concrete over fully prestressed concrete are numerous, for example:

(1) Prestressing steel is more expensive than ordinary unprestressed reinforcing due to its high strength. Partially prestressed concrete uses less prestressed steel than fully prestressed concrete and hence the members can be more economical. (Obviously there is an optimum ratio of the amount of prestressed steel to the amount of unprestressed steel in a given situation). In the case of post tensioning, a reduction in the amount of prestressed steel also leads to a saving in the cost of end anchorages.

(2) The initial upward camber before loading is less than that of a fully prestressed member due to the reduction in prestress. If the live load is large and mostly transient in nature, such upward camber can increase to undesirable values due to creep.

1 PARTIALLY PRESTRESSED CONCRETE

1.1 Introduction

The purpose of this dissertation is to examine the crack behaviour of different partially prestressed concrete sections. Initially a brief historical overview of partially prestressed concrete is presented and the benefits of using partially prestressed sections are enumerated.

Partially prestressed concrete members are members in which cracking is permitted under full service load, while containing both prestressed and unprestressed steel. This form of structural element is now widely accepted and has been promoted by many researchers over the last forty years or so.

The origin of partial prestressing is generally credited to Emperger[1], an Austrian engineer. Not satisfied with the cracking and deflection characteristics of some reinforced concrete beams he had been designing, he tried to improve their serviceability behaviour by adding some pretensioned wires to his design. Abeles[2] took the concept further when he realised the problem of prestress losses. Having investigated this problem, he convinced British Railways in the 1940's to use partially prestressed sections in all their new bridge designs.

Due to their superior performance over reinforced concrete members, partially prestressed concrete members can be smaller making them more aesthetically pleasing, while they are more economical than fully prestressed concrete members. The term fully prestressed describes a member containing only prestressed steel, whereas a reinforced concrete member contains only unprestressed

β_1	residual crack width
β_2	bond factor for Bennett and Veerasubramanian
κ_1	bond factor for CEB/FIP 1978
κ_2	loading type factor
ε_1	strain at the level considered
ε_{ct}	concrete tensile strain corresponding to the fictitious tensile stress, f_{ct}
ε_m	average strain
ε_s	incremental steel strain in non prestressed steel
ε_{su}	strain in non prestressed steel after decompression of concrete at level of prestressed steel
$\Delta\varepsilon_{su}$	additional strain in non prestressed steel occuring between decompression of concrete at the tensile face and decompression at the level of the prestressed steel
η_1	bond factor
η_2	stress type factor
ρ	ratio of tensile steel to concrete area (bd)
ΣO	sum of circumferences of all tensile steel, prestressed and non prestressed
ϕ	bar diameter

	prestressed steel
h	depth of section
h_0	crack height remote from a reinforcing bar
h_1	distance from centroid of tension steel to neutral axis
h_2	distance from extreme tension fibre to neutral axis
i_p	prestressing index
I_c	second moment of area of concrete section
k	cracking factor, usually dependent either on the combination of prestressed and non prestressed steel present or the type of prestress used (has various subscripts as defined in the text)
k_0	constant related to the stiffness of the aggregate
M	bending moment due to applied loads
M_c	cracking moment
M_d	moment due to dead load
M_{dec}	decompression moment
M_l	moment due to live load
$M_{u,ps}$	ultimate moment sue to prestressed steel
$M_{u,s}$	ultimate moment due to non prestressed steel
PPR	partial prestressing ratio
s	tension bar spacing
s_c	crack spacing
t_b	distance from extreme tension fibre to centre of adjacent bar
t_s	distance from the side of the beam to the centre of the adjacent bar
w	crack width
W	point load
x	depth to neutral axis
x_1	smaller dimension of a link
α	strength factor related to aggregate characteristics

LIST OF SYMBOLS

Symbol	
a	crack spacing
a'	distance from compression face to point at which crack width is being calculated
a_{cr}	distance from crack considered to nearest longitudinal bar
a_{min}	minimum crack spacing
A_c	effective tension zone area
A_{ps}	area of prestressed steel
A_s	area of non prestressed steel
A_t	area of concrete below the neutral axis
b	width of section
c	concrete cover, measured to surface of bar
c_0	crack height directly over a reinforcing bar
c_{min}	minimum cover to tension steel
d	effective depth to total area of tension steel
d_c	concrete cover, measured to centre of bar
d_p	depth to centroid of prestressed steel
d_s	depth to centroid of non prestressed steel
E_c	modulus of elasticity of concrete
E_{ps}	modulus of elasticity of prestressed steel
E_s	modulus of elasticity of non prestressed steel
f_{cu}	characteristic concrete cube strength
f_{ct}	fictitious concrete tensile stress
f_{pb}	tensile stress in prestressed steel st ultimate limit state
f_{ps}	incremental stress in prestressed steel
f_{pu}	characteristic strength of prestressed steel
f_{py}	characteristic yield strength of prestressed steel
f_s	incremental stress in non prestressed steel
f_y	characteristic yield strength of non

where:

- β_1 is a constant which was derived from the values of residual crack width obtained after removing the load from the test beams. The suggested value for deformed bars is 0,02 mm
- β_2 is a constant depending on the bond characteristics of the unprestressed steel. For deformed bars, β_2 = 6,5
- ε_s is the incremental stress in the unprestressed steel after concrete decompression at the soffit of the beam
- d_c is the concrete cover to the centre of the nearest bar

They do not state whether the calculated crack width is at the level of the tensile steel (prestressed or unprestressed) or at the tensile face. It should be noted that equation [2.9] does not take the bond characteristics or the type of prestressed steel into account. Note also that cover, d_c, has been included in the equation, but there is no mention of the composition of steel areas. The term ε_s, the steel strain, is simply the steel stress divided by the elastic modulus, E_s, assuming that the load lies in the elastic range.

(5) CP 110[17], BS 8110[26], SABS 0100[27], BS 5400[28]

The equation predicting crack width in the above codes is based on the work by Beeby[16] on reinforced concrete and included the changes recommended by Beeby et al[29] that were necessary for prestressed concrete. Scholz[4] states that this equation is complex and therefore can be unattractive to the design engineer. The maximum crack width at the tensile face is given by:

prestressing used.

Table 2.4 Values of *k* for Nawy & Huang[21] and Nawy & Chiang[22]

Type of prestress used	k
pretensioning	$5,85 \times 10^{-5}$
post tensioning (unbonded)	$6,51 \times 10^{-5}$

Naaman[23] concludes that this equation includes most of the important parameters that have an effect on the cracking behaviour of partially prestressed members, except that of the concrete cover. However, Nawy[24] believes that the cover is accounted for in the term A_t.

(4) Bennett and Veerasubramanian[25]

The main objective of this study was to compare the cracking behaviour of four different shaped cross sections: rectangular, I, T and composite. Bennett and Veerasubramanian[25] believed that the existing research of the time that had focused solely on rectangular beams was not typical of practice. Hence they wanted to find if there was any correlation between results from rectangular sections and those from I, T and composite sections. It was in fact found that the shape of the cross section had no measurable influence on the crack width. Their proposed equation for predicting maximum crack width was:

$$w = \beta_1 + \beta_2 \varepsilon_s d_c \qquad [2.9]$$

Table 2.3 Values of k_w for Suri and Dilger[20]

Steel combination	k_w
deformed bar-strand	2,55
deformed bar-wire	3,51
strands only	2,65
wires only	4,50

Scholz[14] found that equation [2.7] predicted larger crack widths to those measured in the tests by Tansi et al[15].

(3) Nawy & Huang[21] and Nawy & Chiang[22]

A series of pretensioned I and T beams were tested by Nawy and Huang[21], while Nawy and Chiang[22] tested a series of post tensioned unbonded T beams. Similar equations were derived from the results of both tests and the maximum crack width at the level of the unprestressed steel was suggested to be:

$$w = k \frac{A_t}{\Sigma O} f_s \qquad [2.8]$$

where:

- A_t is the area of concrete in tension below the neutral axis.
- ΣO is the sum of the perimeters of all the bars crossing the section on the tension side
- f_s is the incremental steel stress after the point of decompression at the level of the unprestressed steel
- k is a variable factor depending on the type of

(2) Suri and Dilger[20]

Suri and Dilger[20] used a statistical approach on already existing equations resulting in an equation predicting maximum crack width at the level of the unprestressed steel:

$$w = k_w f_s d_c \sqrt{\frac{A_t}{A_s + A_{ps}}} \times 10^{-6} \qquad [2.7]$$

where:

- f_s is the incremental steel stress after the point of decompression at the level of the unprestressed steel
- d_c is the concrete cover to the centre of the nearest bar
- A_t is the area of concrete in tension below the neutral axis. It was argued that A_t varies as the neutral axis varies and hence the effect of the load level on the crack width would be better represented.
- (A_s+A_{ps}) is the total area of tensile steel. Suri and Dilger[20] chose to include the total area of steel in the equation instead of only the area of unprestressed steel, since for a large value of prestress, the area of the prestressed steel can be of similar size to the area of unprestressed steel. The observation by Bennett and Chandrasekhar[30] that the crack width is influenced by, among other factors, the total area of steel irrespective of the degree of prestress, supports this decision.
- k_w is a variable factor depending on the type of prestressed and unprestressed steel used. Suggested values are:

Table 2.1 Values of k_w for ACI 318-83[18] and CAN3-A23.3-M84[19] by Suri and Dilger[20]

Steel combination	k_w
deformed bar-strand	13,7
deformed bar-wire	20,3
strands only	21.5
wires only	37.2
deformed bar-unbonded tendon	25,0

When Scholz[14] compared the results from equation (2.3) using a factor of k_w = 13,7 to the results of the tests by Tansi et al[15], he found that k_w = 11 in fact gave better results for the deformed bar-strand combination and subsequently suggested reducing all the k_w values suggested by Suri and Dilger[20] accordingly:

Table 2.2 Reduced values of k_w for ACI 318-83[18] and CAN3-A23.3-M84[19] by Scholz[14]

Steel combination	k_w
deformed bar-strand	11
deformed bar-wire	16,4
strands only	17,4
wires only	30,1
deformed bar-unbonded tendon	20,2

However, these reduced values need to be verified by experimental results.

$$w = \frac{11\sqrt[3]{t_b A_e}}{1+\frac{2t_s}{3h_1}} f_s \times 10^{-6} \qquad [2.6]$$

where:

- t_b is the concrete cover to the centre of the nearest bar
- t_s is the distance from the side of the beam to the centre of the adjacent bar
- A_e is as described above for equation [2.3]
- h_1 is the distance from the centroid of the tension steel to the neutral axis
- h_2 is the distance from the extreme tension fibre to the neutral axis
- f_s is the incremental steel stress after the point of decompression at the level of the unprestressed steel

Suri and Dilger[20] re-evaluated equation [2.3] and suggested replacing the factor of $k_w = 11$ by a variable k_w. They found that equation [2.3] worked well for pretensioned strands and deformed bars, but underestimated the crack width for other combinations. The factors they suggested were:

- A_e is the area of concrete in tension around per bar as shown in Figure 2.4

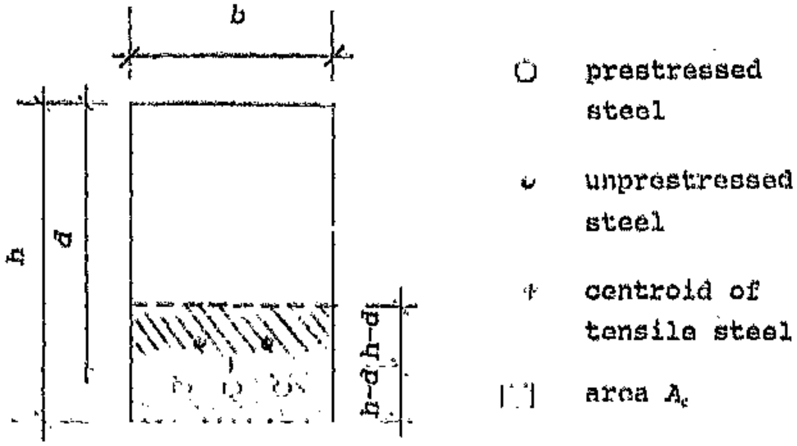

Figure 2.4 Definition of A_e

$$A_e = \frac{2b(h-d)}{no.\ of\ bars} \qquad [2.5]$$

When the tensile steel consists of prestressed and unprestressed steel of different diameters, the "effective" number of bars is calculated by taking the total area of tensile steel and dividing it by the area of the largest bar.

This equation is a modified form of the Gergely-Lutz equation[4] where the maximum crack width is given at the level of the unprestressed steel:

Two types of equations for predicting crack width in partially prestressed concrete are apparent:

(1) crack width is related to the incremental steel stress
(2) crack width is related to the fictitious concrete tensile stress

2.3.1 Equations relating the crack width to the incremental steel stress

The majority of equations in this category are of the form:

$$w = k_w c f_s \qquad [2.3]$$

These equations are developments of the theory described in sections 2.2.1 to 2.2.4.

(1) ACI 318-83[18] and CAN3-A23.3-M84[19]

The maximum crack width at the level of the unprestressed steel is given by the equation:

$$w = k_w f_s \sqrt[3]{d_c A_b} \times 10^{-6} \qquad [2.4]$$

where:

- k_w = 11.
- f_s is the incremental steel stress after the point of decompression at the level of the unprestressed steel
- d_c is the concrete cover to the centre of the nearest bar

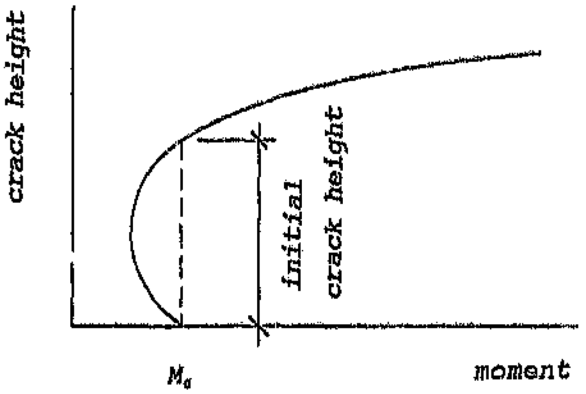

Figure 2.3 (a) Moment-crack height curve for reinforced concrete beam

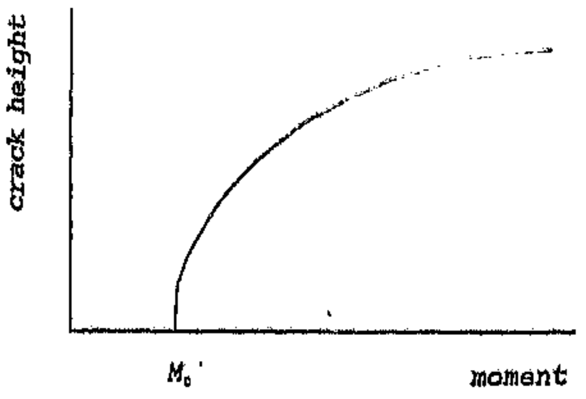

Figure 2.3 (b) Moment-crack height curve for prestressed concrete beam

Beeby's equations[16] for the prediction of crack width were complex, and were therefore not suitable for everyday use by design engineers. As shall be shown, both the equations by Beeby[16] and Gergely & Lutz[13] were adopted by CP 110[17] and ACI 318-83[18] & CAN3-A23.3-M84[19] respectively, and suitably modified for partially prestressed concrete.

2.3 Previous Research and Code Recommendations

As already noted, many of the equations predicting crack width and code recommendations for limiting crack with were modifications of those applicable to reinforced concrete. This modification was necessary due to the difference in cracking behaviour[20]:

- unprestressed reinforcing has different bond characteristics to prestressed steel.

- the cracking behaviour of reinforced and prestressed concrete differ. Figure 2.3 shows the difference between cracking in a reinforced concrete member (Figure 2.3(a)) and a prestressed concrete member (Figure 2.3(b)). In a reinforced concrete member, once the cracking moment has been reached, the moment capacity of the section decreases as the crack height increases. While still applying moment, the crack height will continue increasing and once again the value of the cracking moment will be reached. This height is referred to as the initial crack height. The crack height will then continue increasing with an increase in applied moment, and there will be no change in the crack pattern. In a prestressed concrete member, the initial crack height is very small and the crack height simply increases with an increase in applied moment.

as in (a).

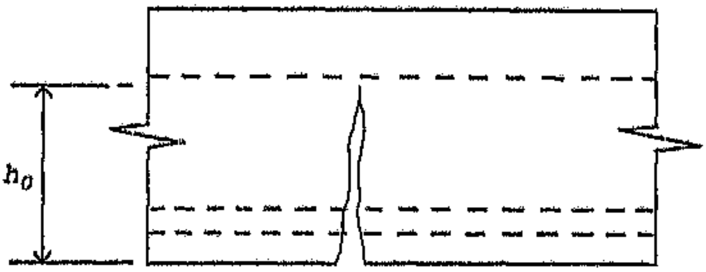

Figure 2.2 (a) Cracking distant from a bar, controlled by h_0

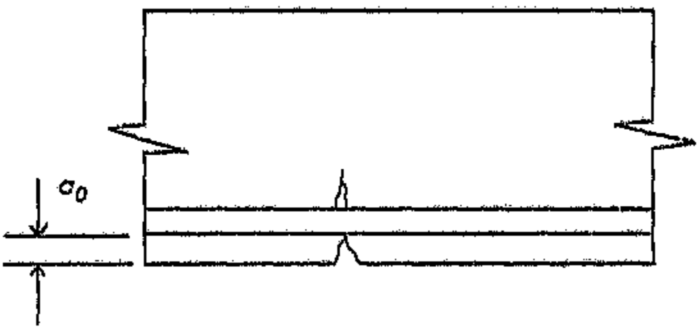

Figure 2.2 (b) Cracking at a bar, controlled by c_0

However, some slip will occur and hence the effective height will be greater than c_0 since the crack width is not zero at the bar surface, leading to behaviour that is intermediate between the h_0 and c_0 cracking patterns. If large slip occurs, the crack pattern will then tend towards that of cracking remote from a reinforcing bar, ie. the h_0 controlled pattern.

Paulay[6] argued that the approach by Gergely and Lutz[13] was unsatisfactory. However, Scholz[14] found that the Gergely-Lutz equation[13] correlates well when compared to measured values from the tests by Tansi et al[15].

2.2.4 Beeby's suggestion of interaction

Beeby[16] found that the crack width and crack spacing increased with the distance from the reinforcing bar until a constant value was reached, at which point both the crack width and spacing were dependent on the crack height rather than the distance from the bar. Beeby[16] then suggested that interaction between two basic crack patterns would lead to the final one.

(a) cracking distant from a reinforcing bar

The crack height h_0 controls the crack pattern and is assumed to almost reach the neutral axis (as shown in Figure 2.2). A crack that is further than h_0 from an existing crack will not significantly influence the concrete tensile stress between two existing adjacent cracks. Therefore cracks will form between h_0 and $2h_0$ indicating an average of $1,5h_0$. However, Beeby's tests[16] indicated an average of $1,33h_0$. Hence the crack width is dependent on crack height and not the distance from the bar.

(b) cracking directly over a reinforcing bar

No slip theory suggests that wedge shaped cracks occur as a result of zero crack width at the reinforcing bar. If the effective height of the crack is c_0, ie. the distance between the tensile face and the reinforcing bar (or the cover), the mean crack spacing is $1,5c_0$ using the same reasoning

3 PROBLEM ASSESSMENT AND DETAILED RESEARCH AIMS

3.1 Appraisal of the equations and methods presented

As has been shown in sections 2.3.1 to 2.3.3, the methods for both calculating and limiting crack width can vary considerably.

For some time, researchers have agreed that the incremental steel stress approach is fundamentally more correct than the fictitious concrete tensile stress. Bennett and Chandrasekhar[30] summarised the reasons why when they noticed that the crack width was closely related to the stress in the steel after cracking which is largely dependent on the total area of steel. The fictitious tensile stress is calculated using the whole section as if in an uncracked state and hence it is quite insensitive to the total area of steel present. This fact was emphasized by Naaman and Siriaksorn[37] when they compared the fictitious tensile stresses for single T, double T, rectangular slab and hollow core sections. For a limiting crack width of 0,2 mm the stresses varied between 3 MPa and 23 MPa.

Scholz[14] compared various equations predicting crack width to the results from the tests by Tanai et al[15]. He found that there was a large scatter of predicted crack widths and suggested that the equation from ACI 318-83[18] and CAN3-A23.3-M84[19] performs best (using his reduced values of k_w as in Table 2.2). Equations from the research by Suri and Dilger[20], the CEB/FIP 1970 recommendations[32] and the hypothetical tension stress method of CP 110[17], BS 8110[26], SABS 0100[27] and BS 5400[28] all seemed to overestimate the measured crack widths, while the equations from the CEB/FIP 1978 recommendations[33], CP 110[17], BS 8110[26], SABS 0100[27] and BS 5400[28] underestimated.

nominal crack width and type of prestressed steel used. This method has the advantage of being easy to use in design, but Scholz[14] shows that the values are conservative when compared to the results from the tests by Tanzi et al[15].

- f_{ct} is the fictitious concrete tensile stress
- A_t is the area of concrete in tension below the neutral axis.
- A_s and A_{ps} areas of unprestressed and prestressed steel respectively

His results compare reasonably well to those from the tests by Tanai et al[15].

2.3.3 Crack width control by limitation of stresses

As with equations predicting crack width, crack control by limitation of stresses can be related to both the incremental steel stress and the fictitious concrete tensile stress.

(1) Crack width control by limitation of incremental steel stress

SIA 162-1968[36]

In the Swiss code SIA 162-1968[36], crack control is achieved by limiting the increase in stress in the prestressed steel to $0{,}1f_{pu}$, but not more than 150 MPa. In bridge design this increase is limited to $0{,}05f_{pu}$, but not more than 150 MPa also.

(2) Crack width control by limitation of the fictitious concrete tensile stress.

CP 110[17], BS 8110[26], SABS 0100[37], BS 5400[28]

The above codes place an upper limit on the tensile stresses in the concrete by calculating the fictitious tensile stress, assuming an uncracked section. The limiting stresses vary with concrete grade, acceptable

$$w = C_2 \varepsilon_{ct} d_c \sqrt[3]{A_t} \qquad [2.24]$$

where:

- ε_{ct} is the fictitious concrete tensile strain
- d_c is the concrete cover to the centre of the nearest bar
- A_t is the area of concrete in tension around per bar as shown in Figure 2.4
- C_1 and C_2 are variable according to the type of steel nearest the tensile face:

Table 2.8 Values of C_1 and C_2 for Meier and Gergely[35]

Type of steel nearest the tensile face	C_1	C_2
deformed bars	12	8,4
strand	16	12

As mentioned earlier, including strand as unprestressed steel in an equation is useless because it is very rarely used in this way.

(4) Scholz[14]

Scholz[14] proposed an equation based on the CEB/FIP 1978 recommendations[33] using the hypothetical tensile stress giving the crack width at the level of the tensile steel:

$$w = 0{,}0003 f_{ct} \frac{A_t}{A_s + A_{ps}} \qquad [2.25]$$

where:

- c is the cover to the surface of the bar nearest the tensile face
- f_{ct} is the fictitious concrete tensile stress
- k is a variable depending on the type of unprestressed steel used:

Table 2.7 Values of k for Bennett and Chandrasekhar[30]

Type of unprestressed steel	k (mm²/N)
deformed bars	435×10^{-6}
strands	725×10^{-6}
wire	1160×10^{-6}

They conclude that the values from the equation compare well with their own measured values form their tests on partially prestressed beams, but better results are obtained from their equation relating the crack width to the incremental steel stress.

(3) Meier and Gergely[35]

Meier and Gergely[35] examined existing equations for crack width prediction. They proposed using the fictitious tensile stress method over the incremental steel stress method because they felt that there was little difference in accuracy between the two, while the fictitious tensile stress method was easiest to calculate. They put forward two equations for calculation of maximum crack width at the tensile face:

$$w = C_1 \varepsilon_{ct} d_c \qquad [2.23]$$

and

(1) Beeby and Taylor[34]

The following equation for calculation of a design crack width at the tensile face was proposed:

$$w = \frac{1,75 f_{ct}(h - x)}{E_c} \qquad [2.21]$$

where:

- f_{ct} is the fictitious concrete tensile stress
- h is the depth of the section
- x is the depth to the neutral axis
- E_c is the elastic modulus of the concrete

Bennett and Chandrasekhar[30] note that the equation performs well when compared to their results, but the inclusion of the neutral axis depth, x, although logical, removes some of the simplicity of the hypothetical tension stress method. They also state that the equation loses some accuracy when the cover is large.

(2) Bennett and Chandrasekhar[30]

In addition to their equation relating the crack width to the incremental steel stress in the prestressed or unprestressed steel, Bennett and Chandrasekhar[30] suggested the following equation using the fictitious tensile stress for calculation of maximum crack width at the concrete tensile face:

$$w = kcf_{ct} \qquad [2.22]$$

where:

$$\xi = 1 - \kappa_1\kappa_2\left(\frac{M_c}{M}\right)^2 \qquad [2.18]$$

κ_1 = 1 for high bond bars
2 for plain bars

κ_2 = 1 for the first load or sustained load
0,5 for a large number of cycles

and

$$s_c = 2\left(c+\frac{s}{10}\right) + \eta_1\eta_2\,\frac{\phi}{\rho} \qquad [2.19]$$

η_1 = 0,4 for high bond bars
0,8 for plain bars

η_2 = 0,25 for axial tension
0,125 for bending without axial force

Scholz[14] found the calculated crack width to be comparable with the values from the tests by Tansi et al[13].

2.3.2 Equations relating the crack width to the fictitious concrete tensile stress

This approach was originally devised by Abeles[2] and was promoted by the research done by Beeby et al[29]. The general form of the equations is:

$$w = kcf_{ct} \qquad [2.20]$$

(8) CEB/FIP 1970[32]

For non repetitive loads, the crack width at the level of the unprestressed steel is given by:

$$w = 0{,}001(f_s - 40) \qquad [2.16]$$

where f_s is the incremental stress after decompression of the concrete at the level of the unprestressed steel. For repetitive loads, the equation becomes:

$$w = 0{,}001 f_s \qquad [2.16]$$

Scholz[14] compared these equations to the measurements by Tansi et al[15] and found that they exceeded the measured results. However, he states that the results could possibly be acceptable for engineering purposes.

(9) CEB/FIP 1978[33]

This equation is an improvement over the one from the CEB/FIP 1970 recommendations[32] since it takes the bond characteristics of the unprestressed steel into account. The suggested crack width at the level of the unprestressed steel is:

$$w = s_c \xi \frac{f_s}{E_s} \qquad [2.17]$$

where s_c is the crack spacing and

As for the tests by Bennett and Chandrasekhar[30], the usefulness of these tests is also doubtful, for exactly the same reasons. Three series of beams were tested, series 1 having pretensioned and unprestressed 5 mm wires, series 2 with post tensioned and unprestressed 5 mm wires and series 3 with pretensioned and unprestressed 8 mm "Dyform" strands. The proposed equation for maximum crack width is (they do not state where the cracks were measured on their test beams):

$$w = \frac{k_b f_{ps}(h-d_p)}{A_{ps} + 0,25A_s} \qquad [2.14]$$

where :

- f_{ps} is the incremental steel stress in the prestressed steel
- h is the overall depth of the section
- d_p is the depth to the centroid of the prestressed steel
- A_s and A_{ps} are the areas of unprestressed and prestressed steel respectively
- k_b varies according to the type of steel used:

Table 2.6 Values of k_b for Bennett and Dave[31]

Type of steel	k_b (mm^4/N)
5 mm smooth wires	$2,8 \times 10^{-3}$
5 mm rusted wires	$1,4 \times 10^{-3}$
8 mm Dyform strand	$1,3 \times 10^{-3}$

probably not relevant for practical use because of the uncommon types of steel used and the method of prestressing. The proposed equation for calculation of maximum crack width at the tensile face is:

$$w = (k_1 \varepsilon_{su} + k_2 \Delta \varepsilon_{su}) c \qquad [2.13]$$

where:

- ε_{su} is the incremental strain in the unprestressed steel after decompression of the concrete at the level of the tendons
- $\Delta\varepsilon_{su}$ is the additional strain in the unprestressed steel occurring between decompression of the concrete at the tensile face and decompression at the level of the tendons
- c is the minimum cover over the unprestressed steel
- k_1 and k_2 are variables depending on the type of unprestressed steel used as shown in Table 2.5

Table 2.5 Values of k_1 and k_2 for Bennett and Chandrasekhar[30]

Type of unprestressed steel	k_1	k_2
deformed bar	3,8	20
strand	3,8	20
crimped wire	5,0	30

(7) Bennett and Dave[31]

A total of forty beams were tested with different prestress and types of prestressed and unprestressed steel.

where:

- M is the service load moment
- x_1 is the distance, measured from the neutral axis to the point at which the strain, ε_1, is sought
- E_c is the elastic modulus of the concrete
- I_c is the second moment of area of the cracked section

Scholz[14] concludes that when compared to the measurements by Tansi et al[15], the calculated crack widths correlate well, giving results similar to ACI 318-83[18] and CAN3-A23.3-M84[19]. However, the calculation is somewhat more elaborate.

(6) Bennett and Chandrasekhar[30]

Bennett and Chandrasekhar[30] tested a series of twenty beams varying the cover, the type of unprestressed steel, and the prestress. They found that deeper cover had an adverse effect on the crack width, that is, as the cover increased so did the crack width.

However, Bennett and Chandrasekhar[30] used unusual steel for the unprestressed reinforcing. For example, as well as using deformed bars which are in common use, three wire prestressing strands and crimped prestressing wire were used without prestress. These two types of steel are not commonly used in this way, because they are more expensive than ordinary deformed bars. Hence the results from these tests are of questionable use. Their method of prestressing, post tensioned grouted wires, is also not in common use. Post tensioned grouted elements usually contain seven wire strand which has better bond qualities and is therefore more desirable.

Their proposed equation for predicting crack width is

$$w = \frac{3 a_{cr} \varepsilon_m}{1 + 2\frac{a_{cr} - c_{min}}{h-x}} \qquad [2.10]$$

where:

- a_{cr} is the distance from the crack considered to the nearest longitudinal bar
- c_{min} is the minimum cover to the tension steel
- h is the depth of the section
- x is the depth to the neutral axis

ε_m, the average strain at the level under consideration, allowing for tension stiffening is calculated from:

$$\varepsilon_m = \varepsilon_1 - \frac{b(h-x)(a'-x)}{3E_s(A_s+A_{ps})(d-x)} \qquad [2.11]$$

where:

- b is the width of the section
- a' is the distance from the compression face to the point at which the crack width is being calculated
- d is the effective depth to the centroid of the total area of tensile steel
- E_s is the elastic modulus of the unprestressed steel
- A_s is the area of the unprestressed steel
- A_{ps} is the area of the prestressed steel

and ε_1, the strain of the fully cracked section at the level under consideration, is calculated from:

$$\varepsilon_1 = \frac{M}{\frac{1}{2}E_c I_c} x_1 \qquad [2.12]$$

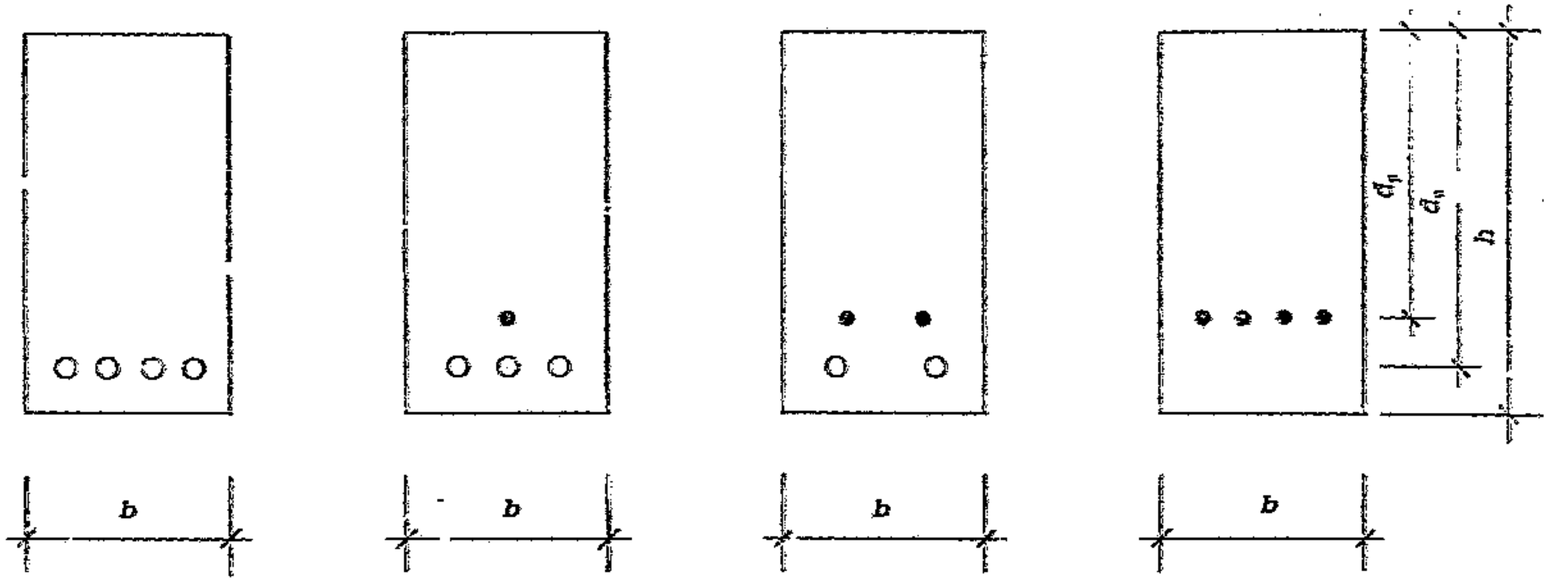

Figure 4.1(c) Sections of the test beams from series C (pretensioned strands and deformed bars)

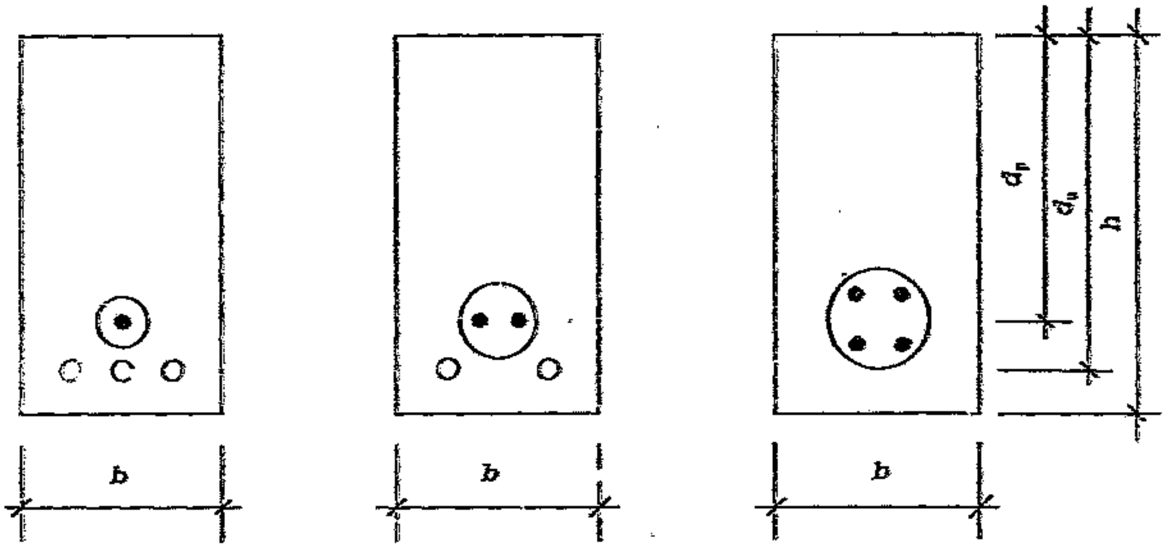

Figure 4.1(b) Sections of the test beams from series B (post tensioned unbonded strands and deformed bars)

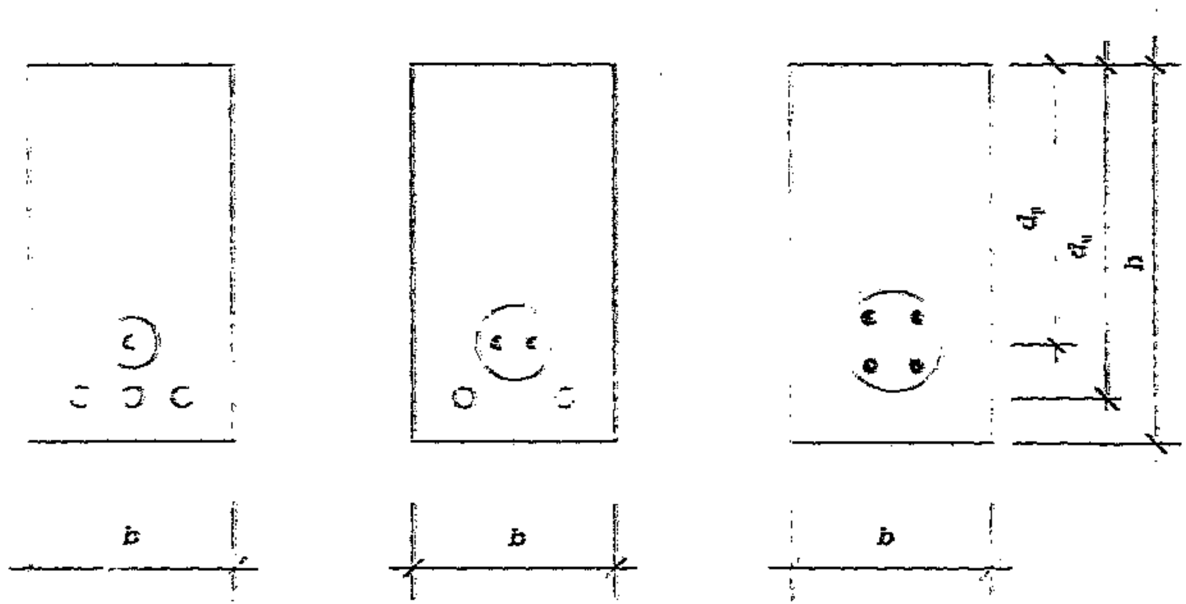

Figure 4.1(a) Sections of the test beams from series A (post tensioned bonded strands and deformed bars)

Table 4.1 Beam properties at the time of testing (continued)

Beam	b (mm)	h (mm)	d_s (mm)	d_p (mm)	A_s (mm²)	A_{ps} (mm²)	P_e (kN)	f_{cu} (MPa)
D2#2	161	305	274	228,5	226	74,84	107,4	48,8
D3#1	161	310	-	228,6	-	149,68	201,9	46,7
D3#2					-	149,68	198,1	43,4

Note: Beam B3#1 failed upon application of the prestress during manufacture

Table 4.1 Beam properties at the time of testing (continued)

Beam	b (mm)	h (mm)	d_s (mm)	d_p (mm)	A_s (mm^2)	A_{ps} (mm^2)	P_e (kN)	f_{cu} (MPa)
C1#1	160,5	302	273	–	452	–	–	57,3
C1#2	161	308	268	–	452	–	–	57,5
C2#1	160	307,5	278	226,5	339	37,42	26,0	54,8
C2#2	161	304	272	228	339	37,42	47,0	54,3
C3#1	161	309	271	226	226	74,84	99,5	41,0
C3#2	161	308	278	225	226	74,84	91,3	44,8
C4#1	161	309	–	224	–	149,68	176,9	44,1
C4#2	160	309	–	229	–	149,68	181,2	44,1
D1#1	161	307	266	229	339	37,42	47,3	54,8
D1#2	160	304	278	228	339	37,42	47,0	54,5
D2#1	159	305	276	227	226	74,84	97,0	63,1

Table 4.1 Beam properties at the time of testing

Beam	b (mm)	h (mm)	d_s (mm)	d_p (mm)	A_s (mm^2)	A_{ps} (mm^2)	P_c (kN)	f_{cu} (MPa)
A1#1	162	308	278	226	339	37,42	58,7	49,5
A1#2	162	309	274	233	339	37,42	55,8	49,9
A2#1	166	301	268	227,5	226	74,84	111,5	49,5
A2#2	172	303	271	228,75	226	74,84	98,3	49,5
A3#1	168,5	301	–	229,25	–	149,68	166,7	49,5
A3#2	173	302	–	230,25	–	149,68	158,6	49,9
B1#1	170,5	303	267	229	339	37,42	43,5	49,9
B1#2	164	303	267	226	339	37,42	54,5	50,0
B2#1	163	302	264	220	226	74,84	93,7	49,9
B2#2	166	303	256	225,5	226	74,84	90,0	50,0
B3#2	161	309	–	237,5	–	149,68	167,8	50,0

4 BEAMS USED IN THE RESEARCH

4.1 Design of Test Beams

In total, 28 beams were manufactured for testing in the laboratory and they ranged from reinforced concrete beams to fully prestressed concrete beams.

Four series of beams were designed, each series using different types of prestressed steel. Series A, B and C used 7,94 mm diameter seven wire strand while series D used 5 mm diameter smooth wire. Series A was post tensioned and grouted, series B was post tensioned and ungrouted while series C and D were pretensioned. Companion beams were provided in order that greater reliability could be obtained from the results. All beams were designed to have approximately equal ultimate moments of resistance.

The beam sections were rectangular, originally designed to be $b = 160$ mm x $h = 300$ mm, with the prestressed steel centroid at a depth of $d_p = 224$ mm and the unprestressed steel at $d_s = 265$ mm. As may be expected, variations occurred in the manufacturing process mainly due to the fact that the shuttering was not all exactly the same. These dimensions were chosen because similar dimensions were used by a number of researchers, for example, Tansi et al[15], Bennett and Chandrasekhar[10] and Bennett Veerasubramanian[5]. Different sections were not included in the research since Bennett and Veerasubramanian[5] concluded that they had no measurable influence on crack width. The beam properties at the time of testing are shown in Table 4.1, while the section drawings are shown in Figure 4.1(a) to Figure 4.1(d).

control crack width and is in general use by many practising design engineers due to its inclusion in the abovementioned codes. It was also decided that the equation by Suri & Dilger[20] should be improved upon since it is of very similar nature to the one found in ACI 318-83[18] and CAN3-A23.3-M84[19].

The objective of this research would thus be:

(a) To develop a variable "cracking factor" based on the percentage combination of prestressed and unprestressed steel. Such a factor does not yet exist.

(b) To improve on existing cracking formulae with regard to the influence of the type and application of prestressing.

Beams were chosen as the type of flexural member to be tested since they are common, particularly in bridge design where partial prestressing has found favour and also because they would be the easiest both to test and to manufacture.

(3) incremental steel stress (in the prestressed or unprestressed steel)
(4) the effective area of tensile concrete per bar or the area of concrete below the neutral axis
(5) a variable "cracking factor" whose value would be determined by the percentage combination of prestressed and unprestressed steel used.
(6) a factor accounting for the type of prestressed steel used.

At this point, three equations appear to include the majority of these parameters:

(1) ACI 318-83[18] and CAN3-A23.3-M84[19]
(2) Suri and Dilger[20]
(3) Nawy & Huang[21] and Nawy & Chiang[22]

The first two equations have the advantage of having a wide range of suggested values for their cracking factors and Scholz[14] has already focused on their performances, comparing their predicted crack widths to the measured values from the tests by Tansi et al[15]. Ref 5 also recommends both the equations by Nawy & Huang[21] and Nawy & Chiang[22] and those found in CP 110[17], BS 8110[26], SABS 0100[27] and BS 5400[28]. As commented on before, the British codes' approach requires much more effort in calculating crack width than the majority of other equations and hence is probably avoided by the majority of design engineers. The equations by Nawy & Huang[21] and Nawy & Chiang[22] are more than likely not particularly well known among practising engineers since they do not appear in any codes of practice.

Therefore it was decided to focus on the development of the equation found in ACI 318-83[18] and CAN3-A23.3-M84[19] since it contains the most important parameters that both the prestressed and unprestressed steel present

(4) obviously scatter can arise from normal experimental error and differences in workmanship between various tests

(5) some researchers, for example Suri & Dilger[20] and Meier & Gergely[36], based their work on a range of different tests, done by different researchers over a number of years. It would be preferable if variable factors such as they have suggested could be derived from tests performed at one time, that would be subject to the same controlling conditions during manufacture and testing.

3.2 Detailed Aims of the Research

Due to the wide spectrum of equations and recommendations found in the various codes of practice and previous research, there appears to be no method at present that can be considered exactly correct. Ref 5 noted Bachmann's suggestion[39] of replacing values calculated by these equations by sound detailing of the unprestressed steel. However, in certain cases like particularly corrosive envirc ments, or where large cracks could have a harmful effect on finishes, it is obvious that there is a need for calculating crack width in some way.

From the research discussed in sections 2.2.1 to 2.2.4, one can conclude that the ideal equation for predicting crack width should contain all the major controlling parameters:

(1) cover
(2) total steel area

For example, they found that under full live load, the predicted crack width by Bennett and Veerasubramanian[25] is about eight times the value from Nawy and Pontyondy[34] and more than three times that given by the equations of Nawy and Huang[21] and the non repetitive load equation of the CEB/FIP 1970 recommendations[32]. The results given by the repetitive load equation of the CEB/FIP 1970 recommendations[32] and the equations of Gergely & Lutz[13], Bennett & Chandrasekhar[30] and the CEB/FIP 1978 recommendations[33] were quite similar, although higher than the results of Nawy & Huang[21]. This large scatter of results can possibly be attributed to the following:

(1) some of the researchers, for example Bennett & Chandrasekhar[30] and Bennett & Dave[31], used unprestressed steel and types of prestressing that are not in common use. For example it is doubtful whether the results from beams with post tensioned grouted wires can be extended to other types of prestressing, due to different bond characteristics

(2) some of the equations, like those by Bennett & Chandrasekhar[30] and Bennett & Veerasubramanian[25] do not include the area if steel, which influences the steel stress which in turn is one of the controlling factors of the crack width

(3) some of the equations only consider the characteristics of the unprestressed steel. While it plays a major part in distributing cracks and governing their width, the characteristics of both the prestressed and unprestressed steel must be taken into account, as observed by Bennett & Chandrasekhar[30] and Suri & Dilger[20]. Hence the ideal equation for predicting crack width should include a variable that accounts for the type of

Naaman and Siriaksorn[37] compared the values of crack width given by various equations for a hypothetical T section (Figure 3.1(a)). They plotted the results as shown in Figure 3.1(b) and it can be seen that there are large differences depending on the equation used.

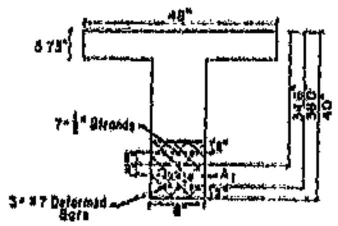

Figure 3.1 (a) idealised section and assumed steel arrangement for Naaman and Siriaksorn[37]

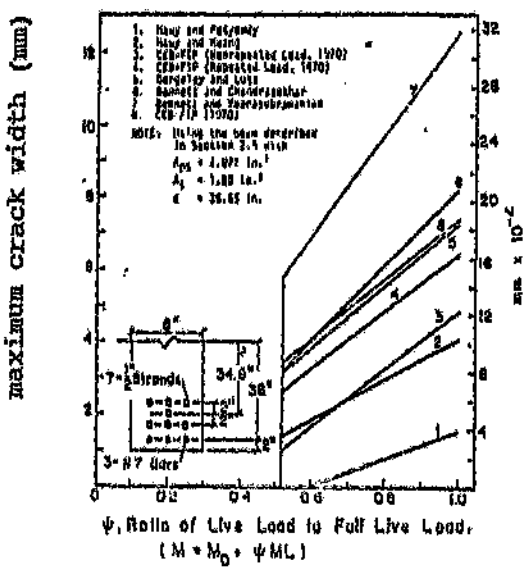

Figure 3.1 (b) comparison of maximum crack widths predicted by different equations for Naaman and Siriaksorn[37]

then grouted, with series B being left ungrouted. The length of each side of the beams were measured as for the pretensioned beams, in order that the prestress would be known at the time of the test.

4.3.3 Stressing of the steel

Using the load-extension curves from Figure 4.2 that had been supplied by the manufacturers, the required extension was found that corresponded to the desired load. Each strand was stressed to $0{,}8f_{pu}$ in order to compensate the loss of anchorage slip, but in some cases the stress was more than $0{,}8f_{pu}$, while in other cases it was less. When the 5 mm diameter wires were being stressed, the wire was simply inserted into the jack, and once stressing was finished, the jack automatically "locked off" or anchored the steel with the barrels and wedges. Due to the 7,94 mm diameter strand not being a common size in South Africa, there were no "jaws" available for Concor's type of jack. Therefore, the strand was inserted through the jack and a barrel and wedge was placed at the back of it. Once the stressing was finished, the steel was anchored "manually" by hammering a piece near the front of the jack, which in turn pushed the wedges firmly in to the barrel.

The prestresses in the test beams at the time of testing are shown in Table 4.1 above.

4.3.1 Manufacture of the pretensioned beams

The pretensioned beams were manufactured singly in an 8,1 m bed. Each wire or strand was stressed separately to the required extension (calculated using the stress-strain curves of Figure 4.2), and was anchored by barrels and wedges which butted against steel anchorage plates at either end of the bed. The concrete was then poured and compacted with poker vibrators, along with three 150 mm cubes per beam. The concrete was steam cured, which greatly reduces curing time, and once it had gained sufficient compressive strength the prestressed steel was cut, so that the anchorages were released. Once the steel had been cut, hence transferring the prestress to the beam, the length of the beam was measured at the level of the centroid of the prestressing steel. This would enable the prestress force at the time of the test to be determined accurately, using the assumption that any change in the length of the beam would correspond exactly to a change in length in the steel.

4.3.2 Manufacture of the post tensioned beams

The post tensioned beams were manufactured in three batches of four beams each. Once the unprestressed steel and the duct positioning had been checked, the concrete was poured and compacted with poker vibrators, as for the pretensioned beams, along with three 150 mm cubes. The beams were cured using conventional methods. The duct was standard mild steel ducting and is used in most post tensioned applications. Once the concrete had gained sufficient strength, the beams were lifted from their shutters and stressed. Each strand was tensioned separately to the required extension, and was anchored by barrels and wedges bearing against 10 mm thick steel plates butting against the end of the beams. Series A was

Table 4.4 Values of cube strength and modulus of elasticity (continued)

Beam	f_{cu} (MPa)	E_{c1} (GPa)	E_{c2} (GPa)
D1#2	54,5	48,5	35,3
D2#1	63,1	52,4	36,6
D2#2	48,8	46,0	33,7
D3#1	46,7	45,0	33,0
D3#2	43,4	43,5	32,0

Note: E_{c1} denotes the value of elastic modulus calculated by equation [3.1] as found in properties of Aggregates in Concrete (Part 1)[40], while E_{c2} denotes the value as found in Table 1 of CP 110[17].

4.2.3 Ducting

The ducting was manufactured from 0,45 mm thick mild steel by Armco Superlite and is used in most post tensioned applications. Three diameters were used: 40 mm (beam type 1), 60 mm (beam type 2) and 80 mm (beam type 3).

4.3 Manufacture of the Beams

All 28 beams were manufactured in a precast yard. It was decided to manufacture two beams of each type in order that greater reliability could be obtained from the test results. Two extra fully prestressed beams from Series D were manufactured since there was excessive slip during testing of the first two of that type.

Table 4.4 Values of concrete cube strength and modulus of elasticity

Beam	f_{cu} (MPa)	E_{c1} (GPa)	E_{c2} (GPa)
A1#1	49,5	46,3	33,9
A1#2	49,9	46,5	34,0
A2#1	49,5	46,3	33,9
A2#2	49,5	46,3	33,9
A3#1	49,5	46,3	33,9
A3#2	49,9	46,5	34,0
B1#1	49,9	46,5	34,0
B1#2	50,0	46,5	34,0
B2#1	50,0	46,5	34,0
B2#2	50,0	46,5	34,0
B3#1	50,0	46,5	34,0
B3#2	50,0	46,5	34,0
C1#1	57,3	46,5	35,1
C1#2	57,5	49,9	35,5
C2#1	54,8	48,7	35,0
C2#2	54,3	48,4	34,9
C3#1	41,0	42,3	31,3
C3#2	44,8	44,2	32,4
C4#1	44,1	43,8	32,2
C4#2	44,4	44,0	32,3
D1#1	54,8	48,7	35,0

be determined otherwise. Two options were available:

(1) Use of the formula

$$E_c = k_0 + \alpha f_{cu} \qquad [3.1]$$

from Properties of Aggregates in Concrete (Part 1)[40]. This formula is a result of research performed on South African aggregates.

(2) Table 1 of CP 110[17]

The elastic moduli from both sources were used in this calculation for comparative purposes, and it was found that there was very little difference in the resulting calculated neutral axis depth and hence the values of the incremental steel stress, f_s or f_{ps}, and the values of k_w. It was subsequently decided that the elastic modulus as calculated by reference 40 would be most applicable to South African conditions. However, a designer is more likely to use Table 1 of CP 110[17], and this is acceptable since there would be no marked difference in the values of neutral axis obtained. As shall be shown in section 6.2.3, the experimental value of the concrete elastic modulus is not essential for calculation of the neutral axis depth, the incremental steel stress or the cracking factor, k_w, in this investigation.

4.2.2 Concrete

The concrete compressive strength used in the original design was 40 MPa at 28 days, which enabled the beams to be safely prestressed without the risk of end zone failure. The concrete mix used in the test beams is shown in Table 4.3.

Table 4.3 Mix proportions for 1 m^3 of concrete

Component	Quantity
cement (OPC)	360 kg
sand	811 kg
stone	1258 kg
water	137 ℓ
superplasticizer	1 ℓ/m^3 concrete

This resulted in a cement:water ratio of 2,63. The cement used was OPC while the stone was 9,5 mm Sterkfontein dolomite. The characteristic cube strength, f_{cu}, for each beam was determined by crushing the three 150 mm cubes that were supplied with each beam. Each cube was kept in a curing tank and was then tested in a wet condition, using a loading rate of 15 MPa/minute, as specified by SABS 0100[27]. The characteristic cube strengths for each beam are shown in Table 4.1, which shows the beam properties at the time of testing.

The elastic modulus of concrete, E_c, could be used to determine the neutral axis (and hence the incremental steel stress and the cracking factor, k_w) in the test beams by calculation. Unfortunately no prisms were cast and hence the elastic modulus of the concrete, E_c, had to

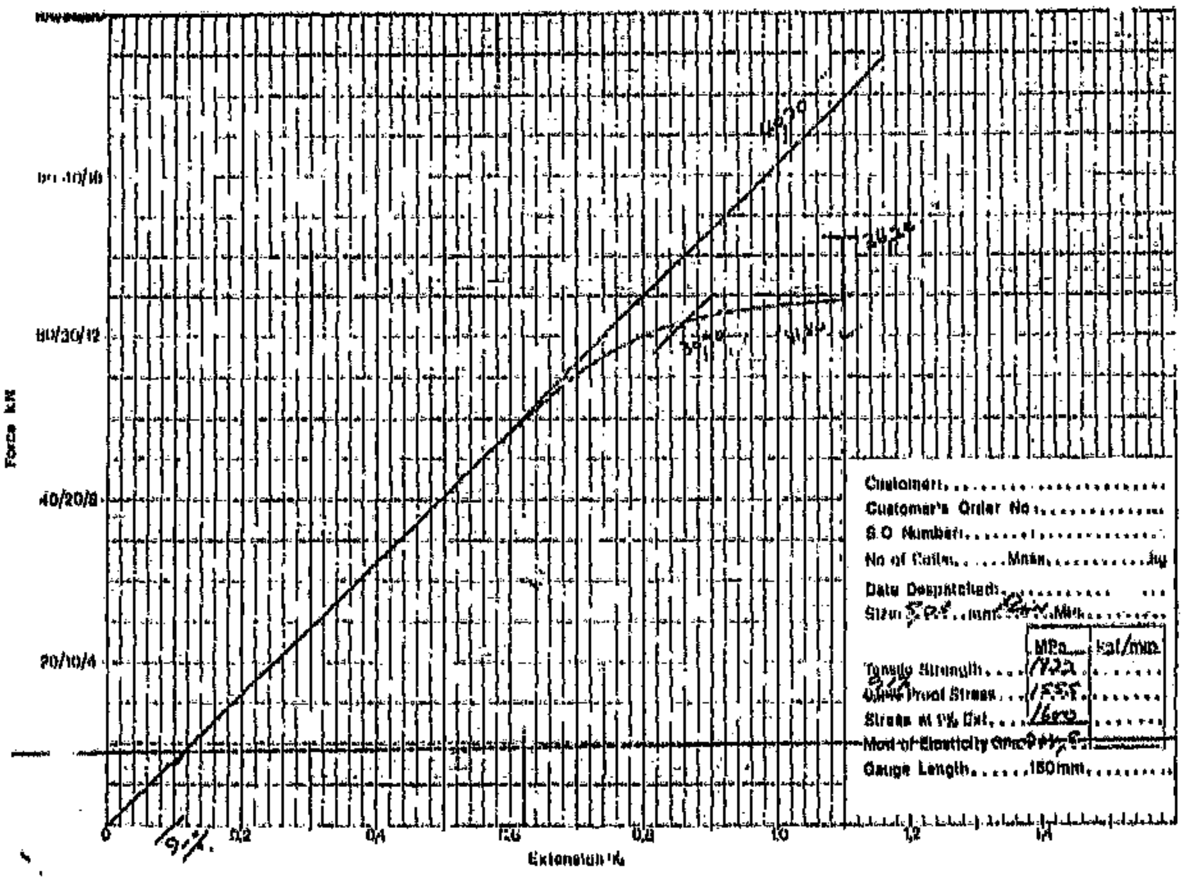

Figure 4.4(b) Typical stress-strain curve for smooth wire type prestressed steel

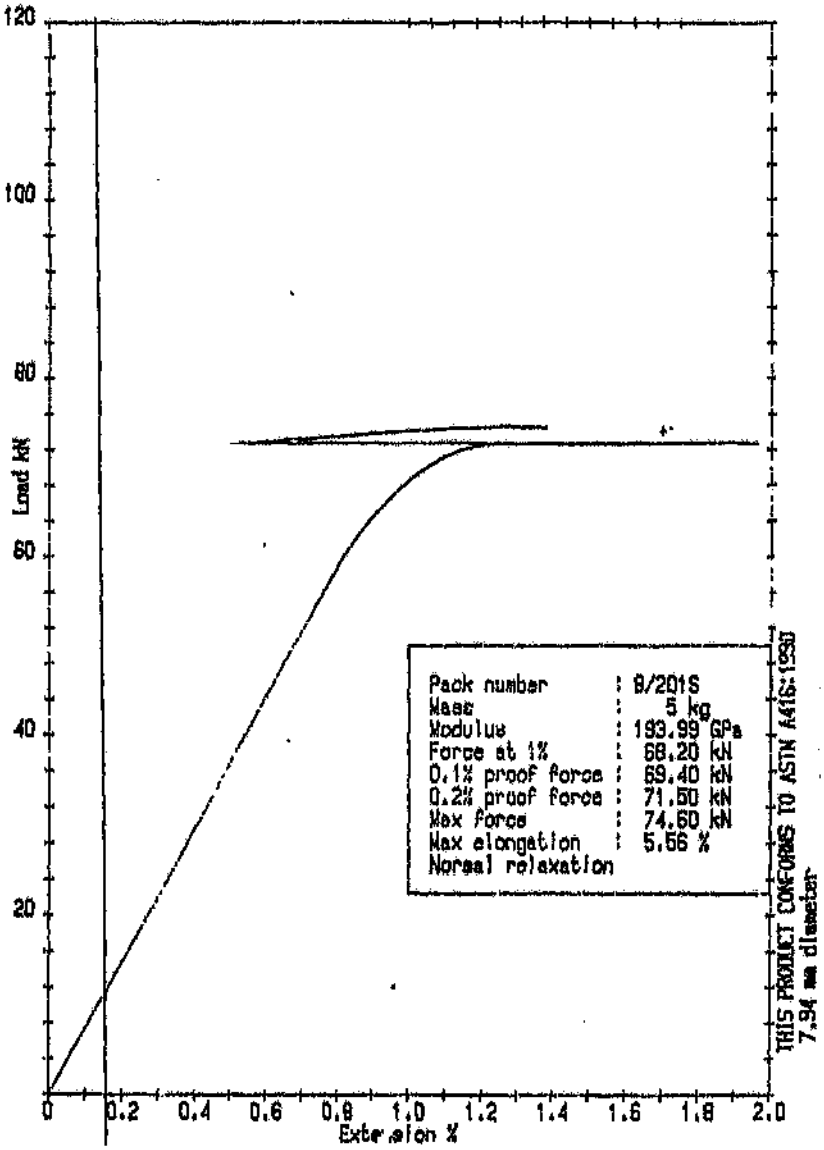

Figure 4.4(a) Typical stress-strain curve for 7 wire strand type prestressed steel

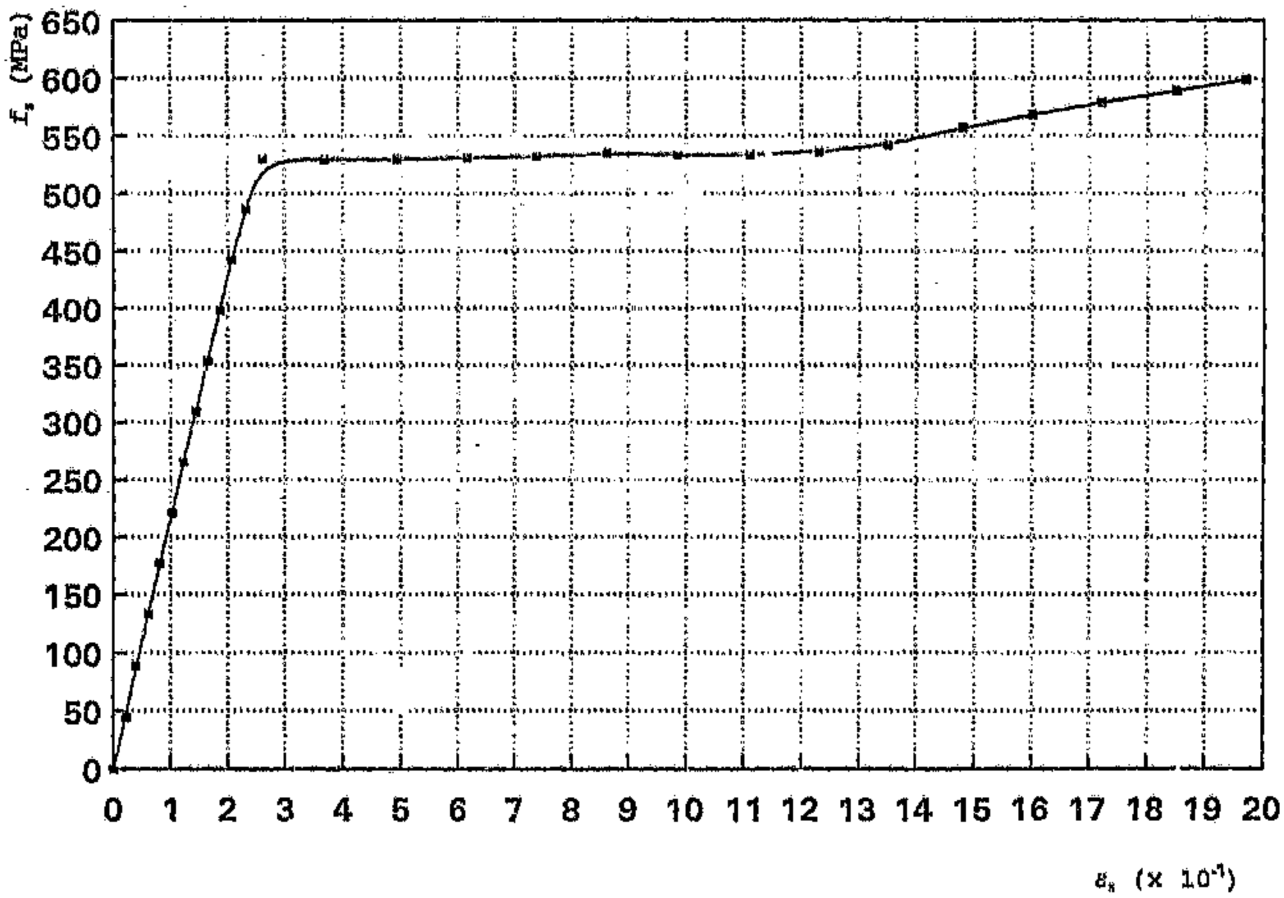

Figure 4.3 Typical stress-strain curve for non prestressed steel

choosing this diameter are that the beams would then correspond with other research, for example Tansi et al[15] and Bennett & Chandrasekhar[30] and Bennett & Veerasubramanian[25], while it gave the desired "step up" in prestress from the partially prestressed beam with lowest prestress to the next beam up and finally to the fully prestressed beam.

- stress relieved 5 mm diameter smooth wire

Their properties are shown below in Table 4.2, while typical stress-strain curves are shown below in Figure 4.3 and Figure 4.4. The remaining stress-strain curves may be found in Appendix A. Note that the modulus of elasticity for all three types of steel is an average value from three different specimens, hence the three stress-strain curves for the unprestressed steel. However, only one curve appears for the two types of prestressed steel since the manufacturer had already averaged the results from the three specimens.

Table 4.2 Properties of prestressed and unprestressed steel.

Type of steel	f_{pu} or f_y (MPa)	E_s (GPa)
7,94 mm diameter 7 wire strand	2000	194
5 mm diameter smooth wire	1822	204,8
12 mm diameter high yield deformed bar	477	210,9

The beams spanned 3,3 m and had 200 mm overhangs past the centrelines of the supports in order that the pretensioned members had sufficient transmission length to develop the required prestress in the beams. Shear reinforcing can initiate cracking in a reinforced concrete member, and hence the test beams were loaded with two point loads situated 800 mm apart and 1250 mm from the centrelines of the respective supports. This loading arrangement provided a pure moment region in the 800 mm distance between the two point loads and therefore required no links. All the crack width measurements were made in this region. A schematic diagram of a typical test setup is shown below in Figure 4.2.

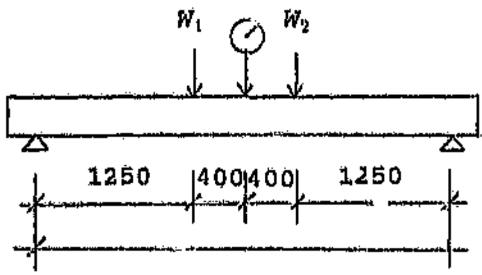

Figure 4.2 Schematic diagram of a typical test setup

4.2 Materials

4.2.1 Tensile steel

The unprestressed steel was high yield deformed bars, while two types of prestressed steel were used:

- normal relaxation 7,94 mm diameter seven wire strand. Although this diameter of strand is not readily available in South Africa, it is manufactured for export markets. The reasons for

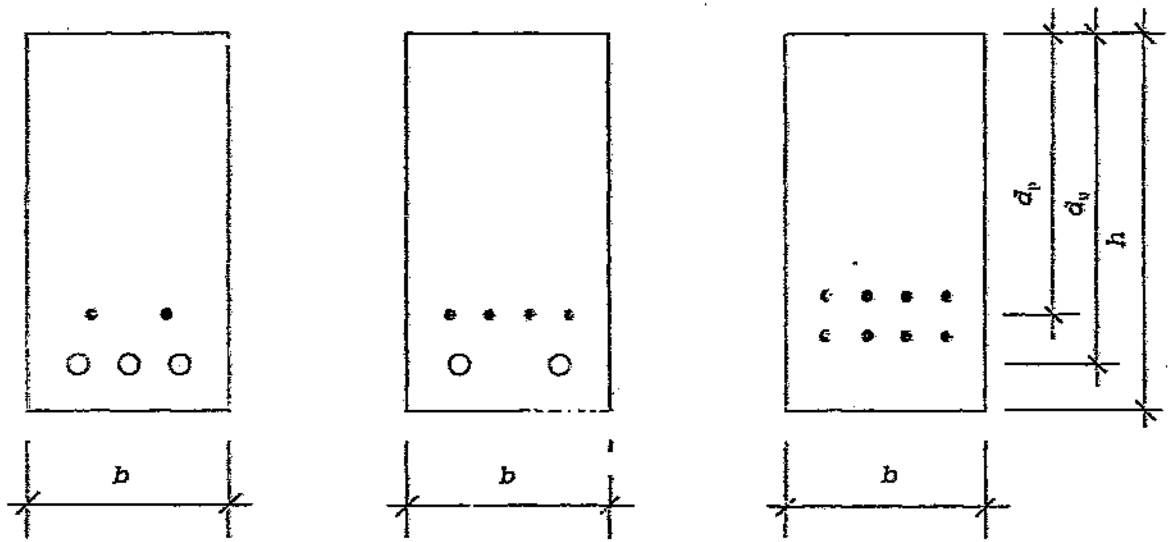

Figure 4.1(d) Sections of the test beams from series D (pretensioned wires and deformed bars)

(4) During the elastic range of the beams behaviour, the central load increment was 10 kN, with demec and deflection readings being taken for every increment. Once the beam had entered the plastic region, it was loaded in increments of 5 mm deflection with the corresponding load being noted. No demec readings were taken at these loads since they were out of the serviceability range. The beams were loaded to a maximum deflection of 50 mm, since this was the maximum extension of the jack. Some beams failed prior to the maximum de lection and hence the ultimate load was known, but for the beams that hadn't failed at or before 50 mm deflection, it was obvious that the failure load had been close, inspecting the resulting load-deflection curves.

after the test. Hence initial readings were also taken from the Huggenberger unit. The initial position of the prestressed steel was marked in order that slip could be monitored, usually by putting a mark 100 mm from the end of the beam on the steel.

(2) The jack was pumped up in increments of 10kN, using the digital reading (which approximately translated to 5 kN at each load point on the beam). The load was then left to settle for approximately a minute. This was necessary because some of the hydraulic fluid would flow backwards from the jack, back to the pump hence releasing some of the hydraulic pressure and therefore reducing the applied load. This is the opposite to what would happen to an element in real structure, ie. the load would remain constant while the element would creep. The two load cell readings for each load point were then taken. A check was made for slip of the prestressed steel by measuring the 100 mm distance that had been marked on the prestressed steel before the test and checking that it had remained constant. Deflection and demec readings were subsequently taken. Since there were six regions of demec targets, each with seven readings to be made, 42 readings per load increment were made. During the time of taking the demec readings, the load was maintained at a constant value.

(3) The cracks in the central pure moment region were then marked on the side of the beam. A mark was then drawn at the top of the crack after each increment indicating the load at which the crack had attained that particular height.

cylinder and the mark on the beam (see Figure 5.2). The beams were checked to be approximately centrally placed in the transverse direction, between the two sets of opposing angles of each column.

Once the test beam had been satisfactorily placed in position, the loading system was connected up. The two steel half cylinders were placed at the load points, 800 mm apart and 1250 mm from each support. The two threaded rods were then held vertically and the bar was placed on top with the two threaded rods passing through the holes drilled in each of its ends. A nut was then threaded on to each of the rods, holding the whole system together.

When the loading system had been successfully connected, it was then brought in to position for the test. The steel plate on top of the jack and the central load cell was almost brought into contact with the head of the column that provided the reaction point. This was done by tightening the nuts on the rods, hence lifting the whole system. While doing this, both the primary steel beam and the two secondary ones were checked to be perfectly level. Once this procedure had been performed, the beam was ready for testing.

5.2 Test Procedure

The beams were subjected to short term test, each test taking approximately 3½ to 4 hours to perform. The procedure took place as follows:

(1) At zero load, initial deflection and demec readings were taken. The central load reading was displayed in kN while the reading obtained from the Huggenberger unit for the other two load cells was given in divisions and had to be converted into kN

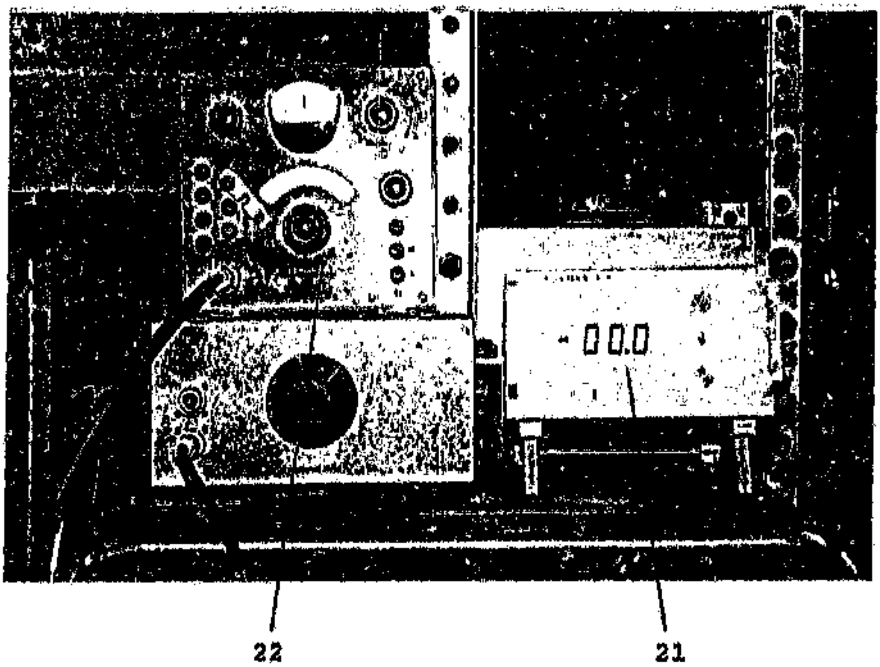

21 digital readout
22 Huggenberger device

Figure 5.7 Readouts for applied loads

5.1.4 Setting the equipment up

All of the test beams were supplied with two lifting points, each situated on top of the beam at the position of the centreline of the support. A crane lowered the beams in between the two sets of opposing angles of each column, the centreline of the beam being approximately lined up with the centreline of the centre column. The centrelines were then lined up exactly, by pushing the beam in the required direction, using the rolling action of the joints. The supports were then tapped into place, lining up the centreline marked on the steel half on the two joints connecting the primary steel beam and the two secondary steel beams of the loading system (see Figure 5.6 overleaf). Also shown is the jack (18) and the tube containing the hydraulic fluid coming from the pump. The central load cell was connected to a digital read out (21) while the other two were connected to a Huggenberger device (22), enabling both readings to be taken off one device (see Figure 5.7 overleaf).

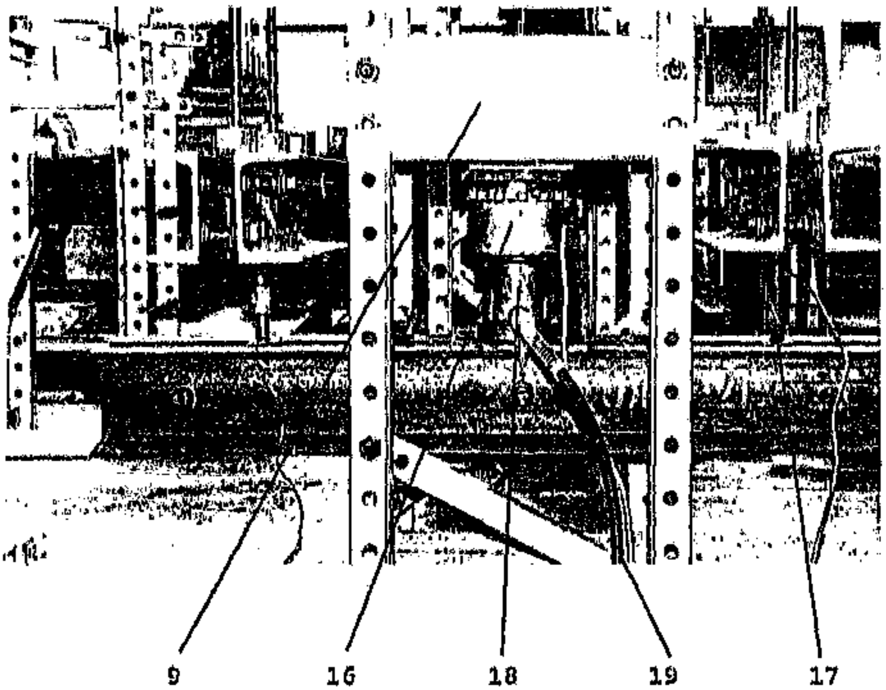

9 central column head
16 primary load cell
17 secondary load cell
18 jack
19 tube from the pump

Figure 5.6 Load cells

5.1.3 Equipment used for measurement of the data

Only three parameters were measured:

- concrete strains
- deflection
- applied load

The slip of the prestressed steel was also monitored although no measurements were recorded since in general, once the prestressed steel had slipped, the beam entered the plastic region of behaviour a short time afterwards.

(1) Concrete strains

The concrete strains were measured with a 203 mm (8") demountable demec gauge. Six regions were measured on the sides of the beams, three on the front and three on the back. These six regions ensured that at least one crack could be measured on each side (if the beam cracked). The beams were marked and demec targets were glued on at 10 mm, 40 mm, 90 mm, 200 mm, 224 mm and 275 mm from the top edge of the beam for the beams in series A and B. In series C and D, the strains were measured at 10 mm, 40 mm, 90 mm, 16L mm, 200 mm, 224 mm and 265 mm from the top edge of the beam. The strains are listed in Appendix C.

(2) Deflection

Deflection was simply measured at each load increment at midspan by a 50 mm dial gauge. Readings were taken to two decimal places.

(3) Applied load

Load cells were positioned on top of the jack (16), and

This facilitated setting the system up for a test, as shall be described in section 5.1.4. Each of the secondary beams (11) had two threaded rods (13) connected to them. These rods transmitted the applied force to a bar (14) which then transferred the load to a steel half cylinder (15), which in turn applied the load to the test beam (2) as shown in Figure 5.5. The extension of the jack was applied by hydraulic pressure from the pump.

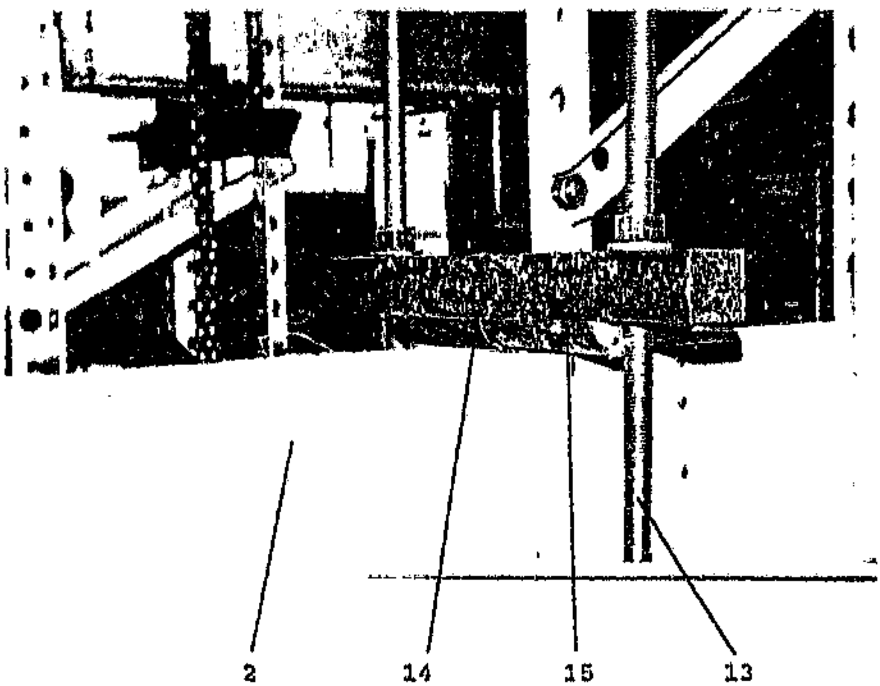

2 test beam
13 threaded rod
14 bar
15 steel half cylinder

Figure 5.5 Transmission of force to the test beam

The central column head (9) provided a reaction point for the jack to push the primary double channel section steel beam (10) downwards. The downward action of the primary steel beam pulls the whole upper assembly down and hence puts load on the test beam. The two secondary steel beams (11) were each connected to the primary steel beam by a joint (12) that allowed the beams to move back and forth along their longitudinal axes (also see Figure 5.4).

11

12

10

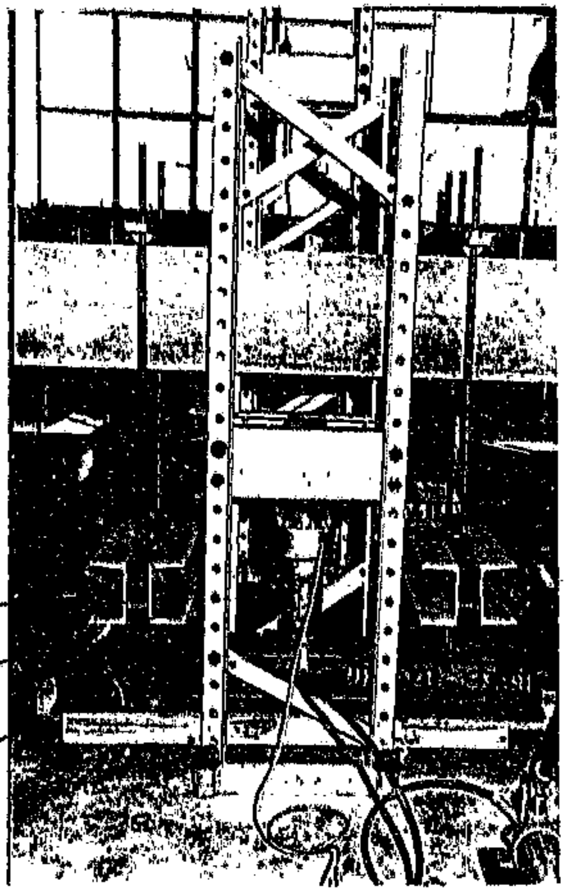

10 primary steel beam

11 secondary steel beam

12 joint

Figure 5.4 Primary and secondary steel beams

5.1.2 Loading system

The loading system, was possibly the most complicated component of the test equipment. Figure 5.3 shows the assembled system as used in the tests.

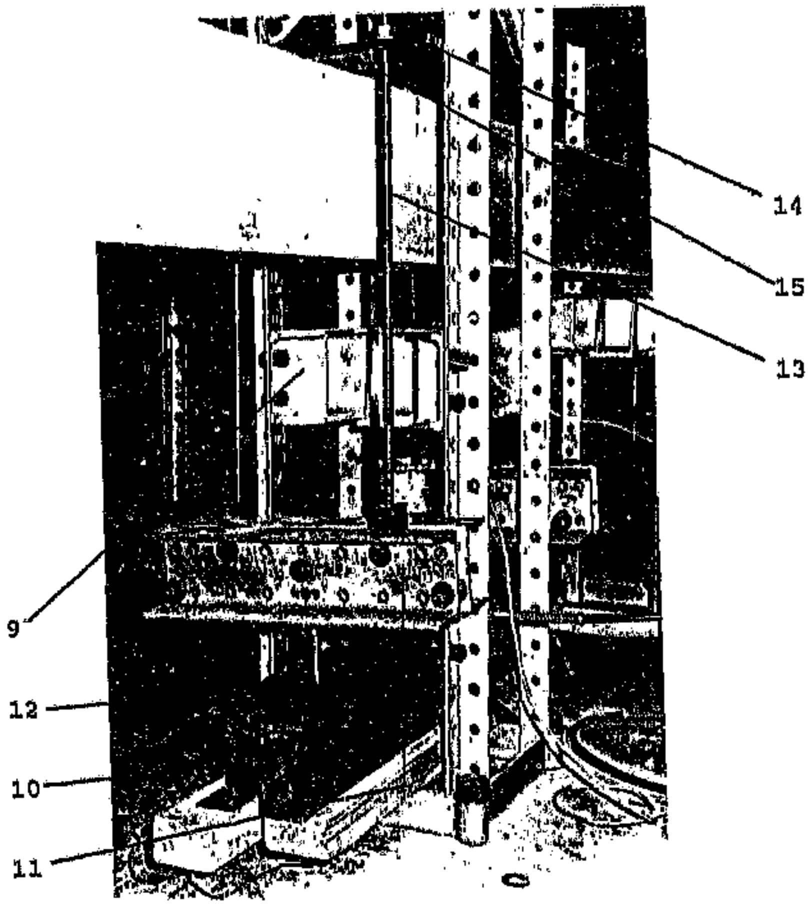

9 central column head
10 primary steel beam
11 secondary steel beam
12 joint
13 threaded rods
14 bar
15 steel half cylinder

Figure 5.3 Loading system

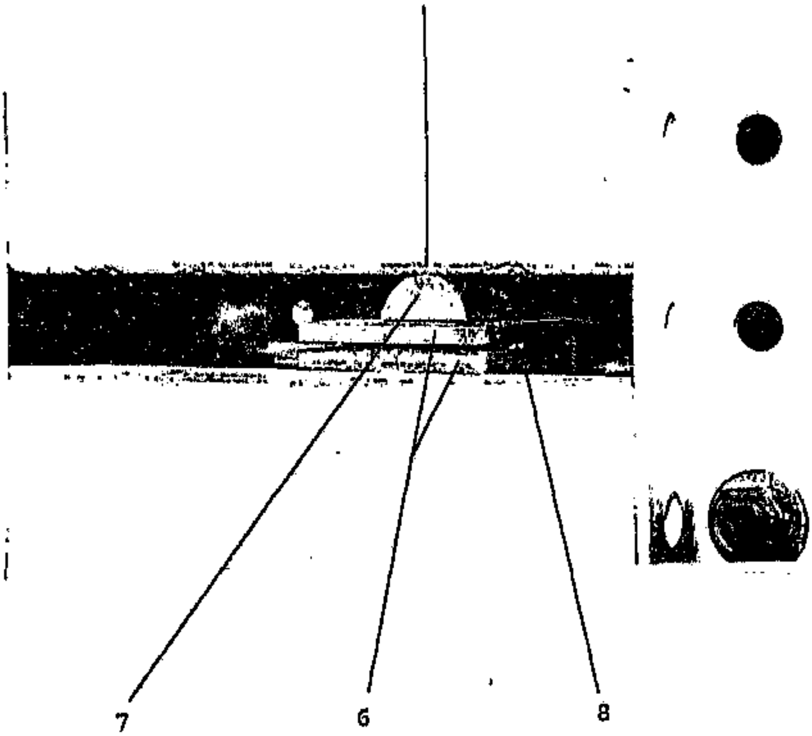

6 flat plates
7 half cylinder
8 roller bearings

Figure 5.2 Roller support

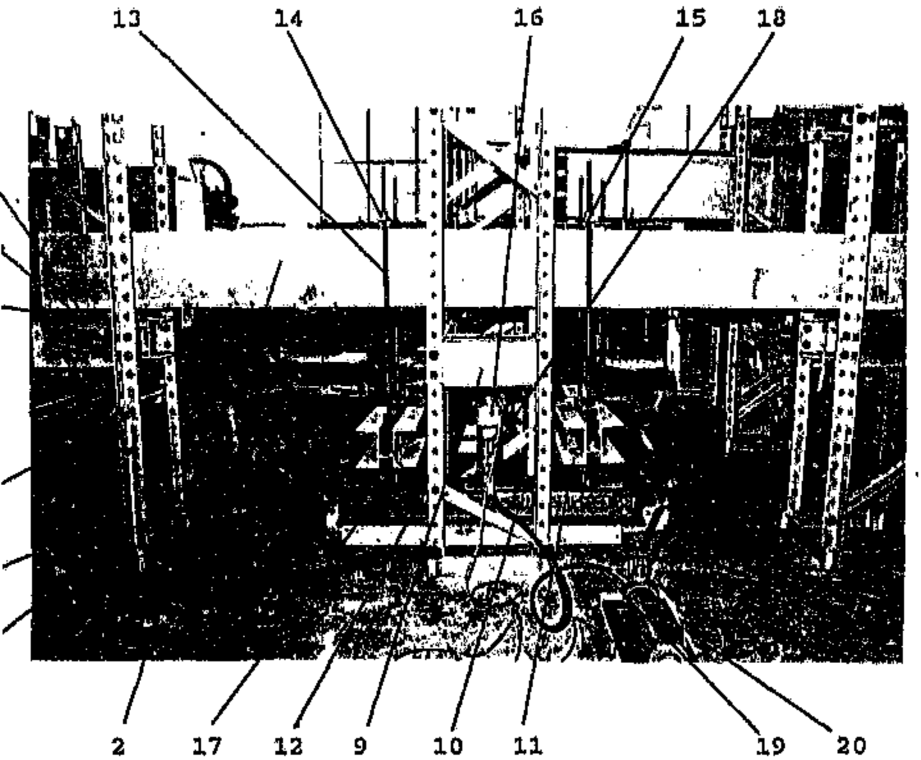

1	column assembly	11	secondary steel beam
2	test beam	12	joint
3	column base	13	threaded rods
4	steel angle section	14	bar
5	column head	15	steel half cylinder
6	flat plates	16	primary load cell
7	steel half cylinder	17	secondary load cell
8	roller bearings	18	jack
9	central column head	19	tube from the pump
10	Primary steel beam	20	pump

Figure 5.1 Test setup and loading arrangement

5 TEST PROGRAMME

This chapter covers a detailed description of the test equipment and the procedure used.

5.1 Test Equipment

All the beams were simply supported on a 3,3 m span and were loaded by two point loads 800 mm apart and 1250 mm from the centreline of each support, as depicted in Figure 5.1 overleaf.

5.1.1 Supports

The column assembly (1) provided support for the test beam (2) 200 mm from either end. Figure 5.1 shows that the column consisted of a base (3) placed on the floor, with four steel angle sections (4) welded vertically to each corner. Another steel member, referred to as the head (5), was then bolted at each of its corners to the angle sections. It was adjustable up and down since the angle members had holes drilled at approximately 75 mm centres along their whole length. The head then had a roller joint placed on top of it, on which the beam rested. The roller joint consisted of two flat plates (6) with a steel half cylinder on top, as shown in Figure 5.2 overleaf. Between the plates were roller bearings (8), providing the rolling action that was required from the support.

The value of the effective prestress at the time of testing was known, hence:

$$T_s + T_{ps} = T - P_e \qquad [6.6]$$

$$\therefore f_s A_s + f_{ps} A_{ps} = T - P_e \qquad [6.7]$$

$$\therefore \varepsilon_s E_s A_s + \varepsilon_{ps} E_{ps} A_{ps} = T - P_e \qquad [6.8]$$

From the known strain distribution shown in Figure 6.8 below, using similar triangles, a relationship between the strain in the prestressed steel and the strain in the unprestressed steel could be found:

$$\varepsilon_{ps} = \varepsilon_s \left(\frac{d_p - x}{d_u - x}\right) \qquad [6.9]$$

Hence the incremental strain in the unprestressed steel could be found:

$$\varepsilon_s = \frac{T - P_e}{E_s A_s + E_{ps} A_{ps} \left(\frac{d_p - x}{d_u - x}\right)} \qquad [6.10]$$

The stress in the unprestressed steel and both the strain and the stress in the prestressed steel could then be found by simple back substitution. A check to ensure that the resulting incremental steel strain was in the elastic region of the steel stress-strain strains measured in the test and the known stress-strain properties of the prestressed and unprestressed steel. Tansi et al[15] also show that a line of best fit can be plotted through the strains measured in the tests. The calculation proceeded as follows:

1. First, the neutral axis depth was interpolated from the concrete strain measurements in the compressive and uncracked tensile zones, using linear regression. Bennett and Chandrasekhar[30] use only the strains in the compressive zone, but when strains in the uncracked tensile zone were also included (as suggested by Tansi et al[15]), it was found that the correlation coefficient would be closer to 1.

2. Using moment equilibrium at the serviceability limit state, the external moment was equated to the total force exerted by the tensile steel, multiplied by the lever arm from the centroid of the concrete compression block to the centroid of the total area of tensile steel, as shown below, in equation [6.4]:

$$M = T(d-0,4x) \qquad [6.4]$$

   This enabled the tensile force exerted by the total area of tensile steel to be obtained.

3. The tensile force exerted by the total area of tensile steel was then expressed as below:

$$T = T_s + T_{ps} + P_e \qquad [6.5]$$

In order to calculate the crack widths, the strain at point A on the curve was subtracted from the strain corresponding to the service moment. Since strain is the change in length divided by the original length, the crack width was found by multiplying the change in strain by the original length of the demec gauge, 203 mm. The measured strains may be found in Appendix C.

6.2.3 Determination of the neutral axis depth, x, and the incremental steel stress, f_s or f_{ps}

The neutral axis depth is needed to calculate the incremental steel stress, either f_s or f_{ps}, for both the equations by Suri and Dilger[20] and the equation found in ACI 318-83[18] and CAN3-A23.3-M84[19]. It is also needed in the equation by Suri and Dilger[20] in order that A_t, the area of concrete below the neutral axis may be calculated.

Suri & Dilger[20] noted that steel stresses could not be obtained from strain measurements, either by using electrical strain gauges on the steel itself, or by member surface strain measurements in the cracked tensile zone because of the large longitudinal variation of stress in the vicinity of the cracks. The depth of the neutral axis and hence the incremental steel stress could then be calculated using two different methods:

(1) Experimental determination of the neutral axis depth and incremental steel stress

Bennett & Veerasubramanian[25], Bennett & Chandrasekhar[30] and Bennett & Dave[31] state that the neutral axis depth and hence the incremental steel stress can be obtained from a cracked section analysis at service, using the concrete compressive

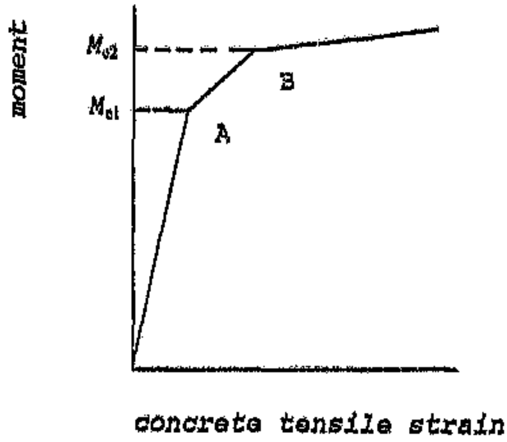

Figure 6.7 Typical curve of concrete tensile strain vs. applied moment

The plotted strain refers to the strain measured at the depth of the unprestressed steel for the reinforced and partially prestressed concrete beams and at the level of the prestressed steel for the fully prestressed beams. Zero applied moment corresponded to zero tensile strain over and above the point of decompression at the bottom extreme concrete fibre. As the moment increased, the tensile strain increased up to point A, where M_{c1}, the moment of first cracking had been reached and cracking had occured. Usually the crack pattern would have established itself fully at this point. The tensile strain would then carry on increasing at a faster rate, after cracking at point A. Sometimes when the crack pattern had not established itself fully after cracking first occured at point A, new cracks would then form again, indicated by point B and corresponding to the second cracking moment, M_{c2}, in Figure 6.7.

the load factor was taken as 1,5, that is, an average of the factors found in load case (1) of clause 2.3.3.1 of CP 110[17]. It was then decided to look at the load factors that other researchers had used, and it was found that they varied between 1,4 and 2,5, the majority of them being in the range 1,4 to 2,0. Therefore a factor of 1,5 seemed reasonable and it was eventually used, since it gave a service moment that was approximately 80% of the maximum elastic moment in most of the beams. However, in some beams the same load factor would give a service moment that was a smaller percentage of the maximum elastic moment and often the resulting values of k_w would be unacceptable due to the low values of incremental steel stress. Hence the service moment would then be increased to approximately 80% of the maximum elastic moment. As may be seen from the moment-deflection curves in Appendix B, some of the beams have a service moment greater than 80% of the maximum elastic moment, using a load factor of 1,5

6.2.2 Determination of crack width from the demec gauge readings

The recorded demec readings had to be converted to concrete strains. For each series, the initial demec reading, corresponding to zero applied moment, was subtracted from the moment corresponding to each increment. This value was then multiplied by the demec gauge factor (the value of strain per division). For each beam, a graph of concrete tensile strain vs applied moment was plotted, a typical curve being shown in Figure 6.7.

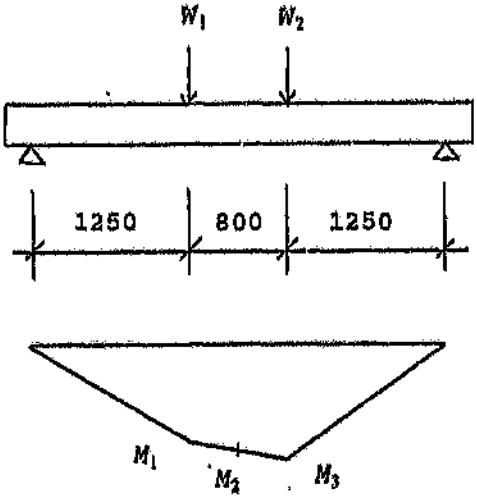

Figure 6.6 Calculation of applied moment

$$M_1 = 0,78W_1 + 0,47W_2 \qquad [6.1]$$

$$M_2 = 0,625W_1 + 0,625W_2 \qquad [6.2]$$

$$M_3 = 0,47W_1 + 0,78W_2 \qquad [6.3]$$

A moment-deflection curve was then plotted. As already mentioned in section 5.2, some of the beams did not fail before or at the maximum jack extension of 50mm. When the moment-deflection curves were inspected, it could be seen that those beams were very close to failure, and therefore it was assumed that the maximum moment on the curve was approximately the ultimate moment. (The moment-deflection curves may be found in Appendix B). The service moment could then be determined by dividing the ultimate moment by an appropriate load factor. Initially,

- determination of k_w
- analysis of the values of k_w

6.2.1 Determination of the service moment

Having obtained readings in divisions from the Huggenberger unit for the two load cells below the loading points, it was necessary to calculate the load in kN. This was easily done by subtracting the initial readings from the readings for each load increment, and then dividing by the cell factor (the number of divisions per kN). The value of each point load on the beam was then known and the moment could subsequently be calculated. The point loads were not exactly the same value, however, W_1 being greater than W_2, and hence the bending moments were calculated thus:

The behaviour of the relevant test beams from series B agreed with this theory, crack widths of 1,6 mm at the service load being obtained in the fully prestressed beam. This beam entered the plastic region of the moment -deflection curve (as may be seen in Appendix B) long before the corresponding fully prestressed beams from series A, C and D and failed well below its calculated ultimate moment. This is because at the section where the large crack forms, the neutral axis moves up rapidly due to the rapidly increasing crack width and crack height, hence making the concrete fail in compression. In prestressed concrete structures, crack widths of up to 0,4 mm are thopught to be safe[5]. These tests clearly demonstrate that cracking at service should not be allowed for unbonded solutions with little or no bonded steel and hence the results from Beam B3#2 have been omitted for this reason and also since no practical value of k_w would have been obtained.

The results from beams A2#2, A3#1, C4#1, D2#2, D3#1 and D3#2 have been omitted since excessively large crack widths and hence values of k_w were obtained. These beams have been discussed in section 6.2.4.

6.2 Processing the Test Data

As already mentioned, the aim of this research was to develop values for the variable cracking factors, k_w, as found in ACI 318-83[18], CAN3-A23.3-M84[19] and in the equation by Suri and Dilger[20]. The processing of the data can be divided into five sections:

- determination of the service moment
- determination of the crack widths
- determination of the the neutral axis depth, x, and the incremental steel stress, f_s or f_{ps}

When a prestressed concrete beam cracks, both the steel and the concrete carry the tensile stress at a crack. With fully prestressed post tensioned unbonded beams that contain no unprestressed steel, a small number of large cracks will form. This is because the unbonded prestressed steel is not in contact with the concrete and it is only the anchorages that transfer the prestress to the concrete. Therefore, when a crack forms, the unbonded prestressed steel elongates along its full length in order to carry the tensile stress over the crack. The crack will then open wider instead of new cracks being formed. This crack pattern can also be seen in a partially prestressed post tensioned unbonded beam that contains a low percenta·e of unprestressed steel, as shown in Figure 6.2. Figure 6.5 below shows the pattern for a fully prestressed unbonded beam. In a beam with bonded prestressed steel, the steel can only fully elongate close to the crack, hence keeping the crack width small, but leading to a pattern of numerous cracks.

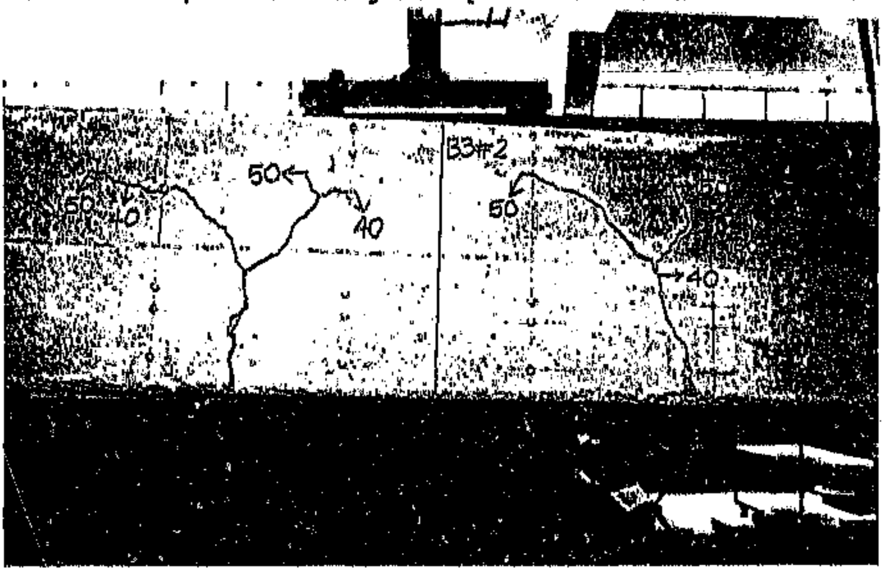

Figure 6.5 Crack pattern of the fully prestressed beam from series B (post tensioned unbonded strands)

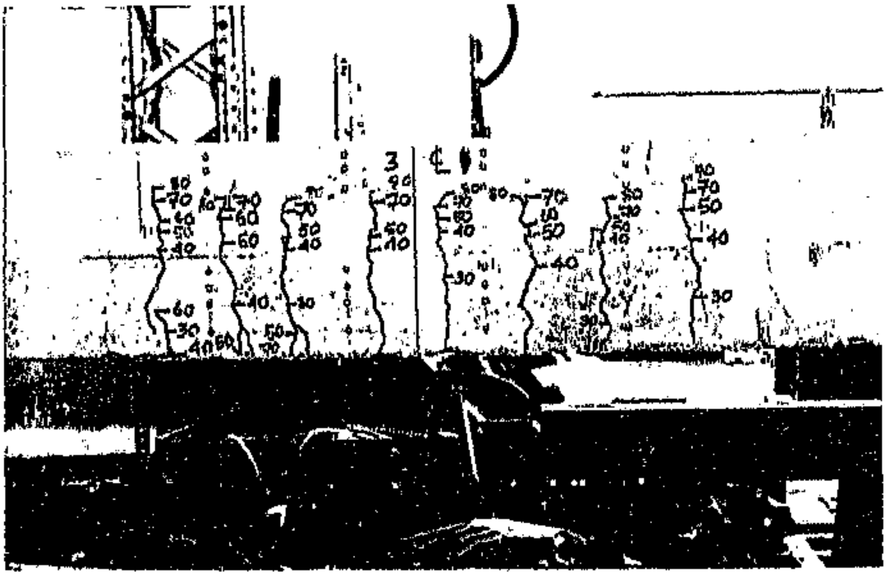

Figure 6.3 Typical crack pattern of series C
(pretensioned strands)

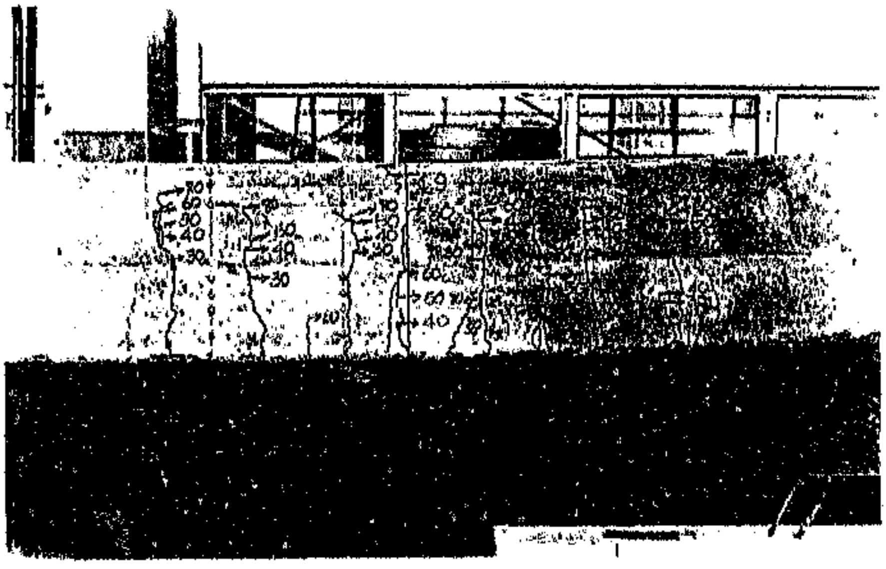

Figure 6.4 Typical crack pattern of series D
(pretensioned wires)

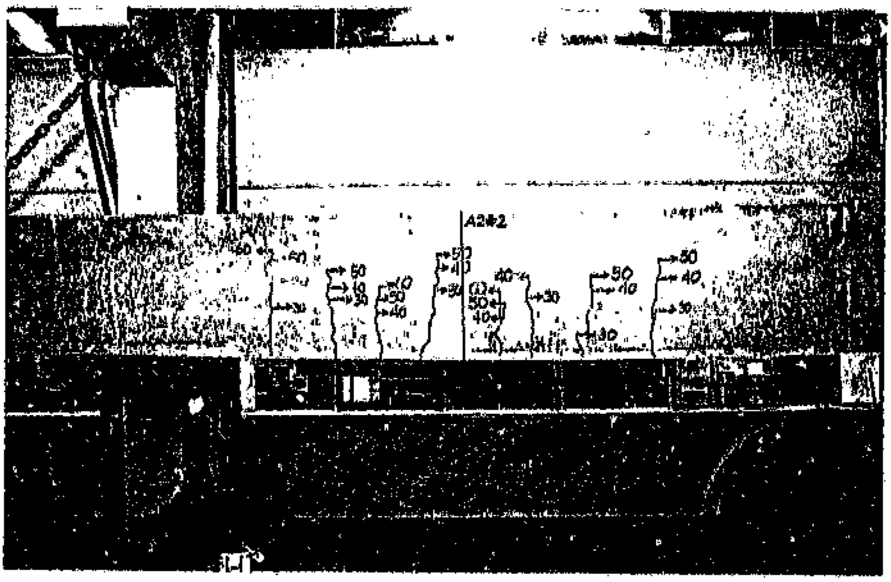

Figure 6.1 Typical crack pattern of series A (post tensioned bonded strands)

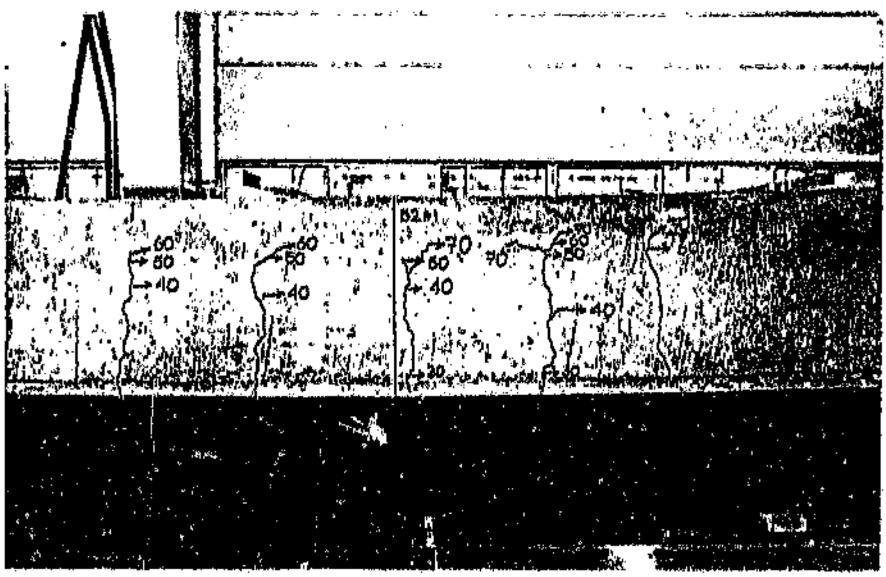

Figure 6.2 Typical crack pattern of series B (post tensioned unbonded strands)

6 TEST RESULTS

Most of the results obtained from the laboratory tests were acceptable for the purpose of this investigation with exception of a few beams as shall be discussed later.

6.1 Observed Beam Behaviour

All crack widths were measured within the pure flexure region between the two point loads. A few cracks would appear initially, once the cracking moment, M_c, had been reached, and then more would appear usually during the following load increment. The cracking pattern established itself quickly, with a few additional cracks sometimes forming at high overload in some of the beams. It is interesting to note the difference in crack patterns between the various types of beams as shown in Figures 6.1 to 6.4. The beams shown are the corresponding ones from each series, ie. they all have similar prestress and ultimate moments of resistance, but are of different prestress type.

It can be seen that the beams from the bonded series A, C and D display similar crack spacings, ie. approximately eight cracks appear between the two point loads, while in the unbonded beam from series B, only five cracks are present, all of larger width than in the beams of series A, C and D.

7 EVALUATION OF TEST RESULTS

7.1 Analysis of the values of k_w

On inspecting the values of k_w obtained from the aforementioned calculations, it was quite obvious that some of the values were of dubious nature, and should be ignored. Elimination by mere inspection was acceptable for obvious outliers, but with other values, it became more difficult to select the values that should be discarded. Hence it was decided that the average crack width should be used to calculate k_w. This approach gave acceptable results since, because of the variable nature of cracks, some cracks would be small and some would be large and hence such results would not affect the average to a large extent.

The values of k_w as determined from the experimental concrete strains obtained from the test beams are listed below in Table 7.1

7.2 Presentation of the Test Results

Previously, suggested cracking factors for the equations in ACI 318-83[18] and CAN3-A23.3-M84[19] and by Suri and Dilger[20], only took the combination of prestressed and unprestressed steel into account. However, on inspection of the test results, it was clear that a relationship existed between k_w and the amount of prestress. Hence the amount of prestress had to be quantified in some manner.

7.2.1 Quantification of the amount of prestress

According to Naaman and Siriaksorn[38], the amount of prestress may be quantified in three ways:

Table 6.1 Important results obtained from the test beams (continued)

Beam	At service				At first cracking		k_w for ACI 318-83 and CAN3-A23.3-M84			k_w for Suri and Dilger		
	w (mm)	δ (mm)	$s_{c,ave}$ (mm)	M (kNm)	δ (mm)	M (kNm)	$k_{w,exp}$	k_{w1}	k_{w2}	$k_{w,exp}$	k_{w1}	k_{w2}
D2#1	0,14	8,1	97,5	30,76	0,55	6,6	25,4	23,3	21,7	4,54	3,84	3,67

Table 6.1 Important results obtained from the test beams (continued)

Beam	At service				At first cracking		k_w for ACI 318-83 and CAN3-A23.3-M84			k_w for Suri and Dilger		
	w (mm)	δ (mm)	$s_{c,ave}$ (mm)	M (kNm)	δ (mm)	M (kNm)	$K_{w,exp}$	k_{w1}	k_{w2}	$K_{w,exp}$	K_{w1}	K_{w2}
C1#1	0,14	8,1	97,5	30,76	0,55	6,6	11,3	13,1	12,9	1,61	1,85	1,88
C1#2	0,18	9,2	99,8	32,55	0,44	6,0						
C2#1	0,16	10,5	95,3	33,25	1,27	11,4	10,9	11,6	11,4	1,83	1,69	1,68
C2#2	0,17	9,8	107,6	37,20	1,95	17,8						
C3#1	0,21	9,6	133,9	32,73	3,82	17,3	13,8	14,5	14,2	2,37	2,19	2,19
C3#2	0,17	9,6	–	34,50	3,21	17,8						
C4#2	0,20	7,8	162,9	33,98	2,54	23,5	17,6	52,9	44,3	1,36	3,99	3,38
D1#1	0,12	6,6	165,8	31,50	0,69	5,6	11,6	12,1	12,3	2,09	1,84	1,91
D1#2	0,15	5,5	163,3	33,50	–	–						

Table 6.1 Important results obtained from the test beams

Beam	At service				At first cracking		k_w for ACI 318-83 and CAN3-A23.3-M84			k_w for Suri and Dilger		
	w (mm)	δ (mm)	$s_{c,ave}$ (mm)	M (kNm)	δ (mm)	M (kNm)	$k_{w,exp}$	k_{w1}	k_{w2}	$k_{w,exp}$	k_{w1}	k_{w2}
A1#1	0,18	10,9	113,1	38,23	1,41	11,8	13,8	13,0	12,5	1,92	1,87	1,80
A1#2	0,15	11,6	114,5	33,75	1,67	11,7						
A2#1	0,18	10,9	140,4	39,00	2,55	18,1	15,1	12,9	12,4	2,07	1,78	1,74
A3#2	0,15	5,2	271,0	31,70	2,47	24,3	29,7	34,7	29,2	2,10	2,56	2,16
B1#1	0,14	10,4	110,7	31,93	1,65	11,9	12,8	12,2	12,0	1,73	1,60	1,63
B1#2	0,16	10,0	112,2	32,77	1,53	11,2						
B2#1	0,30	7,1	209,5	28,59	1,50	12,1	31,4	30,8	32,4	3,71	3,81	4,29
B2#2	0,30	9,8	184,8	30,18	1,65	12,1						

therefore

$$k_w = \frac{w}{f_s d_c \sqrt{\frac{A_t}{A_s + A_{ps}}} \times 10^{-6}} \qquad [6.29]$$

Shown below in Table 6.1 are the values of k_w obtained from the test beams for the equation from ACI 318-83[18] and CAN3-A23.3-M84[19] and also for the equation by Suri and Dilger[20]. The values of k_w for the two beams of each type have been averaged, for example C2#1 and C2#2. However, as explained in section 6.2.4, some of the beams' results have been omitted.

6.2.6 Summary of the test results

Table 6.1 below shows the important test results. Note that the values of k_w obtained by theoretical calculation as in section 6.2.3(2), k_{w1} and k_{w2}, using the two different moduli of elasticity, are very close to each other. However, there are quite large differences between the theoretically and experimentally determined values of k_w, suggesting that the values chosen for the moduli of elasticity may be quite incorrect. Hence the values of k_w determined from the experimental concrete surface strains, $k_{w,exp}$, are probably more reliable and should preferably be used for design instead of the values determined by theoretical calculation. All the stated crack widths are at the level of the unprestressed steel and are "average" values, ie. the values of k_w which were decided to be outliers actually determined which values of crack width would be excluded.

5mm could have occured undetected. When calculating k_w with the effective prestress as determined just before the start of the test, the incremental steel stress was found to be particularly low, which indicated that the prestress was lower than expected, ie. slippage had most probably occured. This led to values of k_w which were extraordinarily large and obviously unrepresentative for the abovementioned beams, initially by inspection, but also by comparing them to the results of the companion beams, where possible. Hence the results from these beams have been omitted.

6.2.5 Determination of k_w

Once the crack width, w, the depth of the neutral axis, x, and the incremental steel stress, f_s or f_{ps}, had been determined, k_w from both the equations in ACI 318-83[18] and CAN3-A23.3-M84[19] and by Suri and Dilger[20] could be calculated. For ACI 318-83[18] and CAN3-A23.3-M84[19] the equation is:

$$w = k_w f_s \sqrt[3]{d_c A_e} \times 10^{-6} \qquad [6.26]$$

therefore

$$k_w = \frac{w}{f_s \sqrt[3]{d_c A_e} \times 10^{-6}} \qquad [6.27]$$

For the equation by Suri and Dilger[20]:

$$w = k_w f_s d_c \sqrt{\frac{A_E}{A_s + A_{ps}}} \times 10^{-6} \qquad [6.28]$$

methods for the fully prestressed beams D3#1 and D3#2, the values of $e = M/P_e$ at service were within the middle third of the section, using the first method, while x as determined from the experimental strains was found to be close to the depth of the section, implying that the section was uncracked. However, during the tests, cracks did appear at the service load in these beams. This cracking could be attributed to three different factors, the first two being more probable:

1. The prestressed steel could have slipped unnoticed, although it was monitored for slippage at each load increment during the test.

2. Cracks could also have formed when the concrete was attempting to shrink, just after casting, as a result of the restraining action of the shuttering. Once the prestress was applied, the cracks would close up and then reappear upon application of the load as soon as tensile stresses occured in the bottom fibre.

3. The prestressed steel could have been overstressed during manufacture, hence sending the incremental stress into the plastic region of the stress-strain curve and therefore allowing the beam to deform to a large extent. This is less likely to have happened than point 1 or 2 above since the jack extensions were carefully measured during manufacture of all the test beams.

Beams A2#2, A3#1, C4#1 and D2#2 all displayed excessively large crack widths, most probably due to slippage, as for D3#1 and D3#2. Since slip of the prestressing steel was not monitored with dial gauges, but rather using the method as described in section 5.2, slip of the order of

From Figure 6.9(a) and 6.9(b) above, the equilibrium of forces gives:

$$\frac{A_c f_c}{2} = A_s f_s \qquad [6.21]$$

and:

$$f_s = \frac{d_u - x}{x} f_c m_s A_s \qquad [6.22]$$

$$\therefore A_c \frac{x}{2} = (d_u - x) m_s A_s \qquad [6.23]$$

The neutral axis may then be found from the resulting quadratic. Now, using the simple bending formula, since the behaviour is elastic:

$$f_c = \frac{M}{I_c} x \qquad [6.24]$$

and by similar triangles:

$$f_s = m_s \frac{M}{I_c} (d_u - x) \qquad [6.25]$$

6.2.4 Problems encountered in calculating the neutral axis depth, x, and the incremental steel stress, f_s or f_{pw}

On attempting to calculate the neutral axis depth and the incremental steel stress by both of the abovementioned the resulting cubic equation in x, and the concrete stress is then calculated from the equilibrium of normal forces as follows:

$$\frac{f_c bx}{2} - \frac{d_u - x}{x} f_c m_s A_s - \frac{d_p - x}{x} f_c m_{ps} A_{ps} - P_e = 0 \quad [6.19]$$

The incremental steel stress in the unprestressed and prestressed steel respectively is calculated from:

$$f_s = \frac{d_u - x}{x} f_c m_s \qquad f_{ps} = \frac{d_p - x}{x} f_c m_{ps} \qquad [6.20]$$

(b) reinforced concrete sections

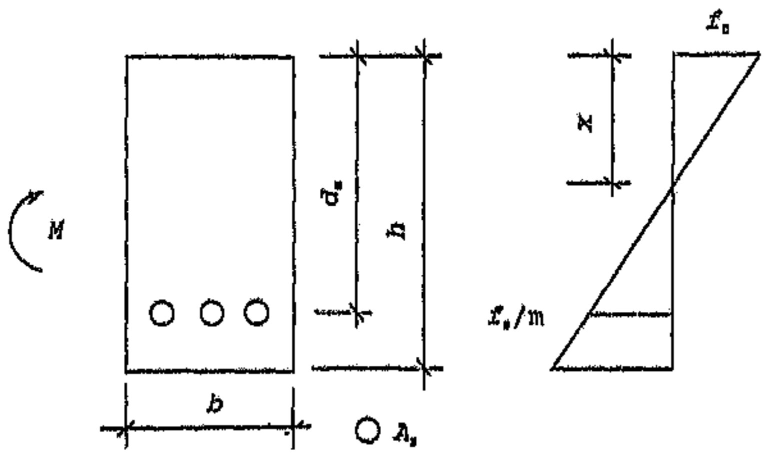

Figure 6.9 (a) reinforced concrete rectangular section
(b) stress distribution at the serviceability limit state

$$m_s = \frac{E_s}{E_c} \qquad m_{ps} = \frac{E_{ps}}{E_c} \qquad [6.11]$$

$$e = \frac{M}{P_e} \qquad e = d_p + k_1 \qquad [6.12]$$

$$\therefore k_1 = \frac{M - P_e d_p}{P_e} \qquad [6.13]$$

From the stress distribution at the serviceability limit state:

$$T_s = f_s A_s = \frac{d_u - x}{x} f_c m_s A_s \qquad [6.14]$$

$$T_{ps} = f_{ps} A_{ps} = \frac{d_p - x}{x} f_c m_{ps} A_{ps} \qquad [6.15]$$

$$C = \frac{f_c b x}{2} \qquad [6.16]$$

Moment equilibrium about point O:

$$f_c A_c (k_1 + x/3) - f_s A_s (d_u + k_1) - f_{ps} A_{ps} (d_p + k_1) = 0 \ [6.17]$$

substituting:

$$\frac{bx^2}{2}(k_1 + x/3) - (d_u - x) m_s A_s (d_u + k_1) - (d_p - x) m_{ps} A_{ps} (d_p + k_1) = 0$$
[6.18]

The neutral axis depth may then be calculated from

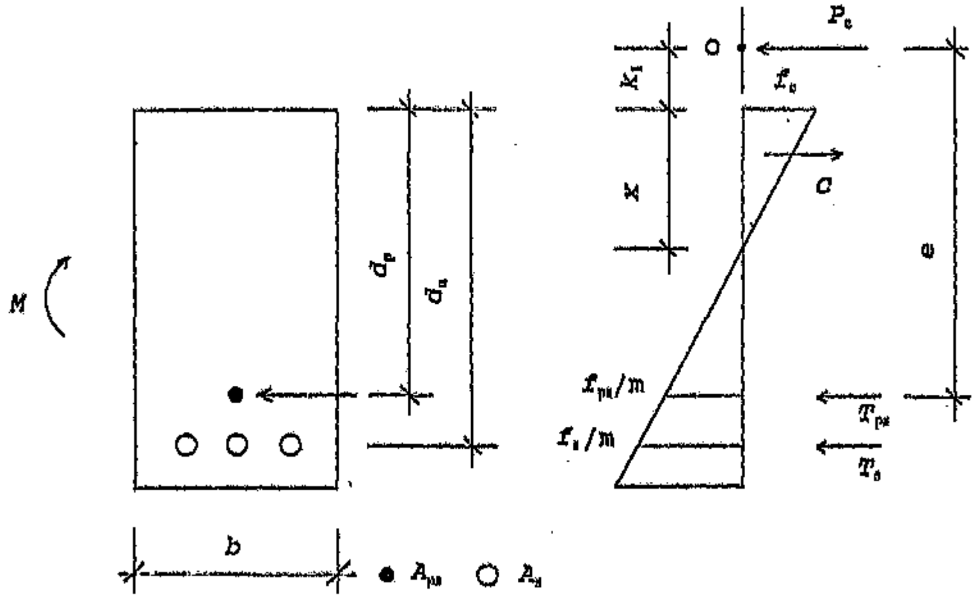

M is the total applied moment at the serviceability limit state

(a) (b)

Figure 6.8 (a) partially or fully prestressed concrete rectangular section
(b) stress distribution at the serviceability limit state

From Figure 6.8(a) and 6.9(b) above:

curve was performed for each calculation, otherwise equation [6.10] could not be used In such a case, the strain would be plotted on the curve and the corresponding stress from the plastic region of the curve could then be read off. However, the behaviour of the unprestressed steel in all of the beams remained in the elastic region of the stress-strain curve for the chosen service moments.

(2) Theoretical determination of the the neutral axis depth and the incremental steel stress

(a) Partially and fully prestressed concrete sections

The following procedure for calculation of the neutral axis depth, x, and the incremental steel stress, either f_s or f_{px}, is a simplified model by Ramaswamy[47]. For a general rectangular partially prestressed section, with a stress distribution at the serviceability limit state as shown overleaf, the calculation is as follows.

Table 7.2(b) Comparisons of measured crack widths from the test beams to values calculated using the equation by Suri and Dilger[13]

Beam	d_c (mm)	$A_s + A_{ps}$ (mm^2)	k_{w1}	w_1 (mm)	k_{w2}	w_2 (mm)
A1#1	30	376,42	1,92	0,18	2,55	0,21
A1#2	35	376,42	1,92	0,15	2,55	0,25
A2#1	33	300,84	2,07	0,18	2,55	0,20
A3#2	71,75	149,68	2,10	0,15	2,65	
B1#1	36	376,42	1,73	0,14	2,55	0,23
B1#2	36	376,42	1,73	0,16	2,55	0,21
B2#1	38	300,84	3,71	0,30	2,55	0,19
B2#2	47	300,84	3,71	0,30	2,55	0,22
C1#1	29	452	1,81	0,14	2,55	0,18
C1#2	40	452	1,81	0,18	2,55	0,27
C2#1	29,5	376,42	1,83	0,16	2,55	0,23

Table 7.2(a) Comparisons of measured crack widths from the test beams to values calculated using the equation from ACI 318-83[18] and CAN3-A23.3-M84[19] continued

Beam	d_c (mm)	A_e (mm²/bar)	k_{w1}	w_1 (mm)	k_{w2}	w_2 (mm)	k_{w3}	w_3 (mm)
C2#1	29,5	2768,00	10,9	0,17	11	0,15	13,7	0,19
C2#2	32	2930,20	10,9	0,17	11	0,15	13,7	0,19
C3#1	38	5280,80	13,8	0,21	11	0,13	13,7	0,16
C3#2	30	4636,80	13,8	0,17	11	0,14	13,7	0,18
C4#2	80	6400,00	17,6	0,20	17,4	0,06	21,5	0,08
D1#1	41	3612,84	11,6	0,12	16,4	0,21	20,3	0,26
D1#2	26	2500,00	11,6	0,15	16,4	0,17	20,3	0,21
D2#1	29	4425,50	25,4	0,20	16,4	0,14	20,3	0,17

Note: k_{w1} indicates the values of k_w obtained from the test beams, k_{w2} the reduced values suggested by Scholz[14] and k_{w3} the original values suggested by Suri and Dilger[20]

Table 7.2(a) Comparisons of measured crack widths from the test beams to values calculated using the equation from ACI 318-83[18] and CAN3-A23.3-M84[19]

Beam	d_c (mm)	A_e (mm^2/bar)	k_{w1}	w_1 (mm)	k_{w2}	w_2 (mm)	k_{w3}	w_3 (mm)
A1#1	30	2848,77	13,8	0,18	11	0,13	13,7	0,16
A1#2	35	3165,48	13,8	0,15	11	0,12	13,7	0,15
A2#1	33	4707,52	15,1	0,18	11	0,12	13,7	0,15
A3#2	71,75	6206,38	29,7	0,15	17,4	0,11	21,5	0,13
B1#1	36	2900,37	12,8	0,14	20,2	0,30	25,0	0,37
B1#2	36	3286,56	12,8	0,16	20,2	0,25	25,0	0,31
B2#1	38	3276,78	31,1	0,30	20,2	0,10	25,0	0,13
B2#2	47	3568,86	31,4	0,30	20,2	0,10	25,0	0,13
C1#1	29	2327,25	11,3	0,14	11	0,12	13,7	0,15
C1#2	40	3220,00	11,3	0,18	11	0,16	13,7	0,19

7.3 Comparison of the Test Results to Previous Research

Comparisons are made in this section in two ways:

(1) The measured crack widths from the test beams are compared to values of crack width predicted using values of k_w previously suggested by Scholz[14] and Suri & Dilger[20].

(2) The applicability of the values of k_w obtained from ther test beams is demonstrated by comparing predicted crack widths using these values of k_w to measured values from previous research. The differences in measured and calculated crack widths are then statistically analysed.

7.3.1 Comparison of measured crack widths from the test beams to predicted values

Table 7.2(a) shows the comparison of measured crack widths from the test beams to predicted crack widths calcualted from the equation in ACI 318-83[18] and CAN3-A23.3-M84[19] using the values of k_w originally suggested by Suri and Dilger[20] and the reduced values of k_w suggested by Scholz[14]. Table 7.2(b) compares the measured crack widths obtained from the test beams to values predicted by the equation by Suri and Dilger[20].

Note:

(1) In the comparisons below, the terms x, f_s or f_{ps}, and A_t have all been omitted, since they are of different value for each of the ranges of the demec targets and hence too voluminous to include

(2) the values of w and k_w shown in Table 7.2(a) and (b) are averages of the values obtained from each of the six ranges of demec targets, excluding the outliers

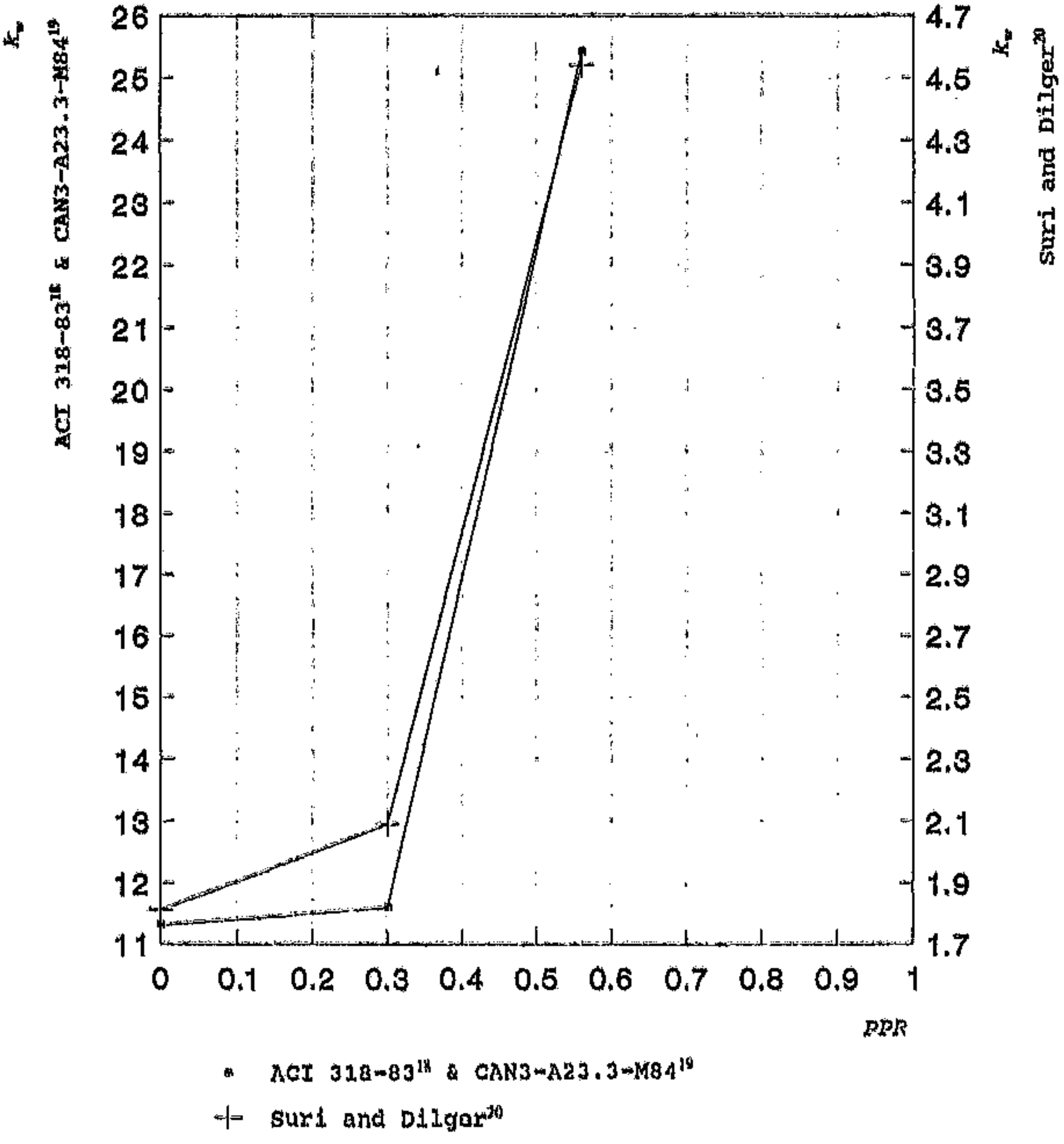

Figure 7.1(d) k_w vs *PPR* for series D (pretensioned wires and deformed bars)

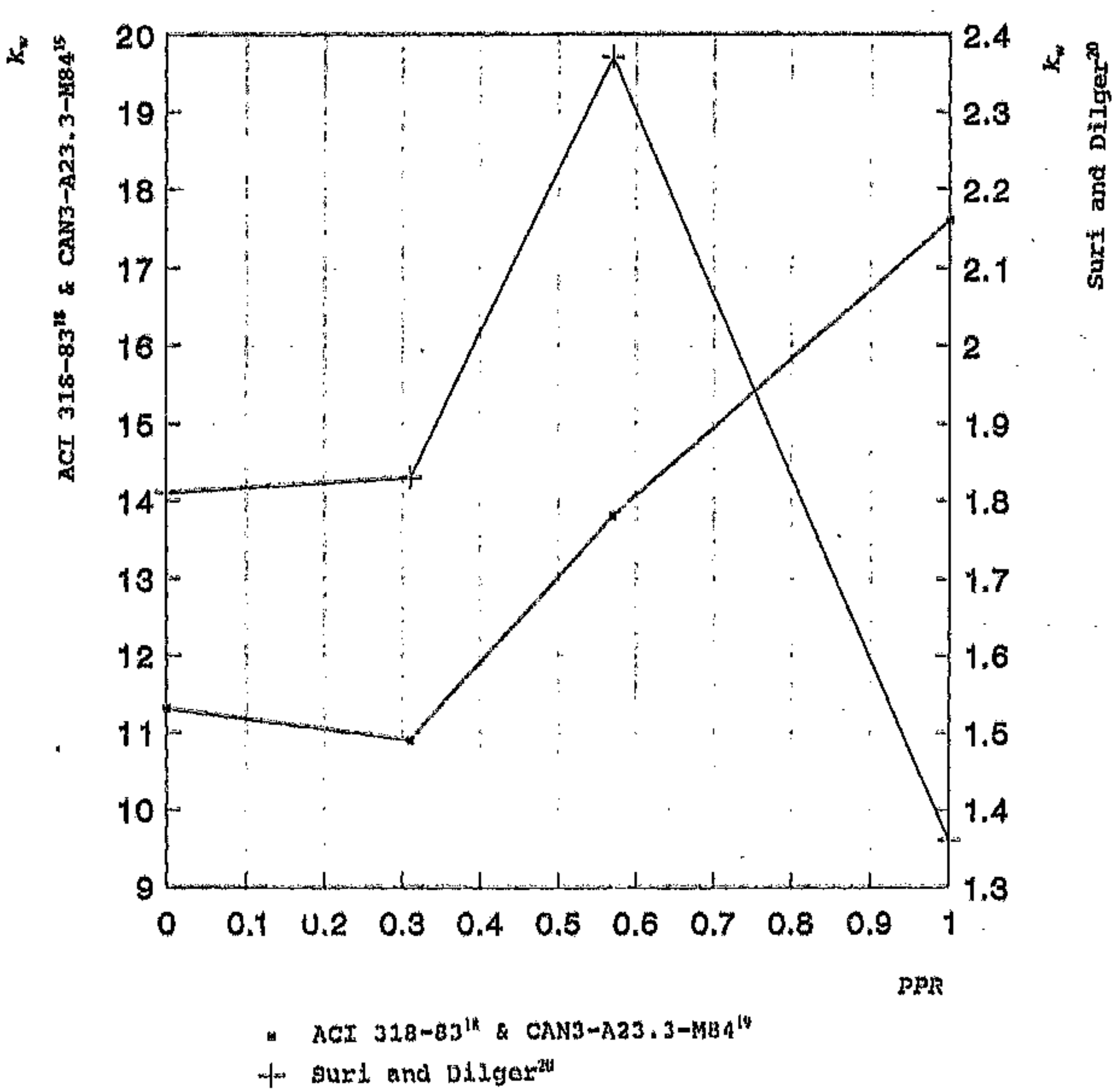

Figure 7.1(c) k_w vs PPR for series C (pretensioned strands and deformed bars)

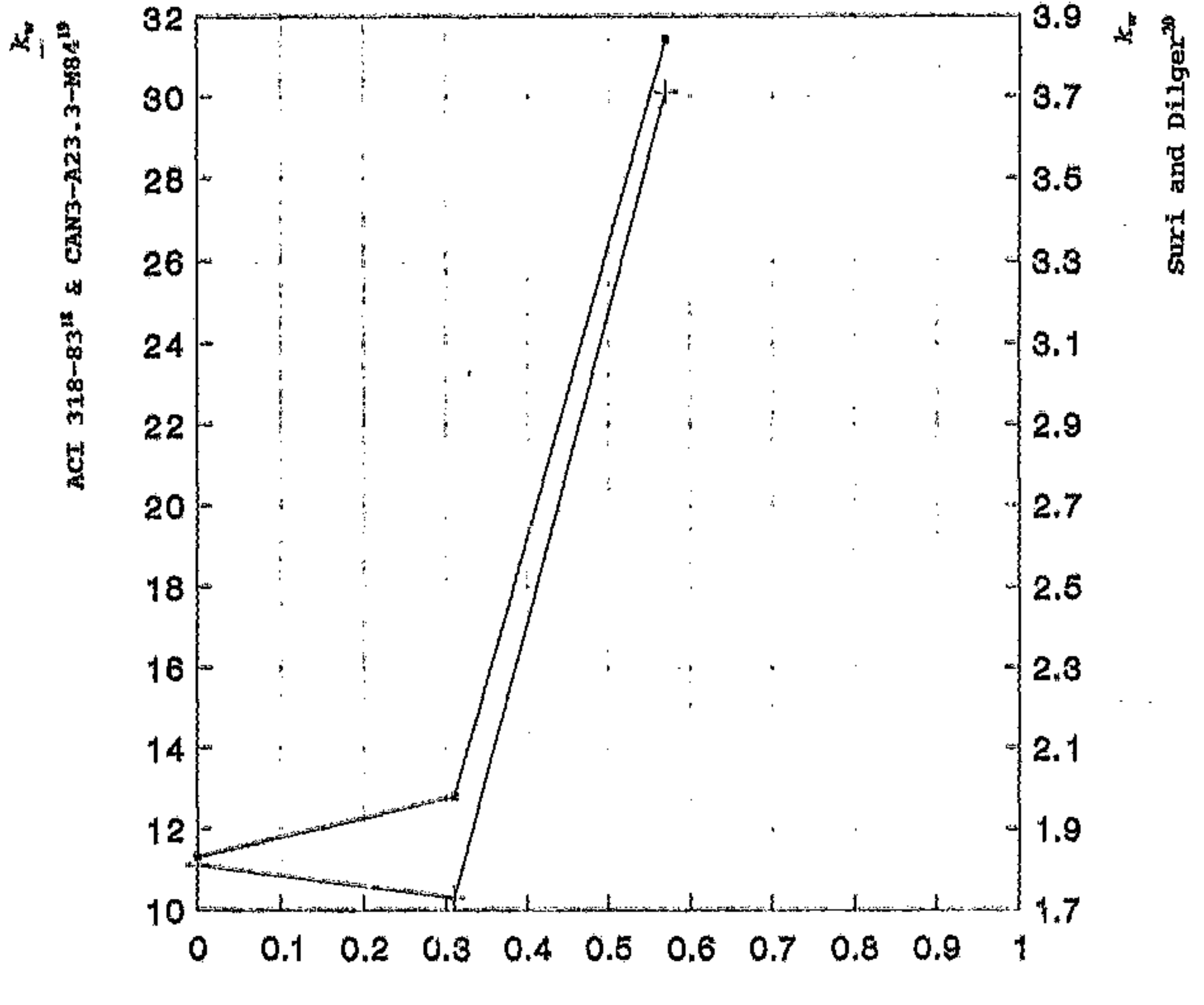

ACI 318-83[18] & CAN3-A23.3-M84[19]

Suri and Dilger[20]

Figure 7.1(b) k_w vs *PPR* for series B (post tensioned unbonded strands and deformed bars)

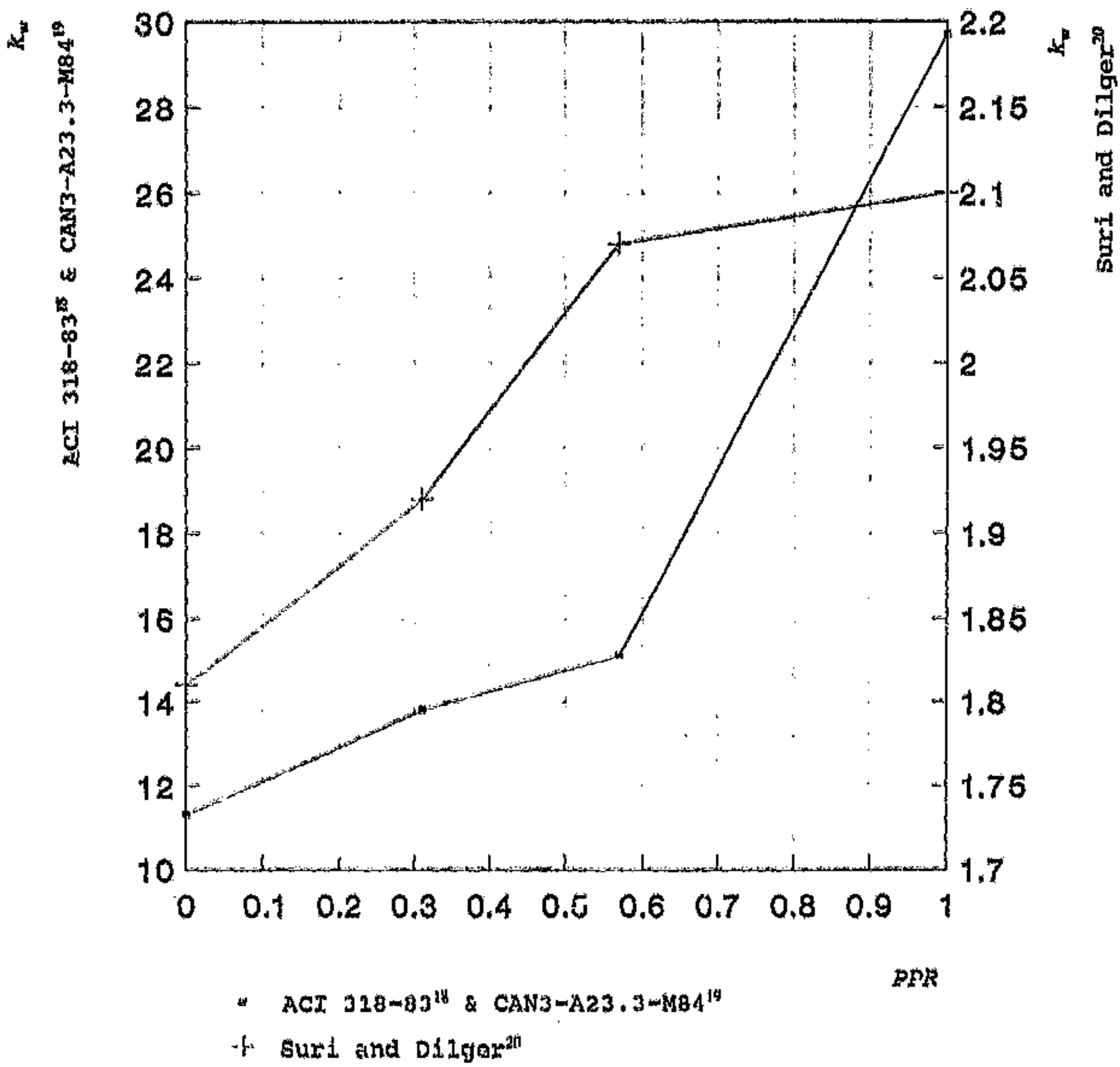

Figure 7.1(a) k_w vs *PPR* for series A (post tensioned bonded strands and deformed bars)

shown below in Figure 7.1(a) to Figure 7.1(d). The calculation of the partial prestressing ratios for the test beams is initially shown below along with the values of k_w in Table 7.1.

Table 7.1 Partial prestressing ratio and values of k_w for the test beams

Beam	d_p (mm)	x (mm)	ε_{pb} ($\times10^{-3}$)	f_{pb} (MPa)	PPR	k_{w1}	k_{w2}
A1#1	226	28,2	24,6	1942,8	0,31	13,8	1,92
A1#2	233	28,3	25,3	1942,8	0,31		
A2#1	227,5	29,6	29,6	1942,8	0,57	15,1	2,07
B1#1	229	26,9	26,3	1942,8	0,31	12,8	1,73
B1#2	226	27,8	25,0	1942,8	0,31		
B2#1	220	29,1	23,0	1942,8	0,57	31,4	3,71
B2#2	225,5	29,7	23,1	1942,8	0,57		
C2#1	226,5	25,8	27,2	1942,8	0,31	10,9	1,83
C2#2	228	25,8	27,4	1942,8	0,31		
C3#1	226	36,6	18,1	1942,8	0,57	13,8	2,37
C3#2	225	33,2	20,2	1942,8	0,57		
D1#1	229	25,8	27,6	1751,4	0,31	11,6	2,09
D1#2	228	25,8	27,4	1751,4	0,31		
D2#1	227	23,7	30,0	1751,4	0,57	25,4	4,54

Note: k_{w1} refers to the value of k_w as used in the equation from ACI 318-83[18] and CAN3-A23.3-M84[19], while k_{w2} refers to the value of k_w as used in the equation by Suri and Dilger[20].

index by Thurlimann[41] because the stress in the prestressed steel at the ultimate limit state is calculated rather than assumed to be the yield stress

- it is easier to calculate than the degree of prestress by Ramaswamy[42]

For design, f_{pb} may be calculated in four different ways:

(1) from Table 37 of CP 110[17]
(2) using the design stress-strain curves for prestressed steel from CP 110[17]
(3) from first principles
(4) from experimental strain measurements

However, for the test beams equilibrium conditions at the ultimate limit state were used along with the load-extension curve for the prestressed steel (Figure 4.3). Once the strain in the prestressed steel had been calculated from the equation:

$$\varepsilon_{pb} = 0,0035 \frac{(d_p - x)}{x} \qquad [7.6]$$

the extension could then be plotted on the load-extension curve and the corresponding steel stress obtained, which was found to lie in the plastic region of the curve for all the beams. The partial prestressing ratio was then calculated, the values being shown below in Table 7.1. The calculation was not performed for the reinforced or fully prestressed concrete beams since it was known that their *PPR's* were 0 and 1 respectively.

It was subsequently decided to present the values of k_w obtained from the test beams in graphical form, as is

(2) Prestressing index

Thurlimann[41] suggested using:

$$i_p = \frac{A_{ps}f_{py}}{A_{ps}f_{py} + A_s f_y} \qquad [7.4]$$

This is similar to the partial prestressing ratio, but assumes that the prestressed steel will yield at the ultimate limit state, possibly making it easier to use. However, the yield stress of prestressing steel is rarely quoted in codes of practice, manufacturers specifications or previous research, the characteristic strength, f_{pu}, usually being given.

(3) Degree of prestress

Ramaswamy[42] defined the degree of prestress as being the ratio of the decompression moment to the full service load moment:

$$degree\ of\ prestress = \frac{M_{dec}}{M_d + M_l} \qquad [7.5]$$

All three expressions quantifying the amount of prestress vary from 0 to 1, 0 indicating reinforced concrete and 1 indicating fully prestressed concrete. The partial prestressing ratio was identified as being the most appropriate for the following reasons:

- it is probably more accurate than the prestressing

- partial prestressing ratio
- prestressing index
- degree of prestress

(1) Partial prestressing ratio (*PPR*)

Naaman and Siriaksorn[38] defined this as the ratio of the ultimate moment due to the prestressed steel to the ultimate moment due to the total area of tensile steel:

$$PPR = \frac{M_{u,ps}}{M_{u,s} + M_{u,ps}} \qquad [7.1]$$

According to CP 110[17], the various ultimate moments are calculated thus:

$$PPR = \frac{A_{ps}f_{pb}\ (d_p - x/2)}{A_s f_y\ (d_u - x/2)\ +\ A_{ps}f_{pb}\ (d_p - x/2)} \qquad [7.2]$$

Naaman and Siriaksorn[38] then state that if *d* is defined as the distance from the extreme compression fibre to the centroid of the prestressed and unprestressed steel:

$$PPR = \frac{A_{ps}f_{pb}}{A_s f_y + A_{ps}f_{pb}} \qquad [7.3]$$

This equation assumes that the unprestressed steel will reach its yield stress at the ultimate limit state, which is generally true.

on cracking.

Four series of beams were tested, series A containing post tensioned seven wire bonded strands and deformed bars, series B post tensioned unbonded seven wire strands and deformed bars, series C pretensioned seven wire strands and deformed bars and series D pretensioned smooth wires and deformed bars. In each series beams were tested with the partial prestressing ratio varying between 0 and 1.

The results obtained from the tests were presented in graphical form, the cracking factor k_w being plotted against the partial prestressing ratio (*PPR*). In contrast to previously recommended values for k_w, the graphs enabled a variable value of k_w to be determined, not only for a certain combination of prestressed and unprestressed steel, but also for the amount of prestress, indicated by the partial prestressing ratio. This is required since the crack width depends upon, among other controlling parameters, the total area of steel, a factor which had been acknowledged by previous researchers but had not been included and quantified. On the whole the values of k_w from the tests generally gave better predictions of crack width when compared to previous research, although only marginally in some instances.

Some unexpected results occurred, for example certain beams entered the plastic zone of behaviour at a moment much lower than expected therefore giving values of k_w that were unrepresentative. Hence these results were not included. The post tensioned unbonded beams with little or no unprestressed steel had excessively large cracks as predicted by theory. However, such members such members containing only unbonded steel would in practice not be

8 CONCLUSIONS AND RECOMMENDATIONS

8.1 Summary and Conclusions

Prestressed concrete structures can be designed for no cracking under full service load, but in general, this leads to an uneconomical and non aesthetically pleasing structure due to the size required of such a member. There is also the possibility that such sections become overreinforced or overprestressed with respect to the ultimate limit state. This often results in brittle failure due to lack of ductility, while also making the member unsuitable for moment redistribution or plastic analysis and design. Partially prestressed concrete is hence a viable alternative to fully prestressed concrete, but with the reduction in prestress, flexural cracking at service will occur and must be controlled. Due to the high strength of prestressing steels, a relatively small loss of its cross sectional area lost due to corrosion can lead to a considerable reduction in ultimate strength of the member. Therefore a reliable method to predict crack width is needed.

It was shown that many of the existing equations are inadequate, mainly because they were adapted from reinforced concrete or they have been derived from a statistical analysis of a number of different tests, all with different controlling conditions and experimental error. Hence it was decided that a full range of commonly used prestressing steels in combination with deformed bars should be used in an experimental study. Those tests would have the advantage over other previous research of being subjected to the same controlling conditions and experimental error, therefore highlighting the true differences of the effect of different prestressing steels and a variation in the partial prestressing ratio

The predictions of crack widths by thee equation from ACI 318-83[18] and CAN3-A23.3-M84[19] correlate reasonably well with the measured values, when the values of k_w from the test beams or the reduced values of k_w as suggested by Scholz[14] are used. The values of k_w suggested by Suri and Dilger[20] do not compare well. The equation by Suri and Dilger[20] compares badly with the measured crack widths, especially when the values of k_w as originally suggested by Suri and Dilger[20] are used, as they give large overestimations.

Table 7.4(c) Percentages differences of measured and calculated and measured values for Tansi et al[15]

Beam	Equation from ACI 318-83 and CAN3-A23.3-M84			Equation by Suri & Dilger	
	Test beams	Scholz	Suri & Dilger	Test Beams	Suri & Dilger
R1	13,3%	13,3%	40,0%	33,3%	86,7%
R2	-17,6%	-17,6%	5,9%	5,9%	47,1%
R3	64,7%	29,4%	64,7%	111,8%	123,5%
R4	70,0%	70,0%	30,0%	80,0%	250,0%
I1	13,3%	6,7%	33,3%	0	40,0%
I2	5,9%	11,8%	35,3%	11,8%	52,9%
I3	12,5%	-6,3%	12,5%	6,3%	6,3%
I4	4,9%	4,9%	-19,5%	0	92,7%
Mean	20,9%	14,0%	25,3%	31,1%	87,4%
Std. Dev.	30,4%	26,5%	25,4%	42,2%	75,0%

Table 7.4(b) Comparison of measured and calculated values for Tansi et al[15] using the equation by Suri and Dilger[38]

Beam	f_s (MPa)	d_c (mm)	A_t (mm^2)	$A_{ps}+A_{ps}$ (mm^2)	w (mm)	PPR	Test Beams		Suri & Dilger	
							k_w	w (mm)	k_w	w (mm)
R1	284,63	43	35171,20	440	0,15	0	1,81	0,20	2,55	0,28
R2	240,43	43	34384,00	370,6	0,17	0,32	1,83	0,18	2,55	0,25
R3	322,63	43	34160,00	301,2	0,17	0,59	2,42	0,36	2,55	0,38
R4	116,51	84	28976,00	162,4	0,10	1	1,36	0,18	2,55	0,35
I1	281,66	42	24157,12	440	0,15	0	1,81	0,15	2,55	0,21
I2	320,76	43	20093,04	370,6	0,17	0,32	1,83	0,19	2,55	0,26
I3	242,39	36	18579,00	301,2	0,16	0,59	2,42	0,17	2,55	0,17
I4	362,21	73,5	20330,09	162,4	0,41	1	1,36	0,41	2,55	0,79

Table 7.4(a) Comparison of measured and calculated values for Tansi et al[15] using the equation from ACI 318-83[18] and CAN3-A23.3-M84[19]

Beam	f_s (MPa)	d_c (mm)	A_e (mm^2/bar)	w (mm)	PPR	Test Beams		Scholz		Suri & Dilger	
						k_w	w (mm)	k_w	w (mm)	k_w	w (mm)
R1	284,63	43	3440,00	0,15	0	11,3	0,17	11	0,17	13,7	0,21
R2	240,43	43	3751,71	0,17	0,32	11,0	0,14	11	0,14	13,7	0,18
R3	322,63	43	5693,27	0,17	0,59	14,0	0,28	11	0,22	13,7	0,28
R4	116,51	84	6636,00	0,10	1	17,6	0,17	11	0,11	13,7	0,21
I1	281,66	42	3350,86	0,15	0	11,3	0,17	11	0,16	13,7	0,20
I2	320,76	43	3377,87	0,17	0,32	11,0	0,18	11	0,19	13,7	0,23
I3	242,39	36	4502,35	0,16	0,59	14,0	0,18	11	0,16	13,7	0,19
I4	362,21	73,5	4105,75	0,41	1	17,6	0,43	11	0,27	13,7	0,52

All the values of k_w, for both equations, underestimate the crack width of Beam RB3604. Table 7.3(c) shows that the predicted crack widths vary considerably between the different values of k_w when using the equation from ACI 318-83[18] and CAN3-A23.3-M84[19]. When using the equation by Suri and Dilger[20], the original values of k_w suggested by Suri and Dilger perform better than the values of k_w from the test beams. In general, for the tests by Bennett and Veerasubramanian[25], the equation from ACI 318-83[18] and CAN3-A23.3-M84[19] used with the values of k_w from the test beams, and the equation by Suri & Dilger[20] used with the values of k_w that they originally suggested, give the best predictions of crack width.

Pretensioned strands

Tansi et al[15] tested eight beams, four rectangular sections and four I sections, both series of beams ranging from reinforced to fully prestressed concrete. The comparison between measured crack widths and the values calculated from the equation in ACI 318-83[18] and CAN3-A23.3-M84[19] is shown in Table 7.4(a). Table 7.4(b) compares predicted crack widths from the equation by Suri and Dilger[20] to measured values.

Table 7.3(c) Percentages differences of measured and calculated and measured values for Bennett and Veerasubramanian[36]

Beam	Equation from ACI 318-83 and CAN3-A23.3-M84			Equation by Suri & Dilger	
	Test Beams	Scholz	Suri & Dilger	Test Beams	Suri & Dilger
RB 1302	53,8%	-15,4%	0	0	23,1%
RB 1204	0	-23,1%	-7,7%	-15,4%	7,7%
RB 2404	50,0%	-12,5%	12,5%	-12,5%	12,5%
RB 2208	9,1%	-9,1%	9,1%	9,1%	45,5%
RB 3604	-9,1%	-54,4%	-45,5%	-54,5%	-45,5%
RB 3408	-15,4%	-30,8%	-15,4%	-23,1%	0
Mean	14,7%	-21,2%	-7,8%	-16,1%	7,2%
Std. Dev.	30,0%	16,8%	16,8%	22,1%	30,3%

Table 7.3(b) Comparison of measured and calculated and measured values for Bennett and Veerasubramanian[25] using the equation by Suri and Dilger[20]

Beam	f_s (MPa)	d_c (mm)	A_t (mm^2)	A_s+A_{ps} (mm^2)	w (mm)	PPR	Test Beams		Suri & Dilger	
							k_w	w (mm)	k_w	w (mm)
RB 1302	228,44	25	31889,6	269,34	0,13	0,75	2,08	0,13	2,55	0,16
RB 1204	250,08	24	32710,4	389,00	0,13	0,49	2,02	0,11	2,55	0,14
RB 2404	187,04	24	28469,6	463,84	0,08	0,66	2,08	0,07	2,55	0,09
RB 2208	223,14	43	30587,6	703,16	0,11	0,33	1,93	0,12	2,55	0,16
RB 3604	140,25	24	25034,4	538,68	0,11	0,74	2,08	0,05	2,55	0,06
RB 3408	193,68	43	27496,8	778,00	0,13	0,49	2,02	0,10	2,55	0,13

Table 7.3(a) Comparison of measured and calculated and measured values for Bennett and Veerasubramanian[25] using the equation from ACI 318-83[18] and CAN3-A23.3-M84[19]

Beam	f_s (MPa)	d_c (mm)	A_c (mm²/bar)	w (mm)	PPR	Test Beams		Scholz		Suri & Dilger	
						k_w	w (mm)	k_w	w (mm)	k_w	w (mm)
RB 1302	228,44	25	2945	0,13	0,75	21,2	0,20	11	0,11	13,7	0,13
RB 1204	250,08	24	1821,57	0,13	0,49	14,7	0,13	11	0,10	13,7	0,12
RB 2404	187,04	24	1706,96	0,08	0,66	18,2	0,12	11	0,07	13,7	0,09
RB 2208	223,14	43	1495,68	0,11	0,33	13,9	0,12	11	0,10	13,7	0,12
RB 3604	140,25	24	1621,62	0,11	0,74	20,9	0,10	11	0,05	13,7	0,06
RB 3408	193,68	43	1488,38	0,13	0,49	14,7	0,11	11	0,09	13,7	0,11

7.3.2 Comparison of predicted crack widths using values of k_w obtained from the test beams to measured crack widths from previous research

Measured crack widths from the tests by Bennett and Veerasubramanian[25] and Tansi et al[15] were compared to values calculated from ACI 318-83[18] and CAN3-A23.3-M84[19] and the equation by Suri and Dilger[20]. The values of k_w suggested by Scholz[14], Suri and Dilger[20] and values obtained from the test beams were used in the comparison.

Post tensioned bonded strands

Bennett and Veerasubramanian[25] tested six rectangular post tensioned bonded partially prestressed concrete beams. Table 7.3(a) shows the comparison between the measured crack widths and the values suggested by the equation from ACI 318-83[18] and CAN3-A23.3-M84[19], while Table 7.3(b) compares the measured crack widths and the values calculated by the equation by Suri and Dilger[20]. Table 7.3(c) shows the statistical analysis performed on the differences between the calculated and measured crack widths.

Table 7.2(b) Comparisons of measured crack widths from the test beams to values calculated using the equation by Suri and Dilger[20] continued

Beam	d_c (mm)	$A_s + A_{ps}$ (mm^2)	k_{w1}	w_1 (mm)	k_{w2}	w_2 (mm)
C2#2	32	376,42	1,83	0,17	2,55	0,24
C3#1	38	300,84	[illegible],37	0,21	2,55	0,21
C3#2	30	300,84	2,37	0,17	2,55	0,20
C4#2	80	149,68	1,36	0,20	2,65	0,39
D1#1	41	378,74	2,09	0,12	2,55	0,26
D1#2	26	378,74	2,09	0,15	2,55	0,16
D2#1	29	305,48	4,54	0,14	2,55	0,12

Note: (1) k_{w1} indicates the values of k_w obtained from the test beams, k_{w2} the original values suggested by Suri and Dilger[20]

(2) k_{w1} is the average of the values of k_w obtained from the test beams excluding the outliers

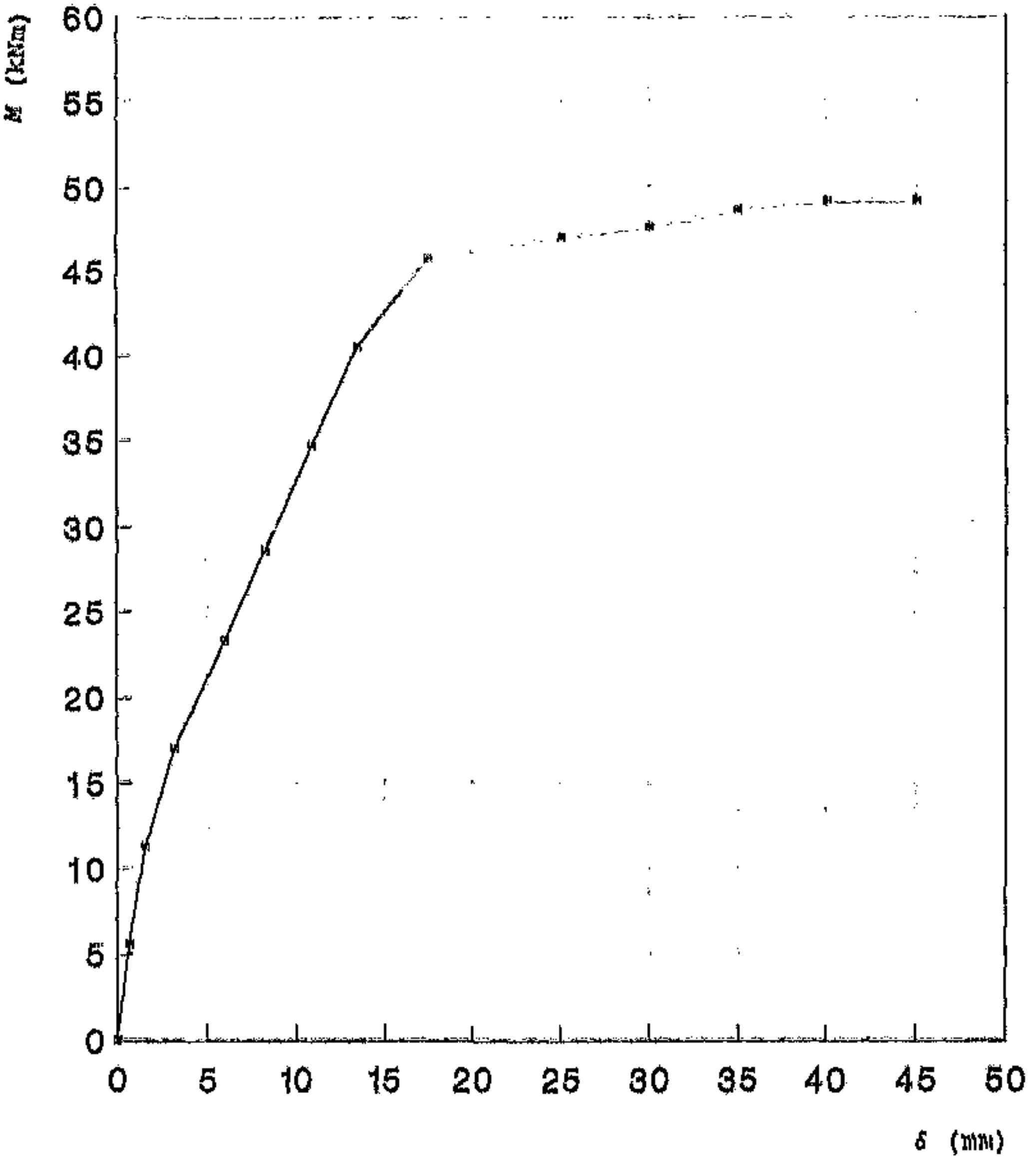

Figure D8 Experimental moment-deflection curve for beam D1#2

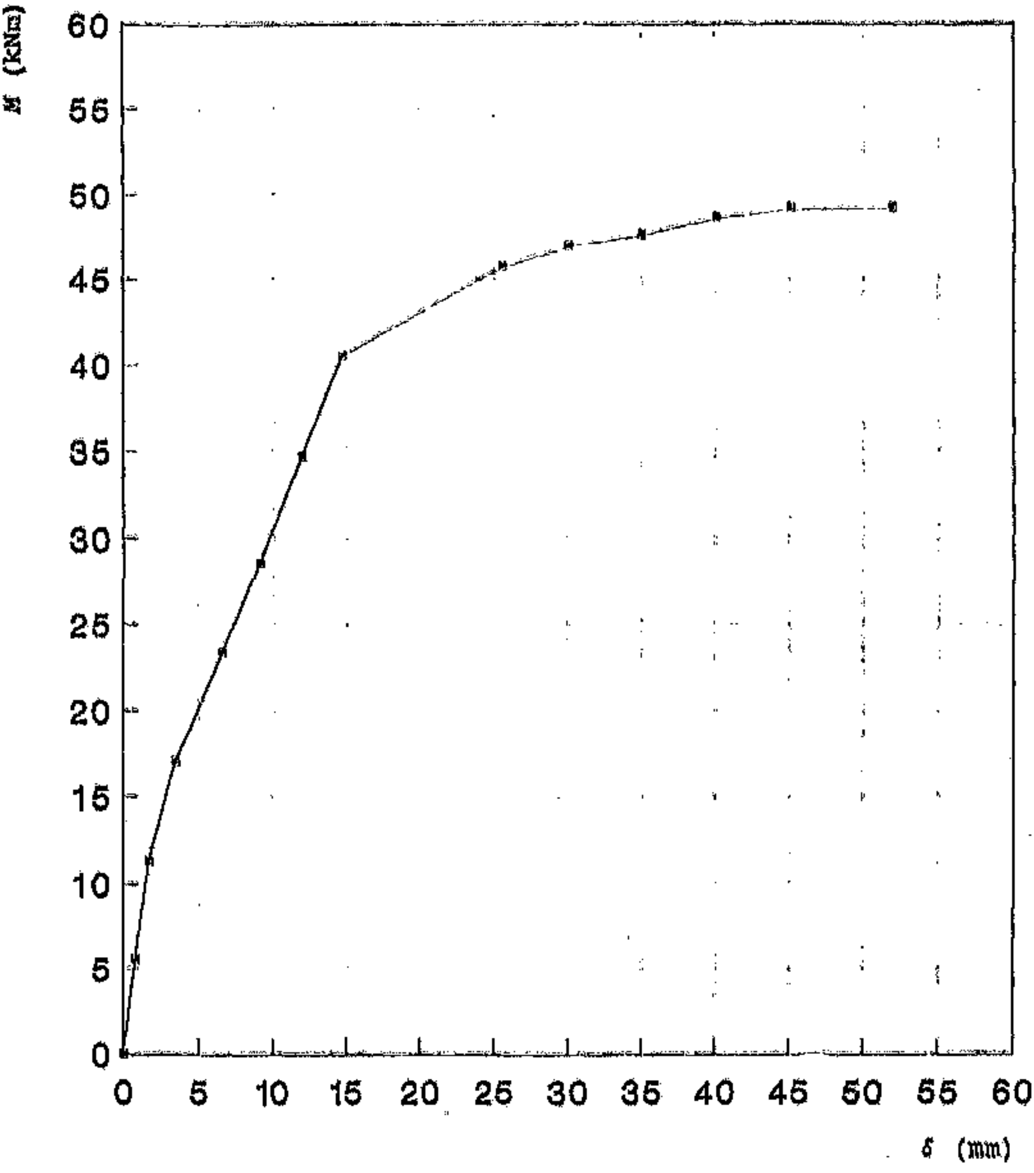

Figure B7 Experimental moment-deflection curve for beam B1#1

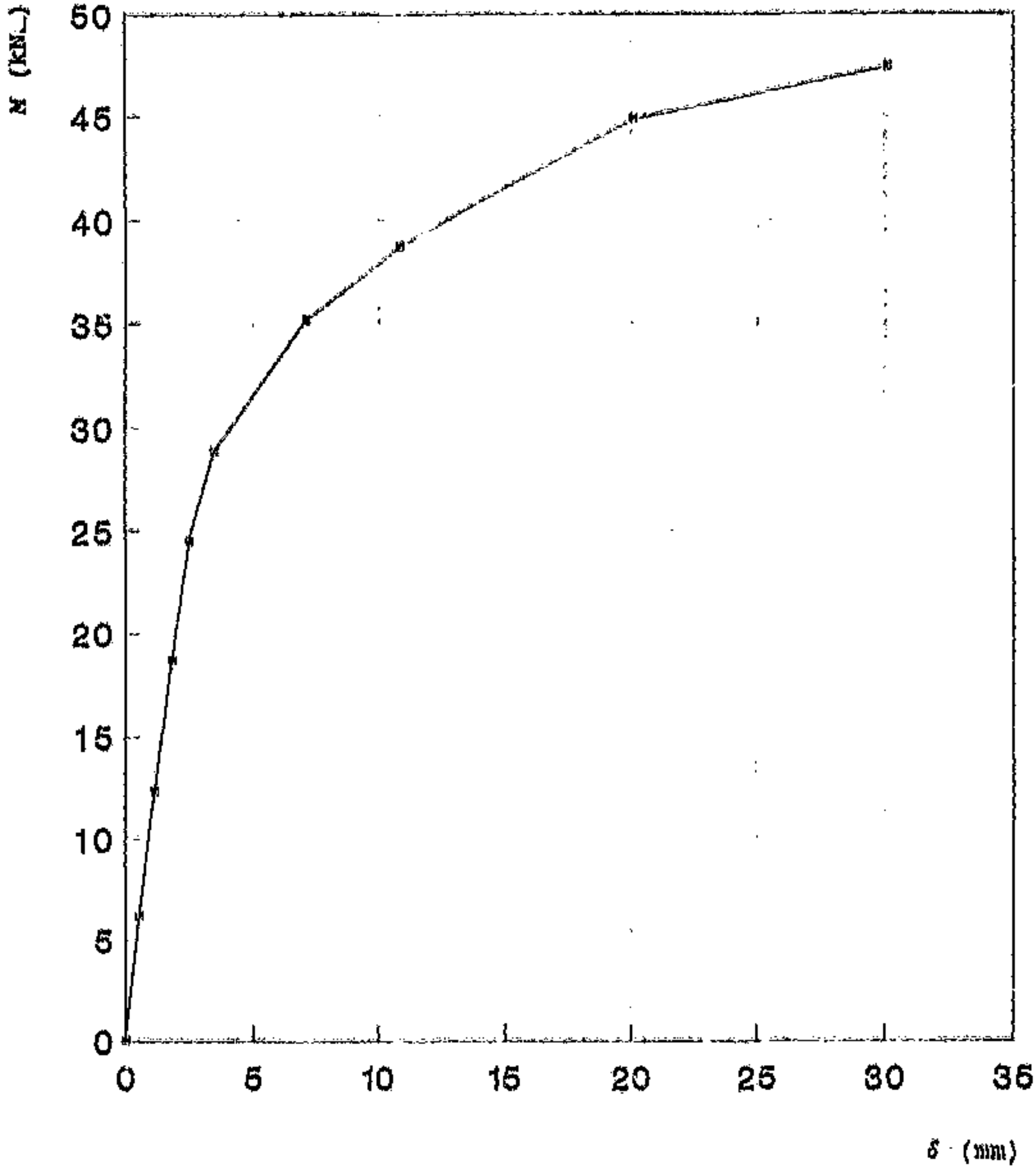

Figure D6 Experimental moment-deflection curve for beam A3#2

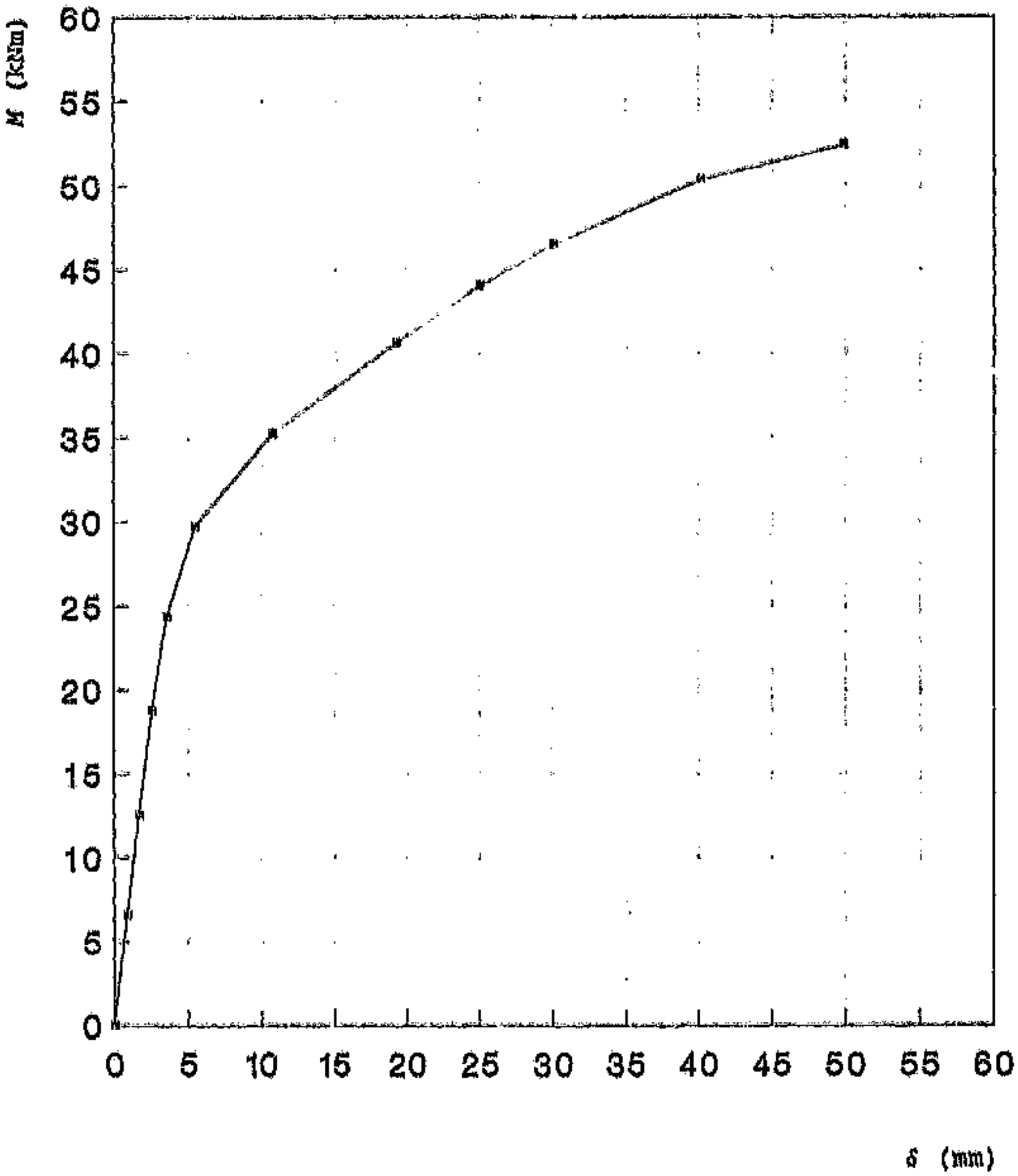

Figure B5 Experimental moment-deflection curve for beam A3#1

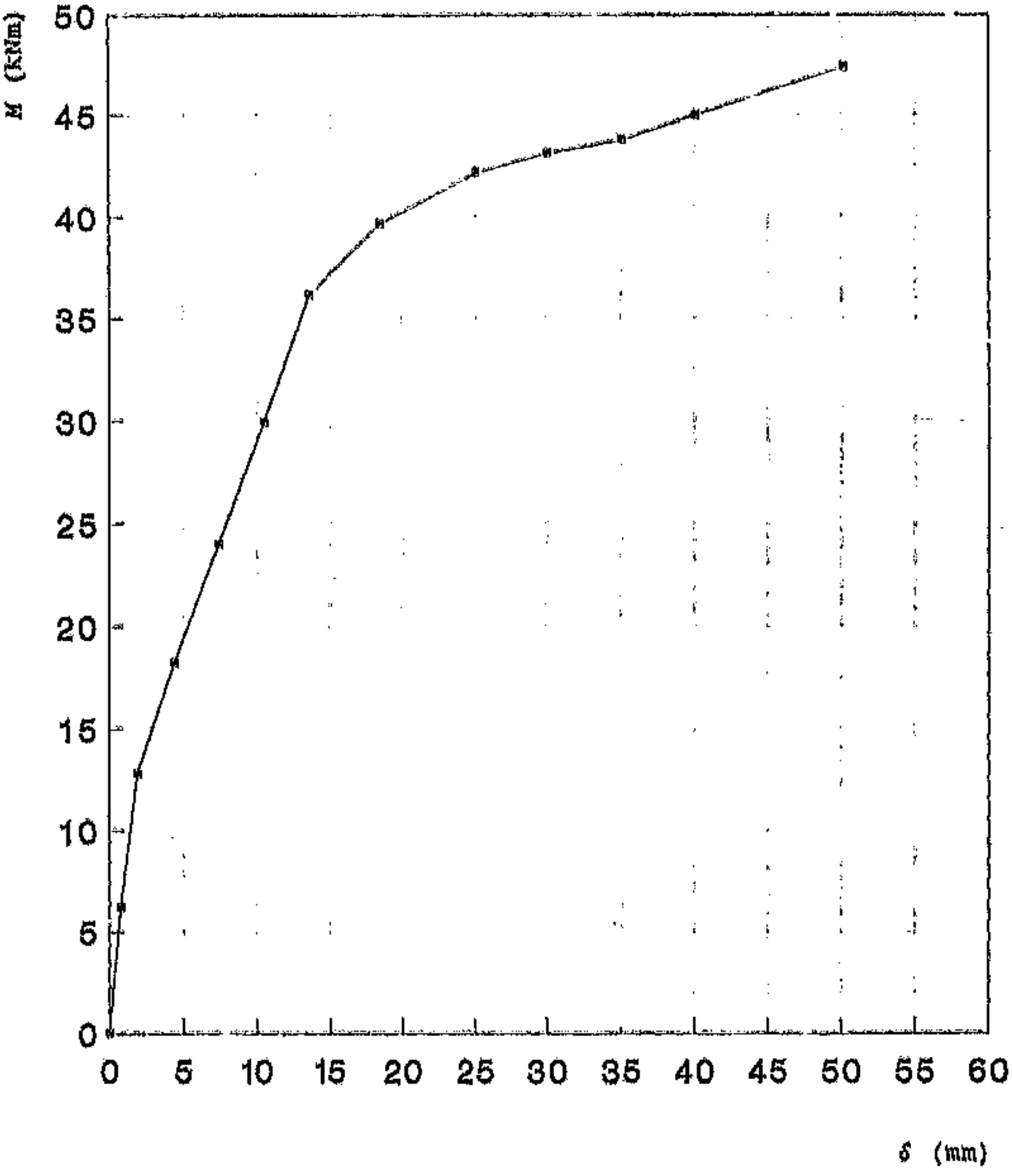

Figure B4 Experimental moment-deflection curve for beam A2#2

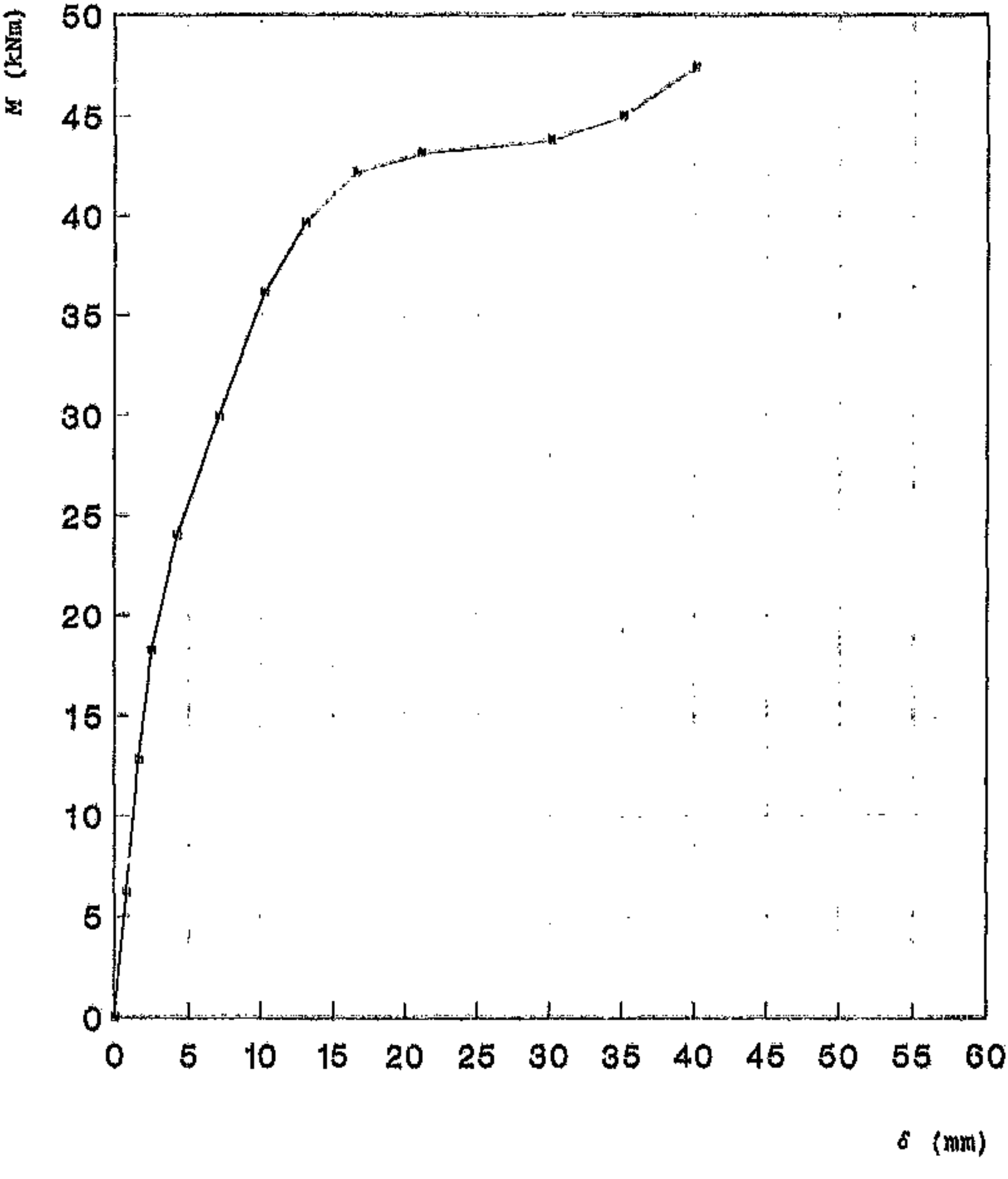

Figure B3 Experimental moment-deflection curve for beam A2#1

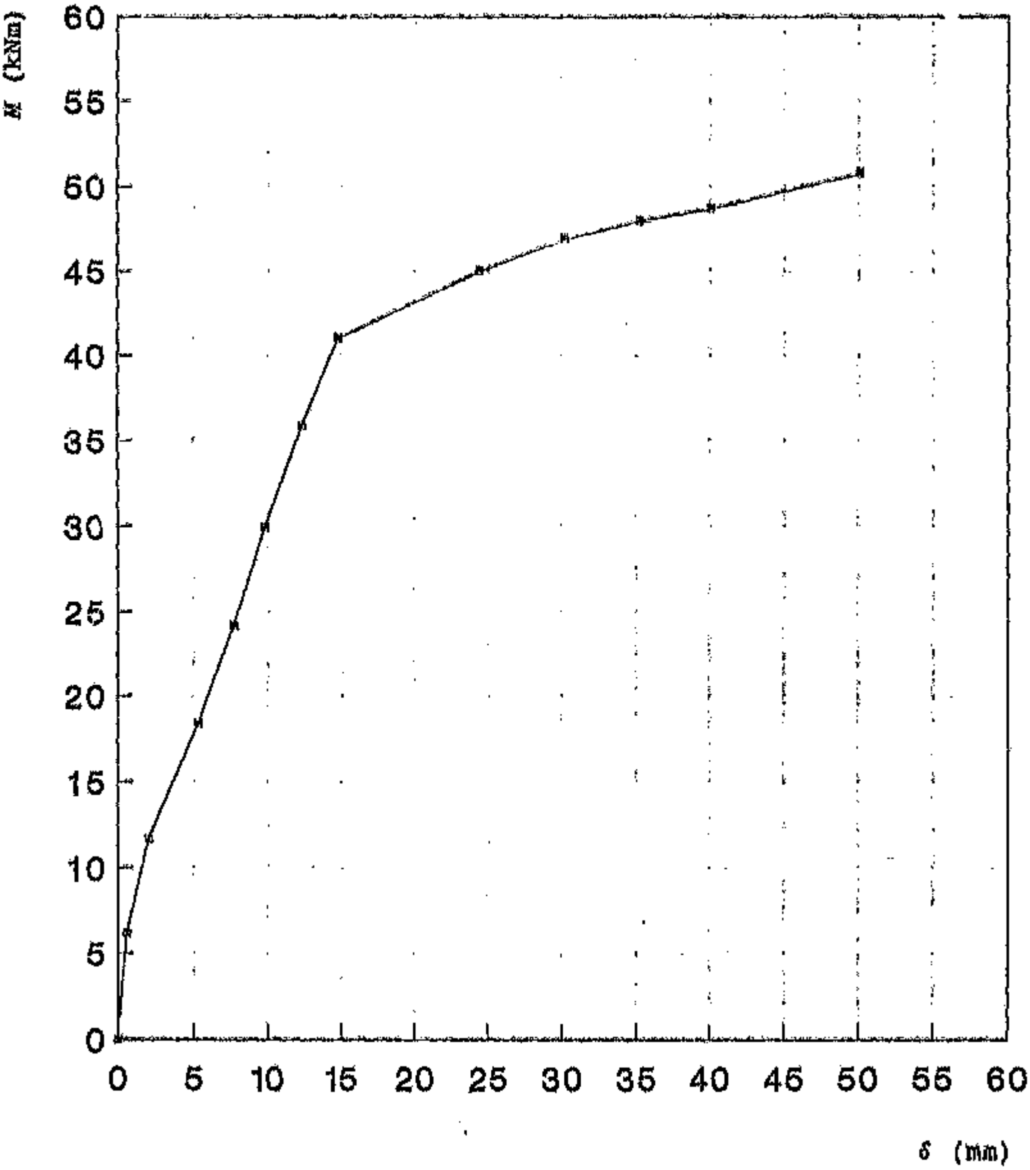

Figure B2 Experimental moment-deflection curve for beam A1#2

EXPERIMENTAL MOMENT-DEFLECTION CURVES FOR THE TEST BEAMS

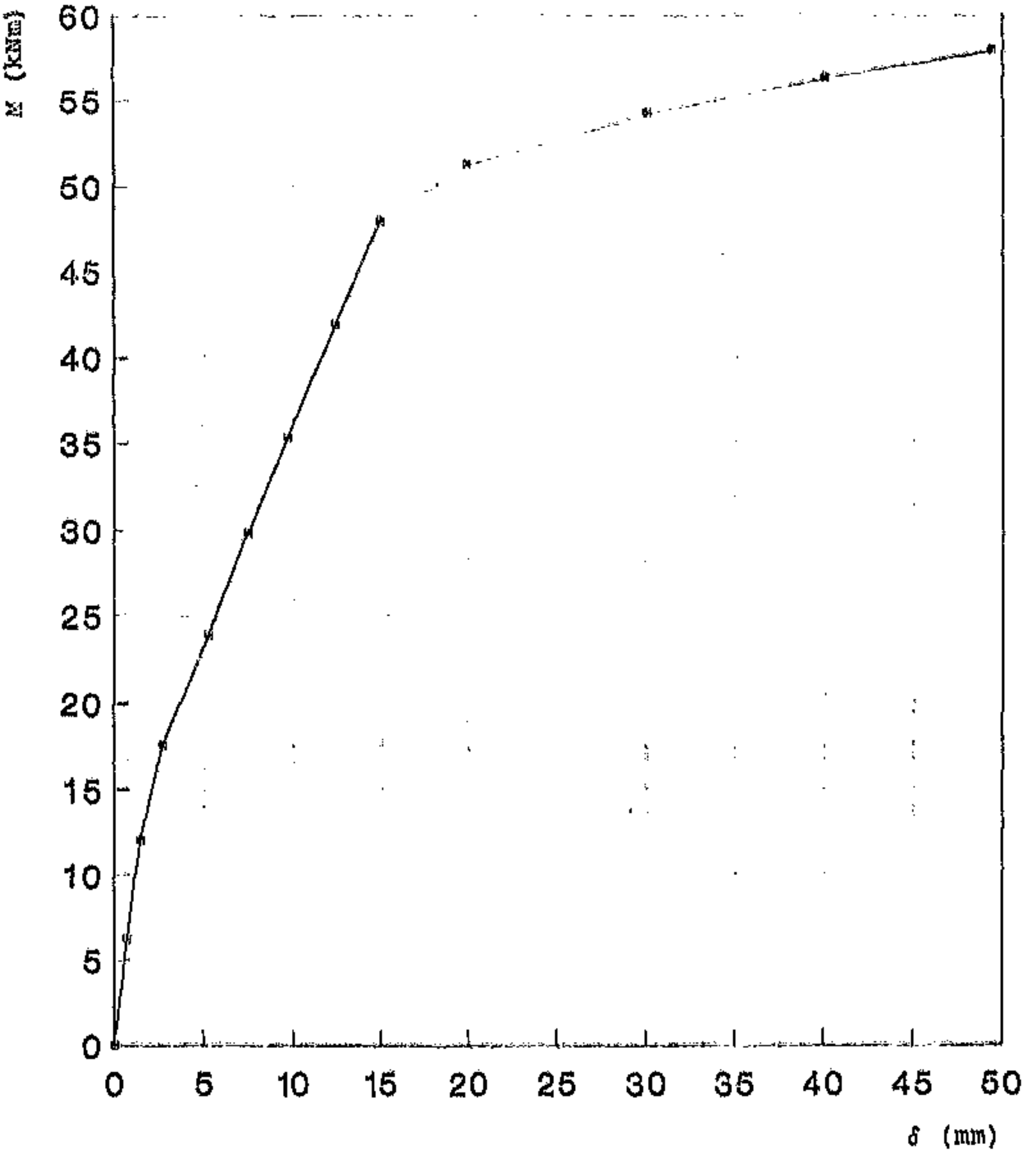

Figure B1 Experimental moment-deflection curve for beam A1#1

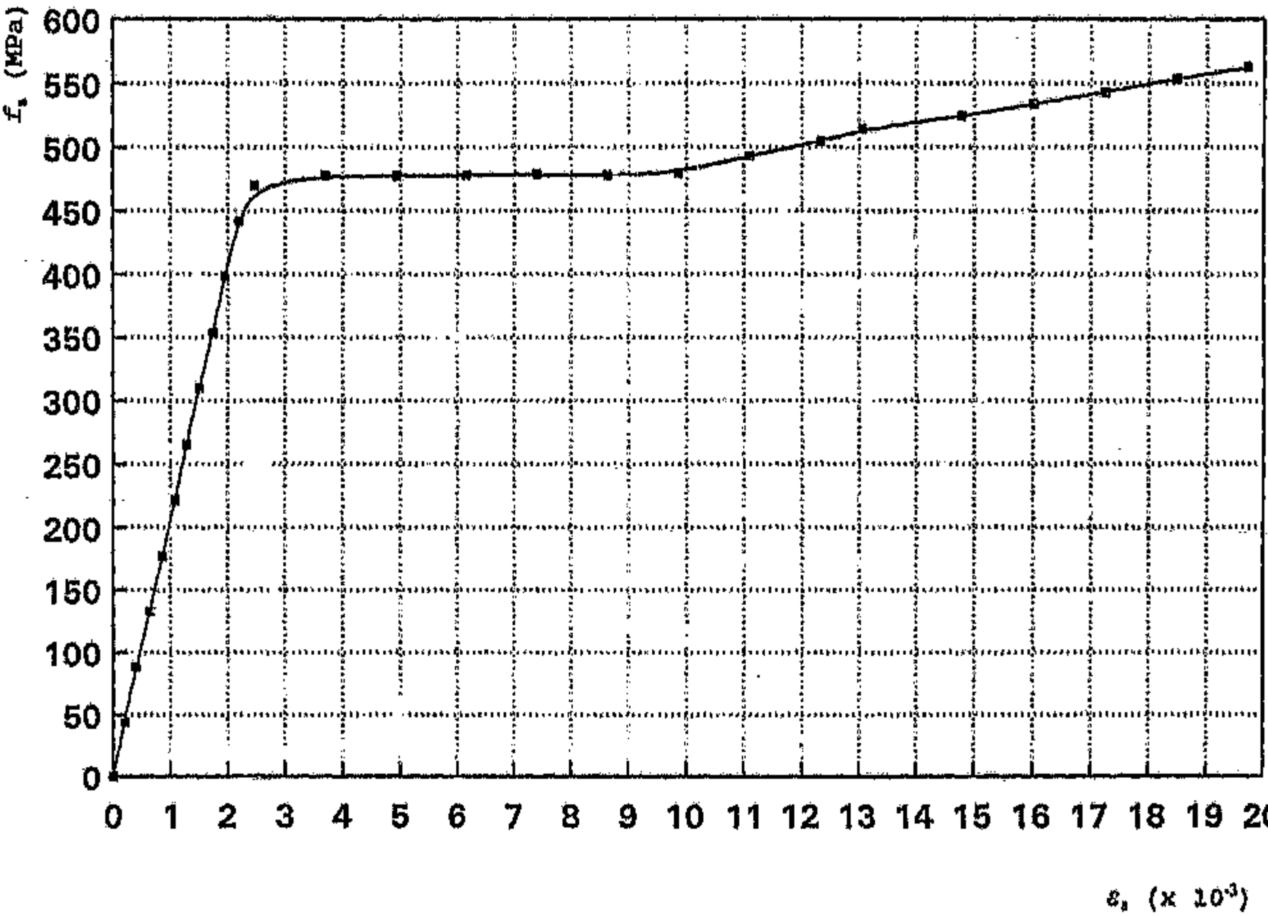
600
550
500
450
400
350
300
250
200
150
100
50
0
f_s (MPa)
0 1 2 3 4 5 6 7 8 9 10 11 12 13 14 15 16 17 18 19 20
ε_s (x 10^{-3})

STRESS-STRAIN CURVES FOR UNPRESTRESSED STEEL AS USED IN THE TEST BEAMS

These are the curves from the remaining two specimens that were not included in the text of section 4.2.1.

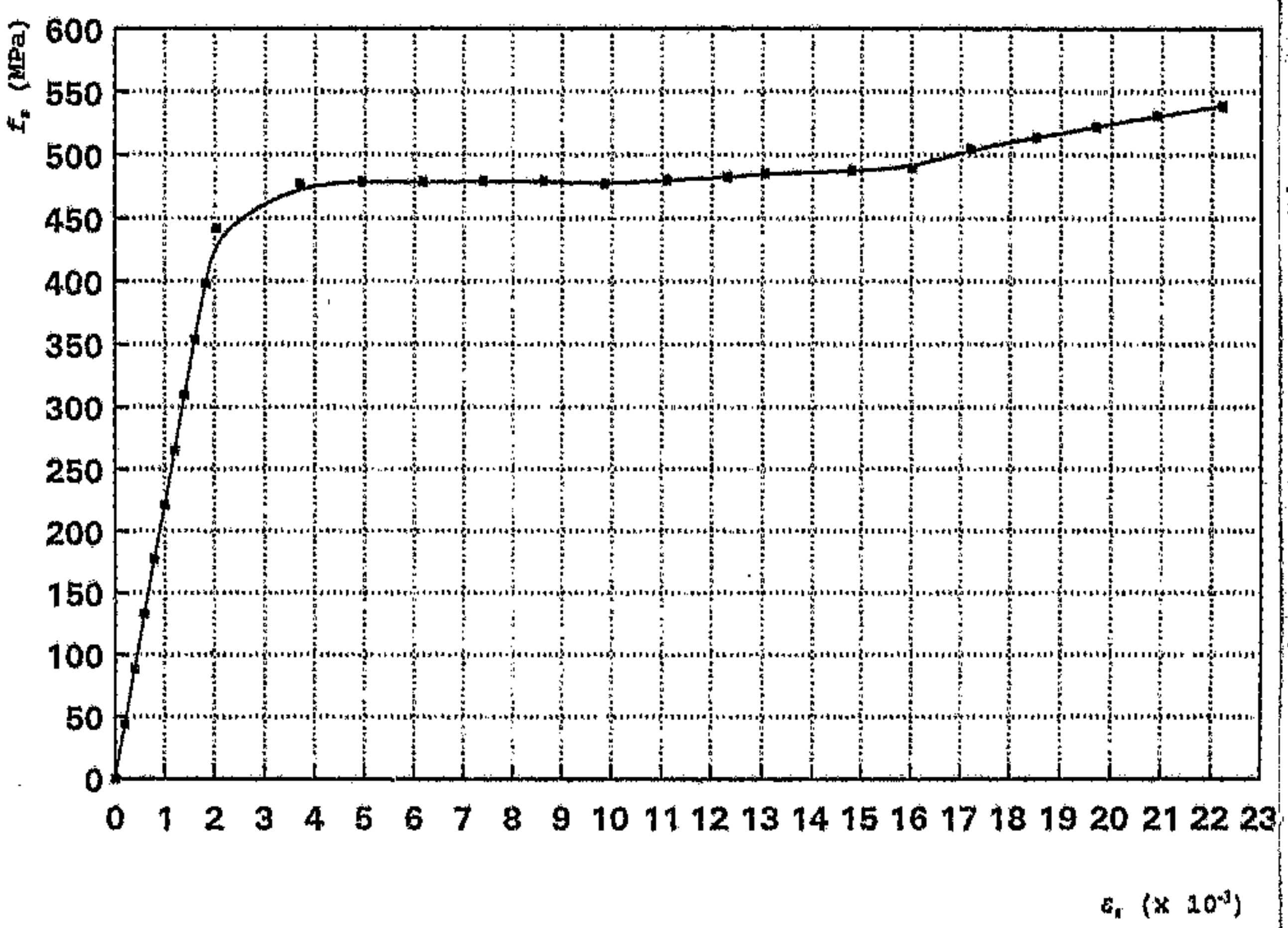

8.3 Recommendations for Future Research

The majority of physical variables of the beams were taken into consideration in this research. The effects of parameters such as the shape of the section and cover were addressed in previous research[26] and therefore were not included in this study. An important factor that cannot be overlooked is that of loading. Future research should focus on repeated and sustained loading.

allowed to crack at service.

8.2 Recommendation for Prediction of Crack Width in Partially Prestressed Concrete Flexural Members

The values of k_w obtained from the tests generally gave better predictions of crack width than the old values by Suri and Dilger[20], but similar results to the reduced values of k_w suggested by Scholz[14] when compared to previous research.

When comparing the performance of the equation in ACI 318-83[18] and CAN3-A23.3-M84[19] to the one by Suri and Dilger[20], their results are very similar for Bennett and Veerasubramnaian[25], when used with the values of k_w from the test beams and the original values of k_w suggested by Suri and Dilger[20], respectively.

Using the tests by Tansi et al[15] as a comparison, the equation from ACI 318-83[18] and CAN3-A23.3-M84[19] used with the values of k_w from the test beams or the ones suggested by Scholz[14] gave the best results. The equation by Suri and Dilger[20] overestimated badly, especially when used with their original values of k_w.

It is thus recommended to use the equation from ACI 318-83[18] and CAN3-A23.3-M84[19]:

$$w = k_w f_s \sqrt[3]{d_c A_o} \times 10^{-6}$$

together with the proposed values of k_w obtained from the graphs of k_w vs. the partial prestressing ratio, or the reduced values of k_w as suggested by Scholz[14].

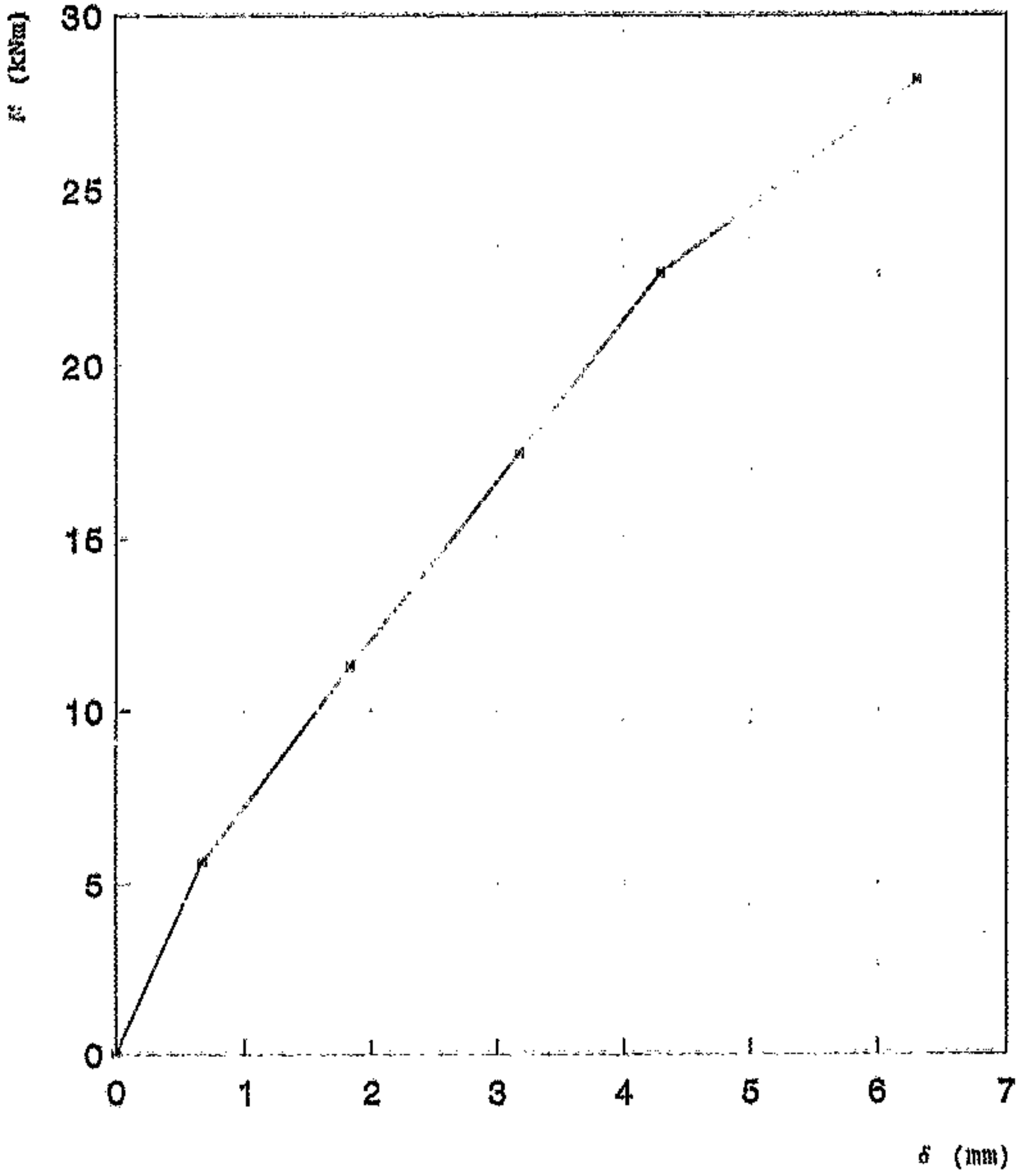

Figure D20 Experimental moment-deflection curve for beam D1#1

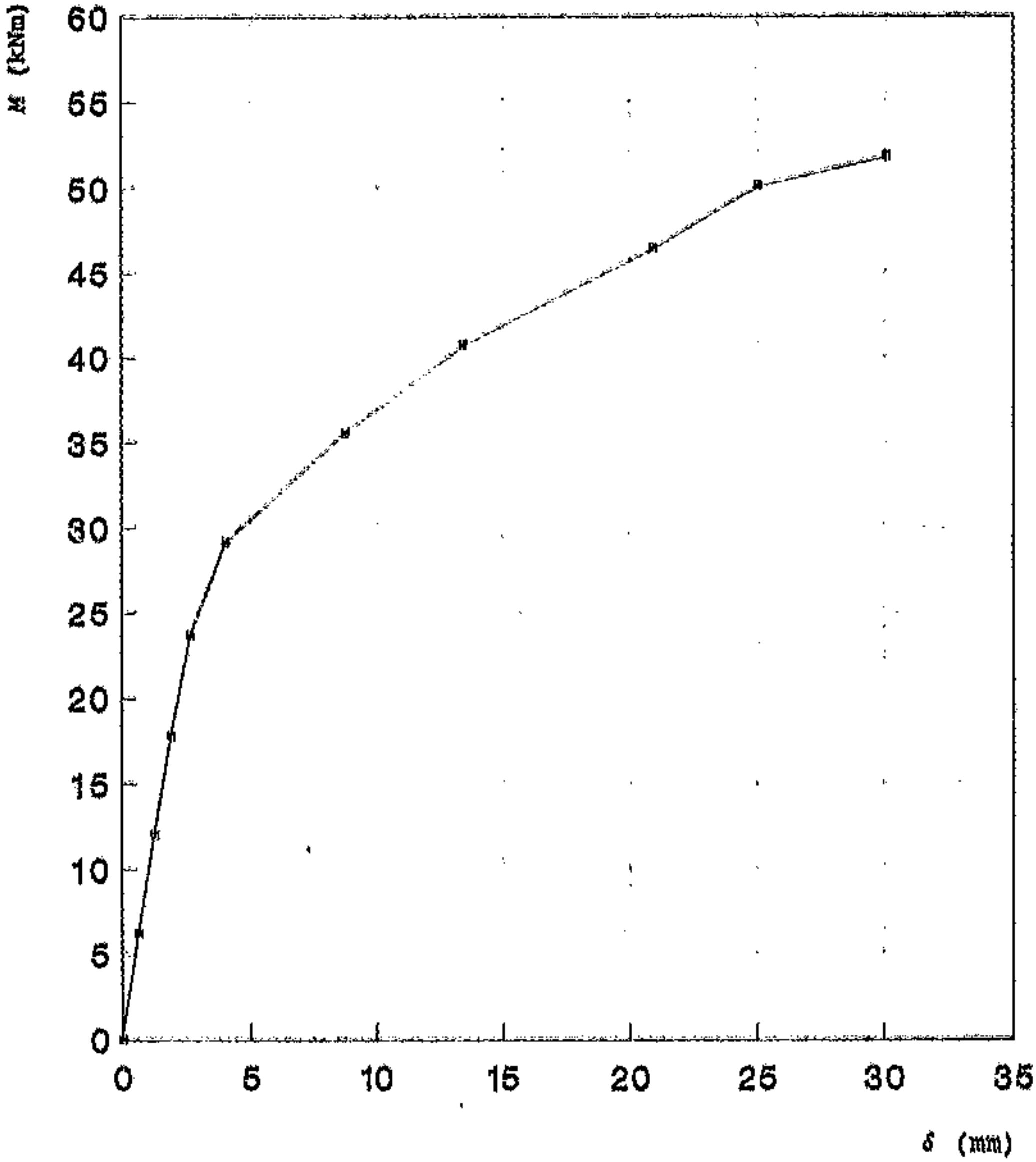

Figure B19 Experimental moment-deflection curve for beam C4#2

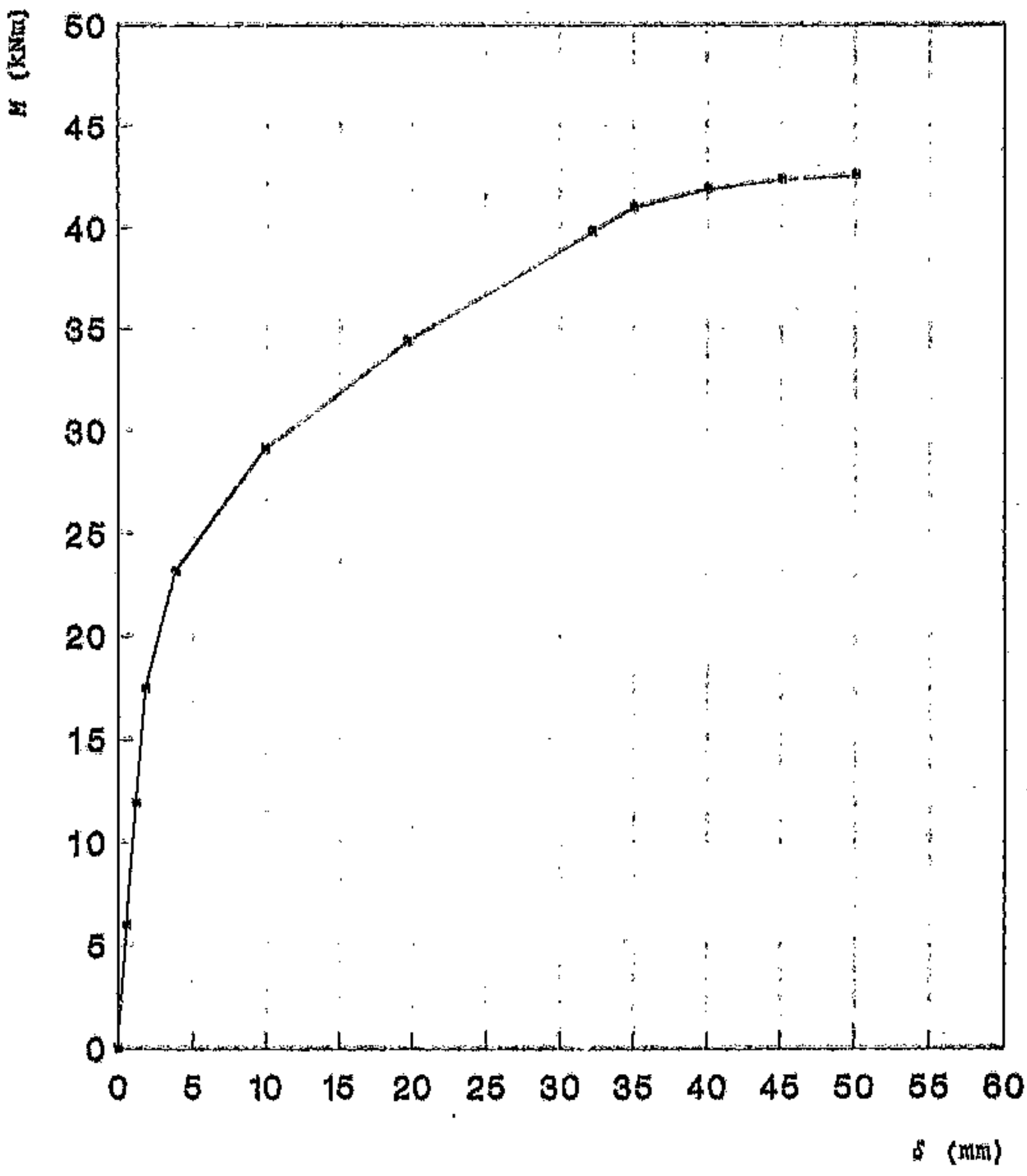

Figure B18 Experimental moment-deflection curve for beam C4#1

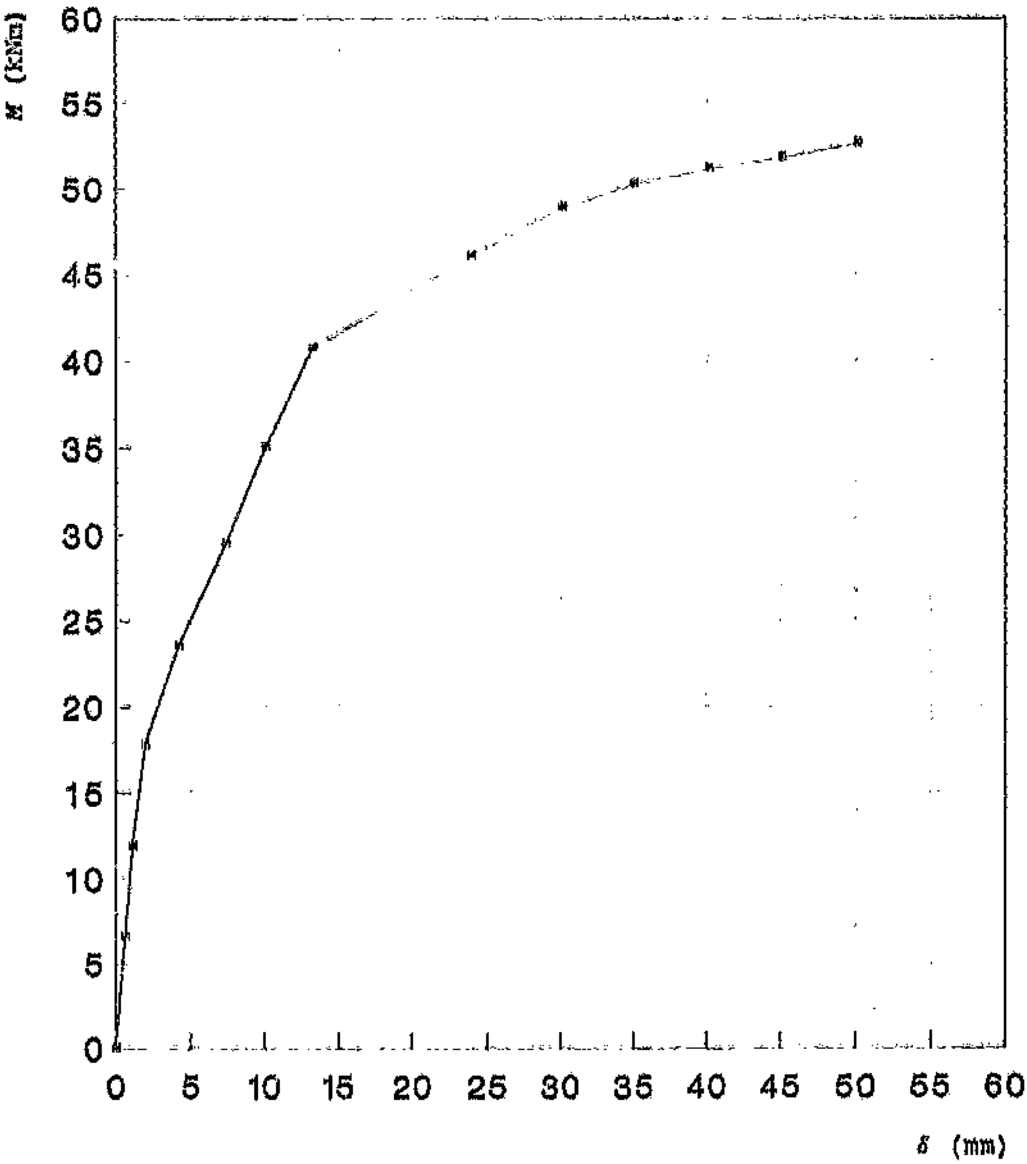

Figure B17 Experimental moment-deflection curve for beam C3#2

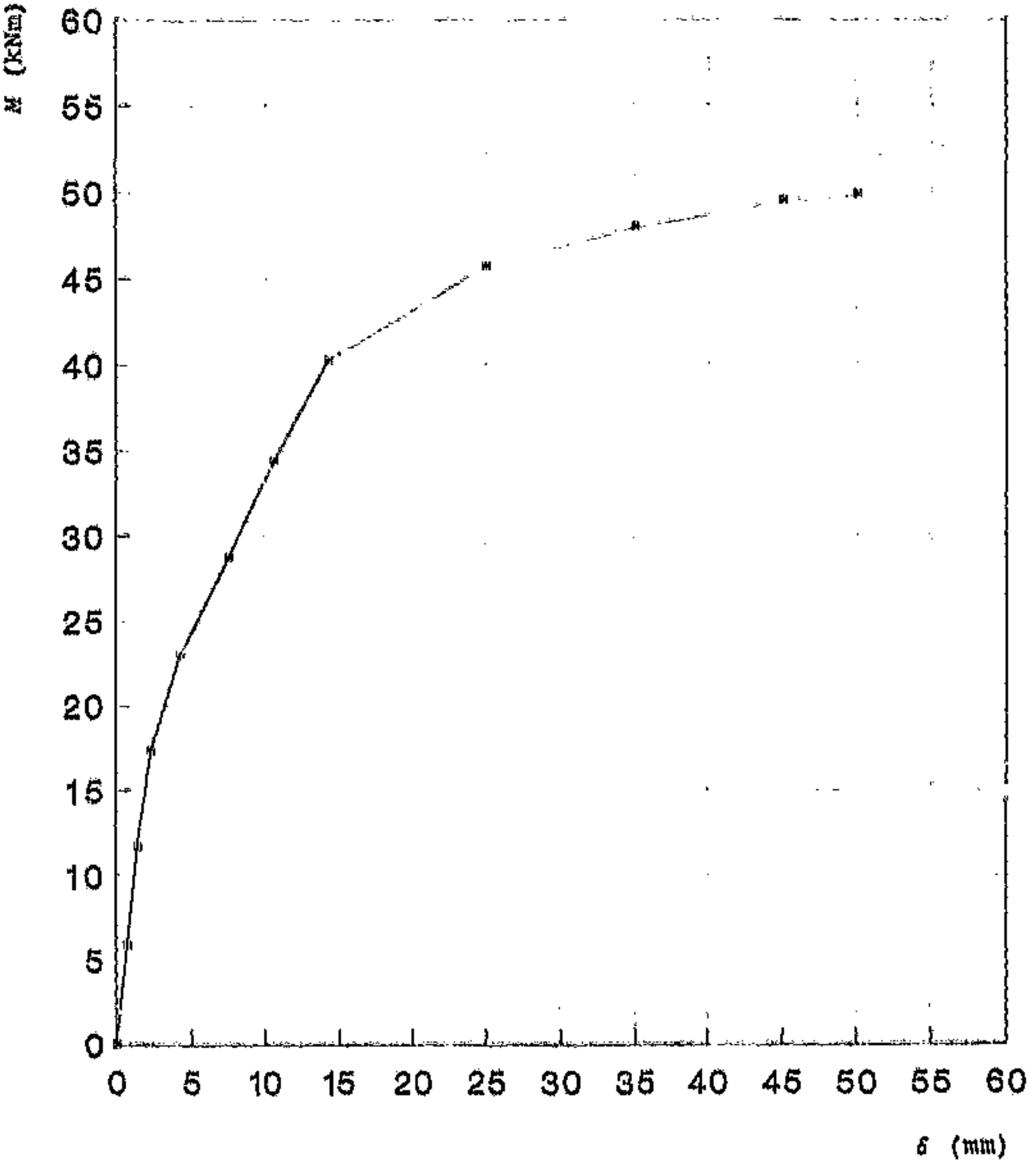

Figure B16 Experimental moment-deflection curve for beam C3#1

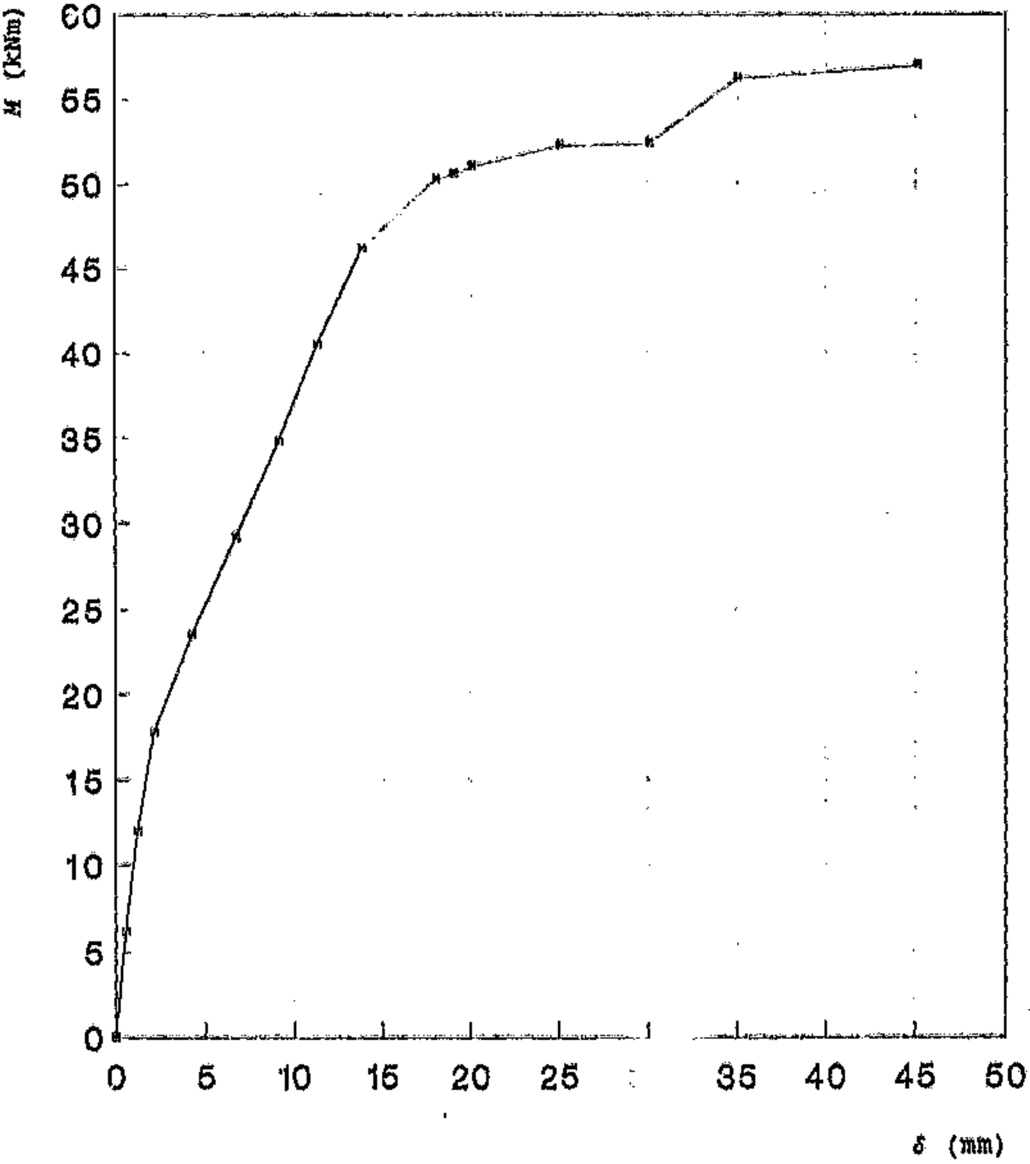

Figure B15 Experimental moment-deflection curve for beam C2#2

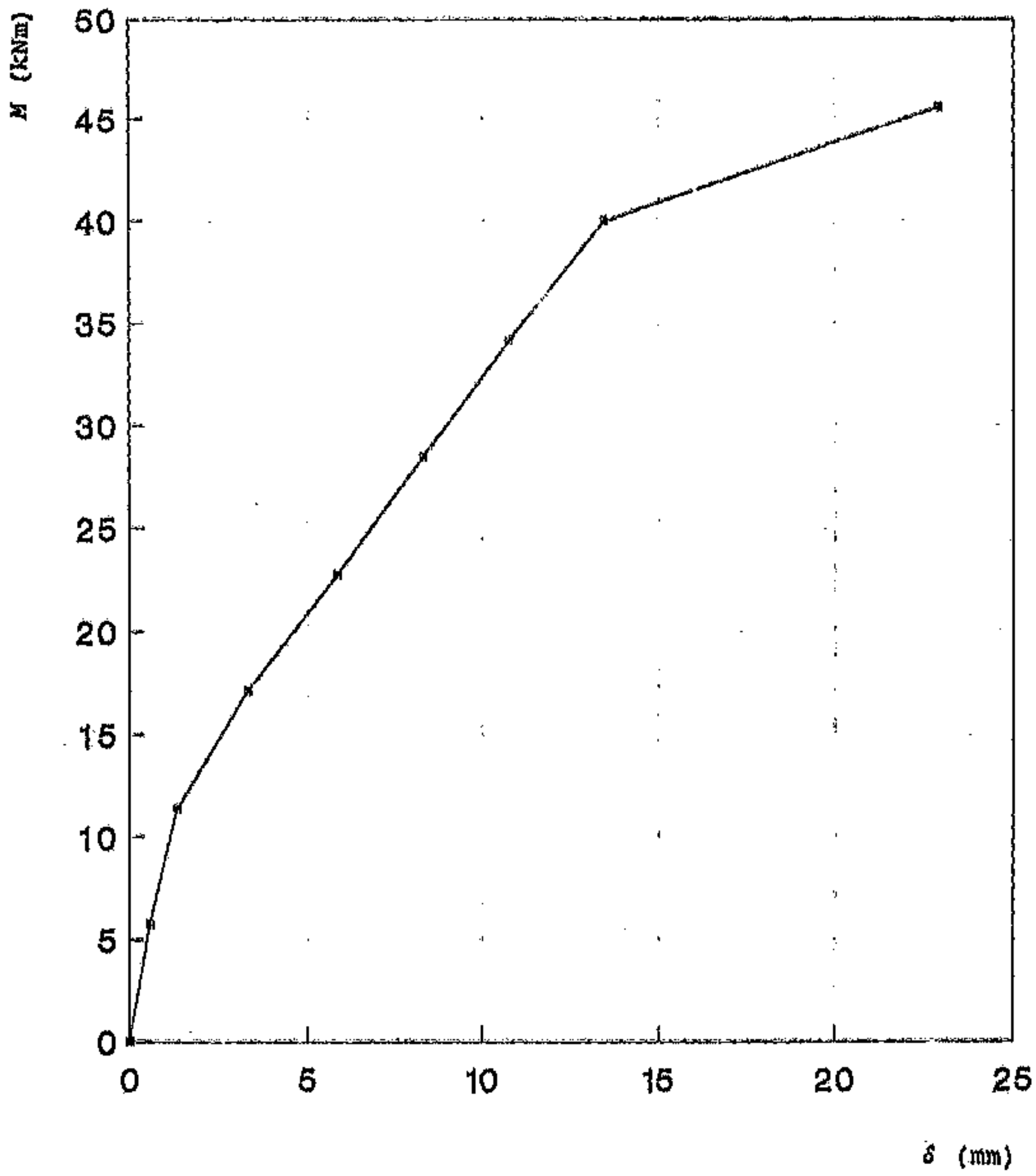

Figure B14 Experimental moment-deflection curve for beam C2#1

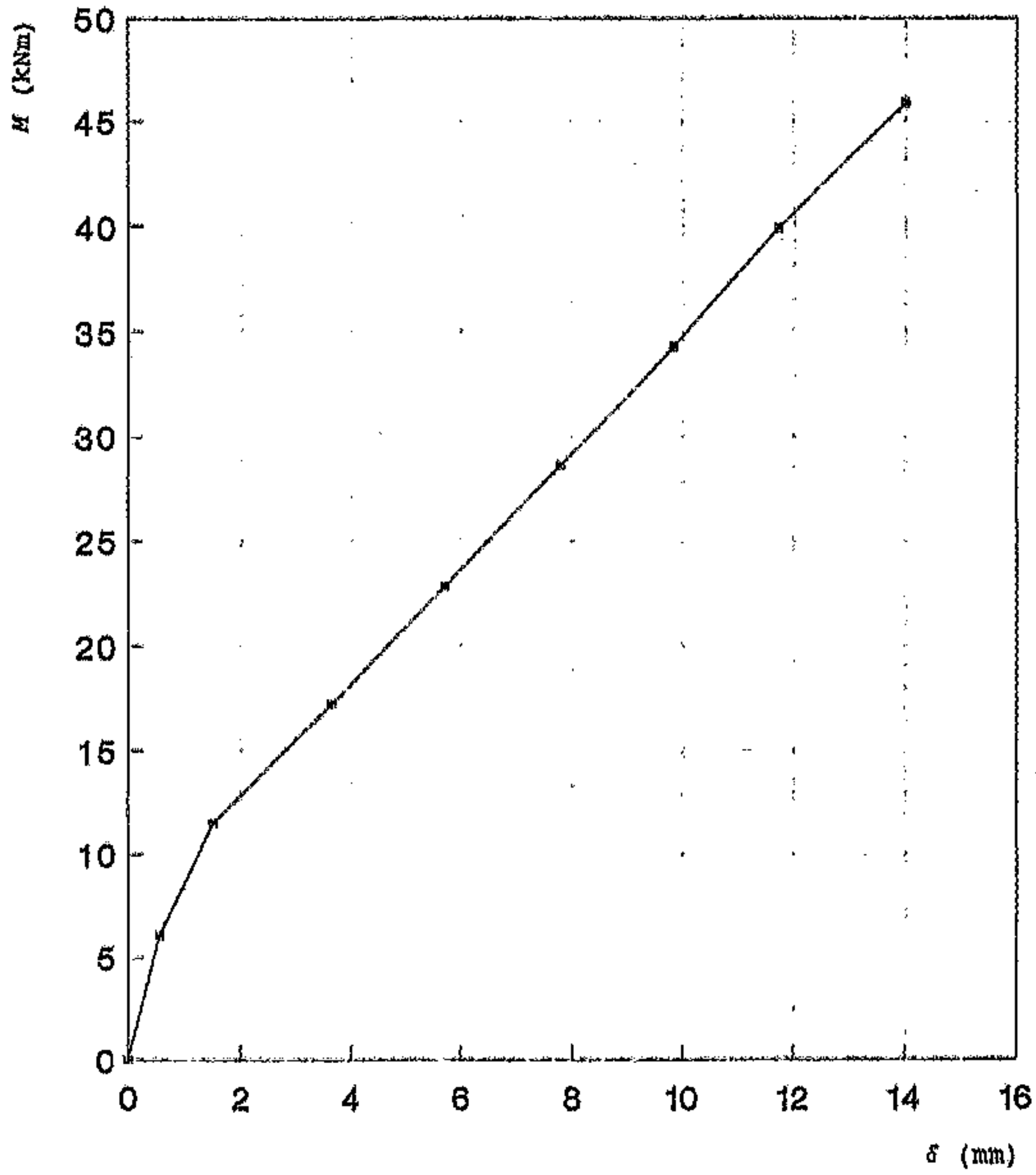

Figure B13 Experimental moment-deflection curve for beam C1#2

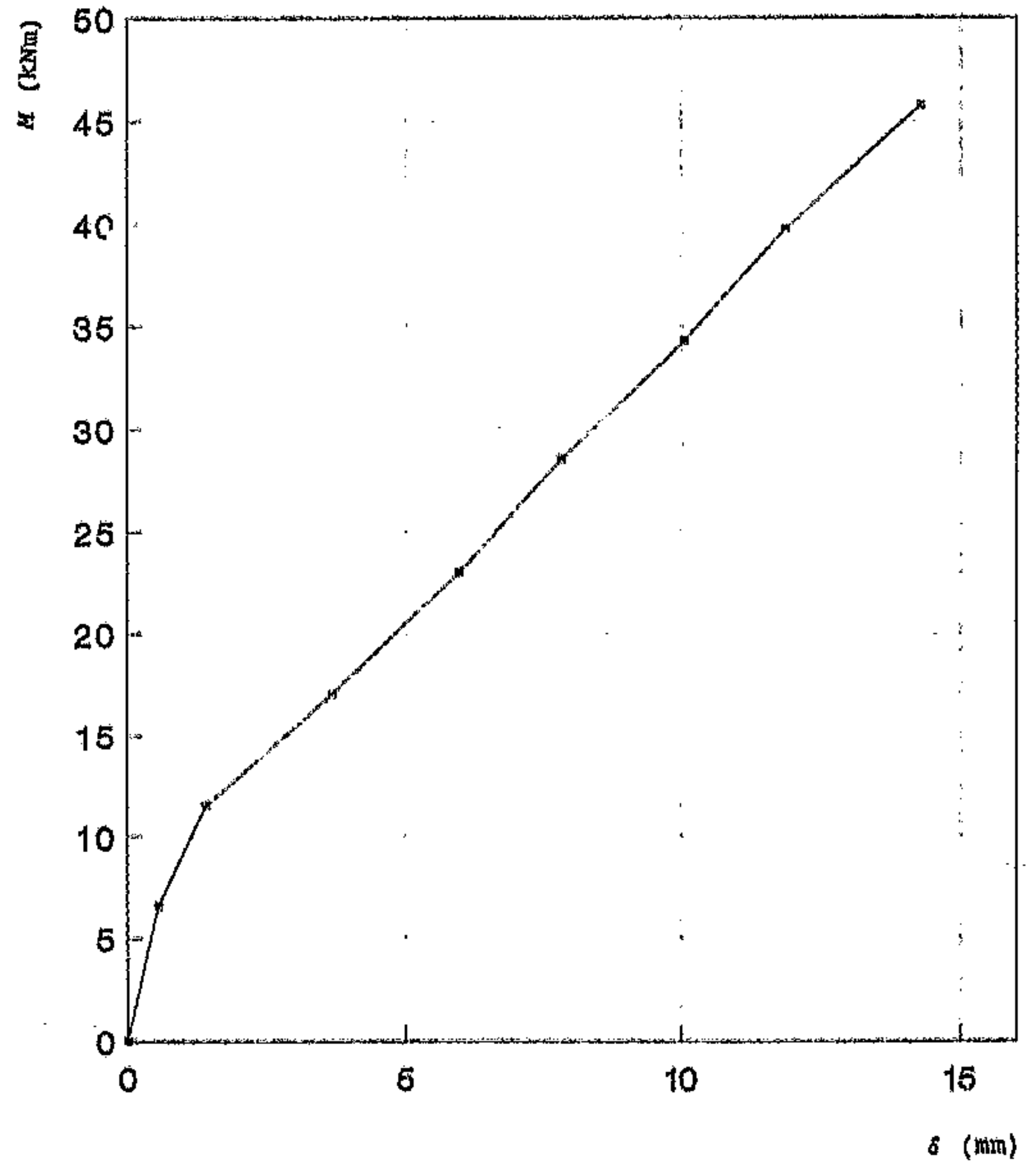

Figure B12 Experimental moment-deflection curve for beam C1#1

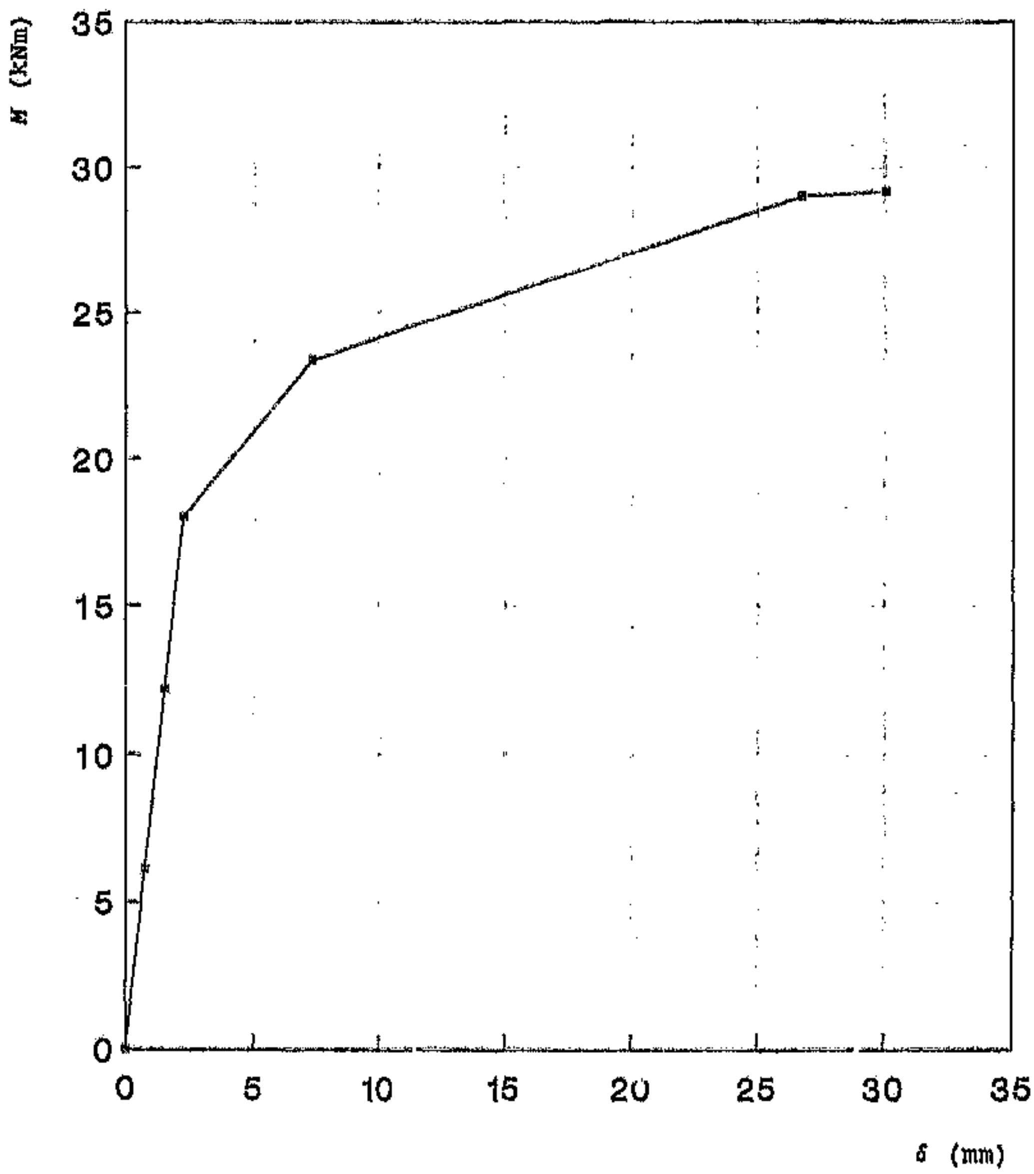

Figure B11 Experimental moment-deflection curve for beam B3#2

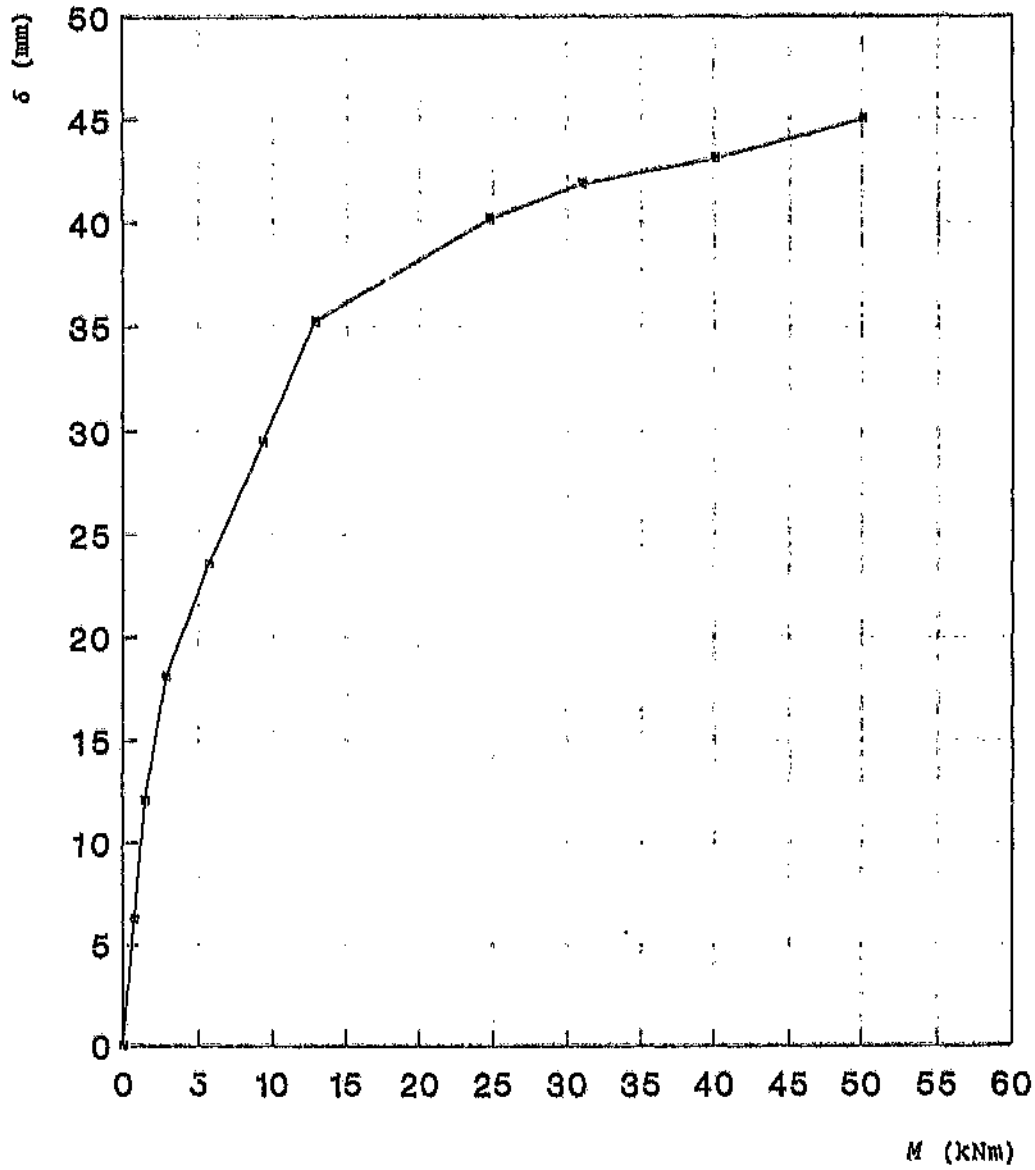

Figure B10 Experimental moment-deflection curve for beam B2#2

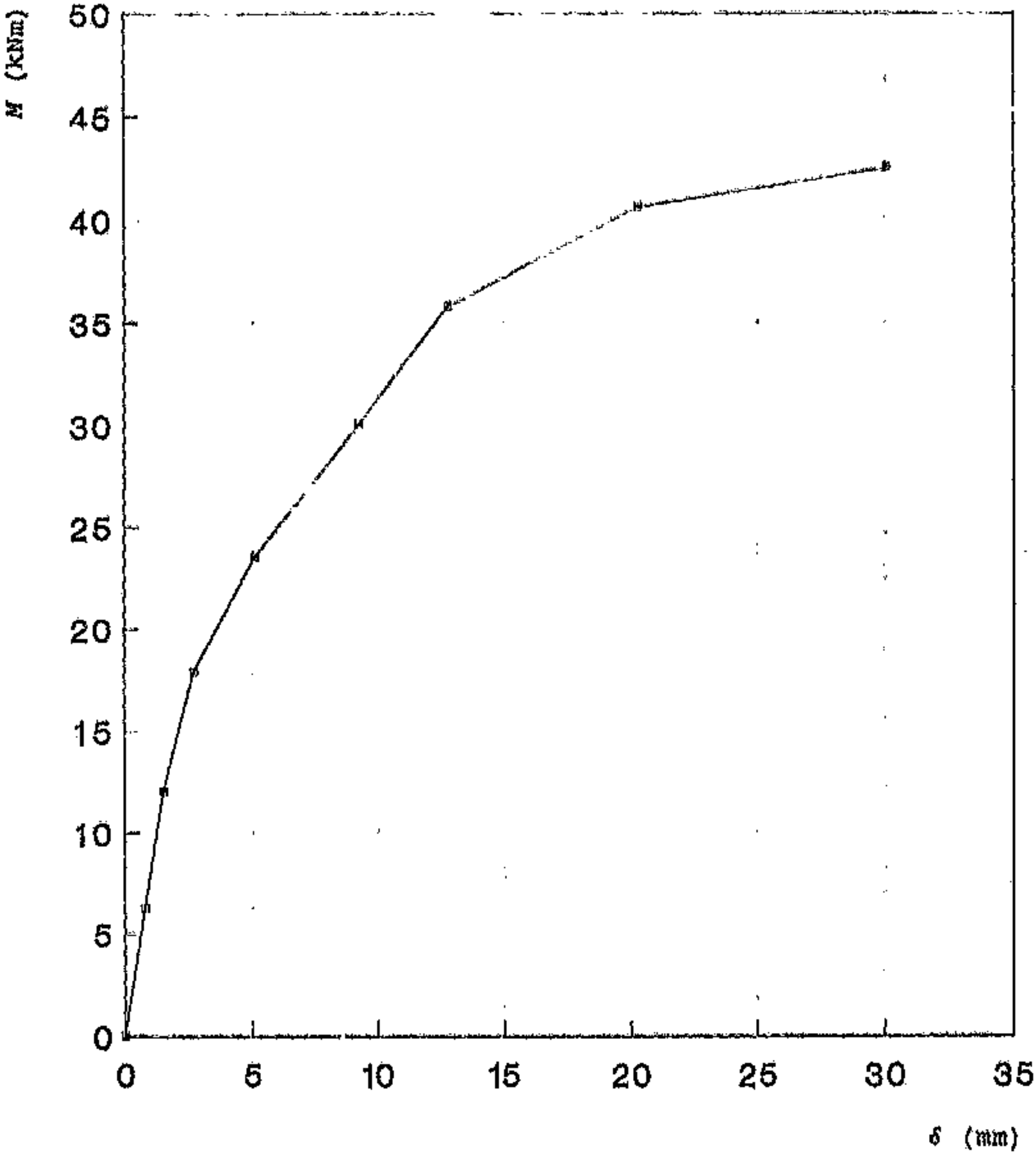

Figure B9 Experimental moment-deflection curve for beam B2#1

REFERENCES

1 Emperger, F. V. *Reinforced Concrete With Additions of High Strength Pretensioned Steel; Research Studies in the Field of Reinforced Concrete*, W. Ernst & Sohn, Berlin , 1939.

2 Abeles, P. W. Fully and Partly Prestressed Reinforced Concrete, *ACI Journal, Proceedings*, Vol 41, No 3, January 1945, pp 181-216.

3 Tadros, M. K. Expedient Service Load Analysis of Cracked Prestressed Concrete Sections, *PCI Journal*, Vol 27, No 6, Nov-Dec 1982, pp 86-111.

4 Pullar-Strecker, P. *Corrosion Damaged Concrete*, Construction Industry Research and Information Association.

5 *The Use of Partial Prestressing for Road Bridges in South Africa*, Research Report RR 89/016/2, Department of Transport, Pretoria, May 1993.

6 Park, R. and Paulay, T. *Reinforced Concrete Structures*, John Wiley and Sons, 769 pp.

7 Park, R. and Gamble, W. L. *Reinforced Concrete Slabs*, John Wiley and Sons, 618 pp.

8 Leonhardt, F. *To New Frontiers for Prestressed Concrete Design and Construction*, PCI Journal, Sept-Oct 1974, pp 54-69.

9 Hognestad, E. High Strength Bars as Concrete Reinforcement, Part 2, Control of Flexural Cracking,

Table C2 continued

Beam		10	40	90	165	200	224	265
D2#1	LF	604	308	178	-922	-1273	-1625	-2078
	CF	667	477	260	-1184	-1292	-1651	-2155
	RF	696	299	187	-1192	-1445	-1510	-1996
	LB	723	527	315	-1013	-1319	-1522	-1981
	CB	815	500	295	-880	-1269	-1615	-2035
	RB	896	669	235	-1460	-1825	-2093	-2777
D2#2	LF	584	471	165	-710	-858	-1077	-1422
	CF	515	360	178	-1340	-1669	-1802	-2387
	RF	529	420	96	-642	-723	-1143	-1308
	LB	646	486	202	-620	-801	-932	-1558
	CB	676	483	216	-1169	-1290	-1680	-2182
	RB	695	)9	223	-609	-765	-976	-1223

Table C2 continued

Beam		10	40	90	165	200	224	265
C4#2	LF	738	564	358	-426	-843	-1064	-1427
	CF	680	559	289	-470	-606	-783	-1056
	RF	634	477	281	-684	-911	-1090	-1586
	LB	572	448	219	-792	-1070	-1278	-217
	CB	649	451	217	-556	-697	-854	-2607
	RB	646	502	248	-724	-923	-1131	-1496
D1#1	LF	-	-	-	-	-	-	-
	CF	582	512	209	-556	-667	-857	-1116
	RF	-	-	-	-	-	-	-
	LB	-	-	-	-	-	-	-
	CB	407	364	84	-636	-751	-922	-1270
	RB	-	-	-	-	-	-	-
D1#2	LF	747	610	286	-673	-691	-1174	-1134
	CF	718	499	250	-989	-1187	-1667	-1776
	RF	648	399	248	-607	-903	-1131	-1540
	LB	808	605	396	-512	-789	-989	-1388
	CB	569	482	45	-1024	-1238	-1460	-1778
	RB	1287	964	613	-863	-1323	-1640	-1802

Table C2 continued

Beam		10	40	90	165	200	224	265
C2#2	LF	655	451	218	-415	-562	-720	-1093
	CF	624	522	290	-877	-899	-997	-1475
	RF	888	499	219	-1402	-1707	-2049	-1312
	LB	764	578	321	-711	-944	-1198	-1429
	CB	770	579	309	-430	-479	-427	-1181
	RB	694	575	318	-714	-1126	-1315	-1725
C3#1	LF	791	543	335	-519	-745	-942	-1293
	CF	563	519	280	-926	-1129	-1185	-1778
	RF	627	464	229	-577	-770	-936	-1448
	LB	632	346	229	-553	-848	-919	-1203
	CB	694	504	269	-915	-1334	-1473	-1507
	RB	703	509	226	-615	-850	-978	-1480
C3#2	LF	740	533	262	-623	-858	-1051	-1393
	CF	759	581	313	-841	-1096	-1378	-1821
	RF	791	592	323	-770	-915	-1289	-1754
	LB	772	470	243	-698	-1176	-1408	-975
	CB	611	451	192	-1039	-1312	-1623	-1916
	RB	642	452	191	-710	-915	-1131	-1472

(2) Series C and D: strains were measured at d = 10 mm, 40 mm, 90 mm, 165 mm, 200 mm, 224mm and 265 mm (from the top extreme concrete fibre)

Table C2 Experimental concrete surface strain measurements (x 10^{-6}) for series C and D

Beam		10	40	90	165	200	224	265
C1#1	LF	430	373	202	-608	-887	-1122	-2646
	CF	444	534	72	-1499	-1563	-1928	-
	RF	434	316	139	-607	-683	-903	-1200
	LB	748	605	209	-441	-591	-888	-1185
	CB	672	266	264	-634	-917	-1062	-1423
	RB	983	772	93	-1177	-1374	-1556	-1778
C1#2	LF	601	419	132	-917	-	-1338	-1830
	CF	535	461	240	-544	-737	-902	-1782
	RF	617	438	171	-1040	-1107	-1319	-1678
	LB	629	292	-7	-612	-1402	-1347	-2081
	CB	465	297	-7	-937	-505	-1767	-1953
	RB	499	254	-27	-1157	-1305	-1591	-2035
C2#1	LF	735	568	291	-1086	-946	-1193	-1846
	CF	750	577	278	-818	-1024	-1218	-2098
	RF	740	546	249	-656	-784	-959	-1230
	LB	546	379	147	-594	-838	-1279	-1525
	CB	555	379	131	-846	-1268	-1290	-1759
	RB	553	357	102	-1611	-1943	-2289	-2663

Table C1 continued

Beam		10	40	90	200	224	275
B1#2	LF	622	651	-69	-1124	-1316	-1723
	CF	651	351	-41	-1326	-1579	-2037
	RF	527	348	-89	-745	-1509	-1377
	LB	653	502	112	-1424	-1659	-1606
	CB	698	371	-1978	-583	-794	-1579
	RB	790	555	-	-1010	-1054	-2009
B2#1	LF	591	308	-120	-1140	-1352	-1864
	CF	575	290	-84	-943	-1116	-1570
	RF	534	290	-107	-1074	-1302	-1728
	LB	505	303	-95	-	-1285	-1720
	CB	503	315	-69	-	-1153	-1573
	RB	558	278	-134	-1148	-1360	-1884
B2#2	LF	650	366	-25	-1122	-1309	-1842
	CF	736	408	-114	-1224	-1461	1955
	RF	738	408	-81	-	-	-
	LB	660	331	-162	-1087	-1327	-3692
	CB	607	256	-116	-1370	-1629	-264
	RB	556	292	-196	-	-2435	-3017

Table C1 continued

Beam		10	40	90	200	224	275
A2#1	LF	757	445	-34	-1373	-1648	-1883
	CF	766	465	-26	-900	-1053	-1801
	RF	768	476	-3	-1130	-1383	-1869
	LB	693	392	-77	-1098	-1313	-1813
	CB	694	412	-92	-1575	-1882	-2409
	RB	735	433	-64	-1109	-1346	-1884
A2#2	LF	466	220	-158	-847	-1006	-3258
	CF	543	176	-558	-2382	-2743	-1502
	RF	535	206	-279	-1414	-1679	-2372
	LB	657	358	-144	-1345	-1606	-2179
	CB	718	381	-246	-1392	-1783	-2441
	RB	667	409	-63	-1369	-1491	-1909
B1#1	LF	679	406	-39	-1068	-1286	-1647
	CF	-	-	-1	-822	-1021	-1452
	RF	-	390	-34	-1303	-1560	-1448
	LB	573	310	-177	-898	-1037	-1459
	CB	394	-	-138	-1243	-1497	-1816
	RB	614	320	-84	-	-933	-1372

EXPERIMENTAL CONCRETE SURFACE STRAIN MEASUREMENTS

(1) Series A and B: strains were measured at d = 10 mm, 40 mm, 90 mm, 200 mm, 224mm and 275 mm (from the top extreme concrete fibre)

Table C1 Experimental concrete surface strain measurements (x 10^{-6}) for series A and B

Beam		10	40	90	200	224	275
A1#1	LF	696	379	-99	-1272	-1594	-1984
	CF	675	415	-59	-1056	-1119	-1739
	RF	682	394	139	-1057	-1269	-1753
	LB	661	355	-77	-1075	-1278	-1727
	CB	667	364	-128	-1131	-1340	-1772
	RB	672	370	-62	-1301	-1552	-2198
A1#2	LF	603	305	-299	-1727	-2010	-2528
	CF	620	308	-140	-1242	-1521	-2065
	RF	593	308	-140	-1242	-1521	-2065
	LB	661	383	-100	-951	-1347	-1552
	CB	725	383	-166	-1093	-1322	-1860
	LB	695	410	-85	-1654	-1947	-2558

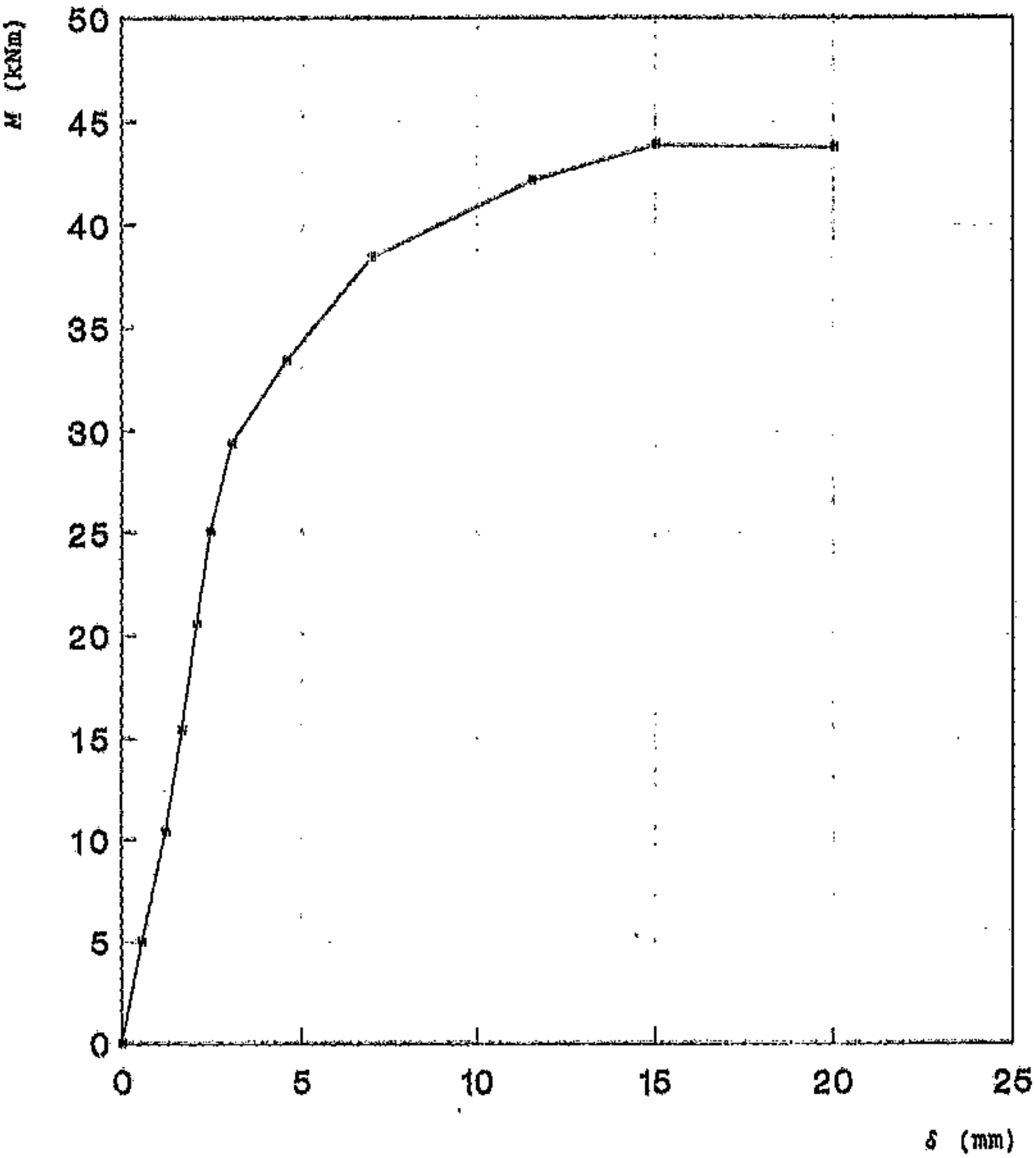

Figure B24 Experimental moment-deflection curve for beam D3#2

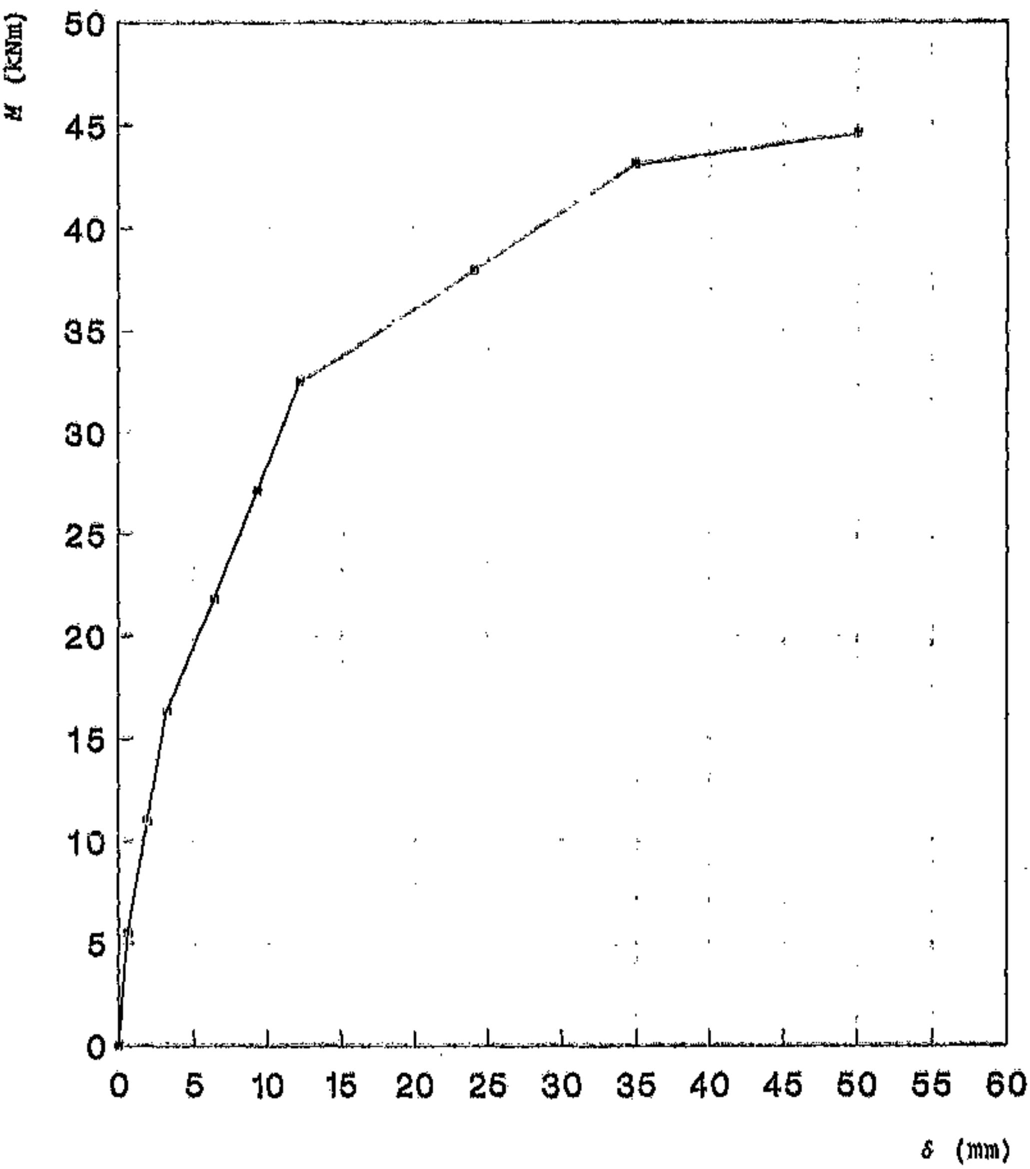

Figure B23 Experimental moment-deflection curve for beam D2#2

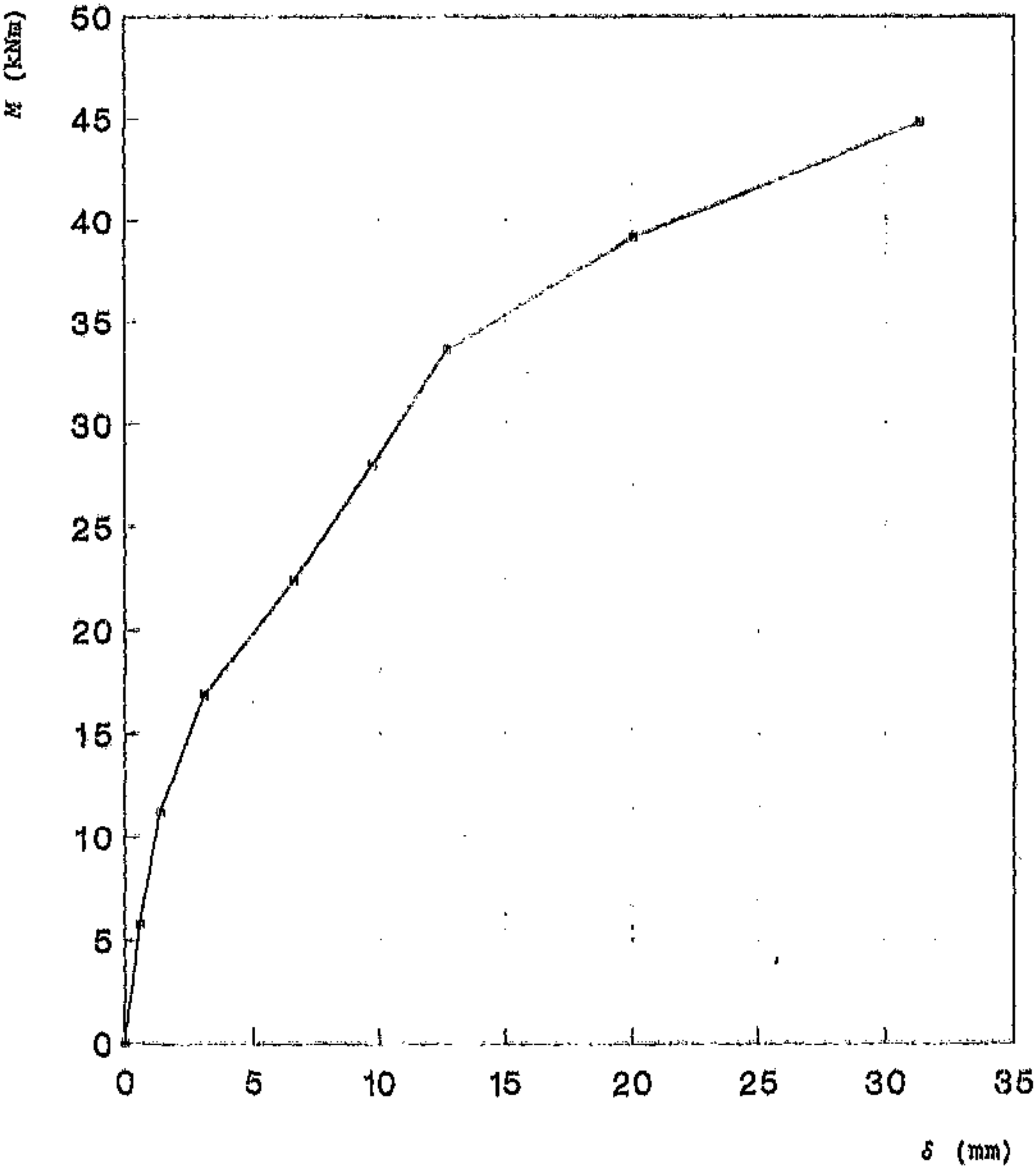

Figure D22 Experimental moment-deflection curve for beam D2#1

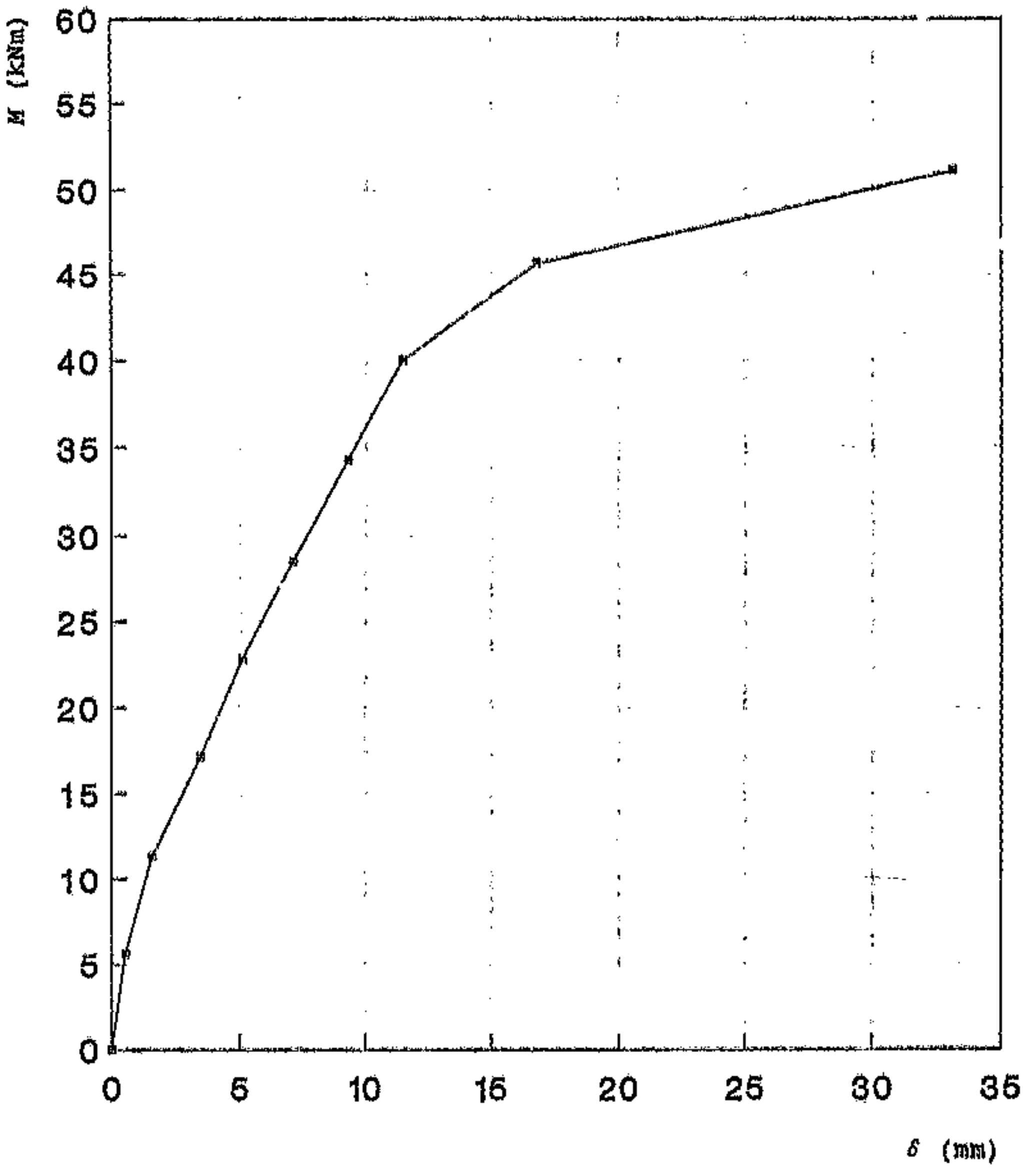

Figure B21 Experimen'al moment-deflection curve for beam D1#2

42 Ramaswamy, G. S. *Modern Prestressed Concrete Design*, Pitman Publications Ltd., London, 1976.

34 Beeby, A. W. and Taylor H. P. J. *Cracking in Partially Prestressed Concrete Members*, FIP Sixth Congress, Prague, June 1970.

35 Meier, S. W. and Gergely, P. Flexural Crack Width in Prestressed Concrete Beams, *ASCE Journal, Proceedings*, Vol 107, No ST2, Feb 1981.

36 *SIA 162-1968, Code for the Analysis, Design and Construction of Structures in Reinforced Concrete and Prestressed Concrete*, Schweizerischer Ingenieur- und Architektenverein, Zürich, 1968.

37 Naaman, A. E. and Siriaksorn, A. Seviceability Based Design of Partially Prestressed Beams (Part 1), *PCI Journal*, Vol 24, No 2, Mar-Apr 1979, pp 64-89, and Seviceability Based Design of Partially Prestressed Beams (Part 2), *PCI Journal*, Vol 24, No 3, May-Jun 1979, pp 40-60.

38 Nawy, E. G. and Pontyondy, J. G. Flexural Cracking Behaviour of Pretensioned I- and T-Beams, *ACI Journal, Proceedings*, Vol 68, No 5, May 1971, pp 355-360.

39 Bachmann, H. Design of Partially Prestressed Conc: ete Structures Bsed on Swiss Experiences, *PCI Journal*, Vol 29, No4, July-Aug 1984, pp 84-105.

40 *Properties of Aggregates in Concrete (Part 1)*, Hippo Quarries Technical Publication.

41 Thurlimann, B. A *Case for Partial Prestressing*, Structural Concrete Symposium, Proceedings, University of Toronto, May 1971, pp 253-301.

No 9, Sept 1972, pp 533-542.

26 *BS 8110-1985, Structural Use of Concrete, Part 1, Code of Practice for Design and Construction*, British Standards Institution, London, 1985.

27 *SABS 0100-1980, Code of Practice for the Structural Use of Concrete*, South African Bureau of Standards, Pretoria, 1980.

28 *BS 5400-1984, Code of Practice for the Design of Concrete Bridges*, British Standards Institution, London, 1984.

29 Beeby, A. W., Keyder, E. and Taylor, H. P. J. *Cracking and Deformations of Partially Prestressed Concrete Beams*, Technical Report, Cement and Concrete Association, Jan 1972, 26 pp.

30 Bennett, E. W. and Chandrasekhar, C. S. Calculations of the Width of Cracks in Class 3 Prestressed Beams, *Proceedings*, Institution of Civil Engineers, Vol 49, July 1971, pp 333 - 346.

31 Bennett, E. W. and Dave, N. J. Test Performances and Design of Concrete Beams With Limited Prestress, *The Structural Engineer*, Vol 47, No 12, Dec 1969, pp 487-496.

32 *CEB/FIP 1970, International Recommendations for the Design and Construction of Concrete Structures: Principles and Recommendations*, FIP Sixth Congress, Prague, June 1970.

33 *CEB/FIP 1978, Model Code for Concrete Structures*, Comité Euro-International du Béton, Paris, 1978.

17 *CP 110-1972, Code of Practice for the structural Use of Concrete*, British Standards Institution, London, 1972.

18 *ACI 318-83, Building Code Requirements for Reinforced Concrete*, American Concrete Institute, Detroit, 1983.

19 *CAN3-A23.3-M84, Design of Concrete Structures for Buildings*, Canadian Standards Association, Rexdale, Ontario, 1984.

20 Suri, K. M. and Dilger, W. H. Crack Width of Partially Prestressed Concrete Members, *ACI Journal, Proceedings*, Vol 83, No 5, Sept-Oct 1986, pp 784-797.

21 Nawy, E. G. and Huang, P. T. Crack and Deflection Control of Pretensioned Prestressed Beams, *PCI Journal*, Vol 22, No 3, May-June 1977, pp 30-47.

22 Nawy, E. G. and Chiang, J. Y. Serviceability Behaviour of Post Tensioned Beams, *PCI Journal*, Vol 25, No 1, Jan-Feb 1980, pp 74-95.

23 Naaman, A. E. Partially Prestressed Concrete: Review and Recommendations, *PCI Journal*, Vol 30, No 6, Nov-Dec 1985, 30pp.

24 Nawy, E. G. Flexural Cracking Behaviour of Pretensioned and Post Tensioned Beams: The State of the Art, *ACI Journal*, Nov-Dec 1985, pp 890-900.

25 Bennett, E. W. and Veerasubramanian, N. Behaviour of Non Rectangular Beams With Limited Prestress After Flexural Cracking, *ACI Journal, Proceedings*, Vol 69,

Journal, Portland Cement Association Research and Development Laboratories, Vol 4, No 1, Jan 1962, pp 46-63.

10 *Compte-Rendu de la 5ème Session de Travail*, Comité Européen du Béton, Bulletin d'Information, No 24, Paris, 1960.

11 Kaar, P. H. and Hognestad, E. High Strength Bars as Concrete Reinforcement, Part 7, Control of Cracking in T Beam Flanges, *Journal*, Portland Cement Association Research and Development Laboratories, Vol 7, No 1, Jan 1965, pp 42-53.

12 Base, G. D., Read, J. B., Beeby, A. W. and Taylor, H. P. J. *Crack Control in Concrete Beams*, Research Report No 18, Cement and Concrete Association, London, Dec 1966, 44 pp.

13 Gergely, P. and Lutz, L.H. Maximum Crack Width in Reinforced Concrete Flexural Members, *Causes, Mechanism and Control of Cracking*, Special Publication SP-20, ACI, Detroit, 1968, pp 87-117.

14 Scholz, H. Appraisal of Deflection and Cracking Models for Partially Prestressed Members, *The Civil Engineer in South Africa*, Jan 1990, pp 23-33.

15 Tansi, P., Heaney, A. C., Warner, R. F., *Serviceability Tests on Partially Prestressed Concrete Beams*, UNICIV report No R-184, University of New South Wales, Australia, May 1979.

16 Beeby, A. W. An *Investigation of Cracking in Slabs Spanning One Way*, Technical Report TRA 433, Cement and Concrete Association, London, April 1970, 22 pp.